AN ABSTRACT OF THE DISSERTATION OF

Anne Jefferson for the degree of Doctor of Philosophy in Geology presented on September 20, 2006.

Title: Hydrology and Geomorphic Evolution of Basaltic Landscapes, High Cascades, Oregon

Abstract approved:

_____

Gordon E. Grant   Stephen T. Lancaster

The basaltic landscapes of the Oregon High Cascades form a natural laboratory for examining how geologic setting and history influence groundwater flowpaths, streamflow sensitivity to climate, and landscape evolution. In the High Cascades, highly permeable young basaltic lavas form extensive aquifers. These aquifers are the dominant sources of summer streamflow for the Willamette River and its tributary, the McKenzie River, whose watershed forms the study area. Groundwater is discharged at large volume, cold springs, and discharge, temperature, and isotopic measurements at seven springs were used to constrain groundwater patterns. Lava flow geometries have a significant influence on groundwater recharge areas and flowpaths, sometimes superseding topographic controls. Transit times to springs are ~3-14 years, and flowpaths are generally shallow and have limited contact with deeper geothermal systems, except at fault zones. Time-series analyses of historical discharge, precipitation, snow, and temperature records reveal that the distribution of permeable rocks and resultant groundwater systems strongly influence streamflow response to climatic forcing. The annual hydrograph is shaped by groundwater storage and release, but inter-annual streamflow variability is largely the result of climatic forcing. Over the past 60 years, warmer winters and earlier snowmelt have lengthened the summer recession period and decreased autumn minimum discharges in a groundwater-dominated watershed. A chronosequence of dated rock units, combined with field

observations and measurements of slopes, contributing areas, and drainage densities, shows that the geologic history of a watershed controls the stage of drainage development. Groundwater flowpaths remain the dominant drainage mechanism for up to one million years, but as chemical weathering, glaciation, and other processes reduce the land surface permeability, channel networks grow up-slope of the springs. Within three million years, water is carried via a fully developed runoff-dominated stream network, groundwater discharge is insubstantial, and the landscape is shaped by fluvial and mass-wasting processes. The geology of a landscape is important for understanding hydrological processes at time scales ranging from a single season to several million years.

Hydrology and Geomorphic Evolution of Basaltic Landscapes,

High Cascades, Oregon

by

Anne Jefferson

A DISSERTATION

submitted to

Oregon State University

in partial fulfillment of
the requirements of the
degree of

Doctor of Philosophy

Presented September 20, 2006

Commencement June 2007

Doctor of Philosophy dissertation of Anne Jefferson presented on September 20, 2006.

APPROVED:

_____

Co-major Professor, representing Geology

_____

Co-major Professor, representing Geology

_____

Chair of the Department of Geosciences

_____

Dean of the Graduate School

I understand that my dissertation will become part of the permanent collection of Oregon State University libraries. My signature below authorizes release of my dissertation to any reader upon request.

_____

Anne Jefferson, Author

ACKNOWLEDGEMENTS

I deeply thank my advisors, Dr. Gordon Grant and Dr. Stephen Lancaster for their assistance, ideas, and encouragement throughout the doctoral process. I express my appreciation for my committee members, Dr. Roy Haggerty, Dr. Wayne Huber, and Dr. Jeff McDonnell, for their contributions to my success. Thanks to Sarah Lewis for her friendship, organizational prowess, analytical skills, and help with my writing and figures. Thanks to Dr. Anne Nolin, Dr. Tim Rose, and Dr. Christina Tague for working with me and co-authoring my papers. Thanks to Mike Farrell, Shawn Majors, Chris O'Connell, Josh Wyrick, and others for amazingly enthusiastic field assistance. Thanks to the wonderful staff of the McKenzie River Ranger District and the H.J. Andrews Experimental Forest for sharing their insight into the McKenzie River watershed and for their help with field work logistics. Thanks to Mike Rowe, Mariek Schmidt, Greg Stewart, Amber Stoner, Rose Wallick, and Peter Wampler for showing me the way forward in graduate school. Most of all, I give thanks to my husband, Joel Lynne, for his unconditional love and support these past four years.

CONTRIBUTION OF AUTHORS

Dr. Gordon E. Grant was involved in the formulation of ideas and the revisions process for Chapters 2 and 4. Dr. Timothy P. Rose assisted with isotopic and noble gas data collection and analysis of results for Chapter 2. Dr. Anne W. Nolin was involved with project design, manuscript revision, and analysis of El Nino-Southern Oscillation and Pacific Decadal Oscillation signals in Chapter 3. Ms. Sarah L. Lewis assisted with project design, data compilation and analysis, and manuscript revision for Chapter 3. Christina Tague provided me with RHESSys model results and assisted with manuscript revision for Chapter 3. Dr. Stephen T. Lancaster was involved in project design and assisted with data interpretation for Chapter 4.

TABLE OF CONTENTS

TABLE OF CONTENTS (Continued)

TABLE OF CONTENTS (Continued)

LIST OF FIGURES

LIST OF FIGURES (Continued)

LIST OF FIGURES (Continued)

LIST OF FIGURES (Continued)

LIST OF TABLES

DEDICATION

I dedicate my dissertation to my mother,

Dr. Carol A. Jefferson, my earliest and best mentor and role model.

Hydrology and Geomorphic Evolution of Basaltic Landscapes,
High Cascades, Oregon

1 Interaction between permeability and hydrological processes: context and setting

1.1 Context and history of research relating to landscape permeability and hydrologic processes

Permeability is a material property that controls the transmittal of fluids. At the landscape scale, permeability is a function of bedrock geology and the geological, hydrological, and biological processes that have acted on the landscape over the course of its history. In turn, permeability influences the partitioning of water between different flowpaths, but fundamentally the questions of how permeable rocks mediate hydrology to shape hydrographs and landscapes are still unanswered. Although the disciplines of hydrogeology, watershed hydrology, and geomorphology have each tackled some aspects of these questions, an improved understanding of the interactions among permeability, hydrology, and geomorphology is necessary to address some of the most pressing scientific challenges of the 21st century.

The linkages between permeability and hydrologic processes are well understood in karst landscapes [e.g., *White*, 2002; *Harmon and Wicks*, 2006], but such integrated knowledge is missing for many other geologic settings. Young basaltic landscapes make excellent laboratories for studying permeability and hydrologic processes, due to basalt's high initial permeability, distribution across the world's climate zones, and availability of absolute dates. In particular, the Oregon Cascades are an ideal location for studies of geologic-hydrologic interactions because of long histories of basaltic volcanism, high precipitation rates, decades of geologic research, and importance for regional water resources.

Hydrogeology is the study of groundwater flow through a geologic porous medium, and characterizing permeability is a central question to hydrogeologic investigations at spatial scales from a single fracture to a regional aquifer [*Freeze and Cherry*, 1979]. While some studies examine the effects of geology on aquifer characteristics and groundwater flow patterns, most research focuses on the current functioning of

groundwater systems [*Koltermann and Gorelick*, 1996]. Groundwater systems have been studied at active volcanoes because of interest in interactions between magmatic and hydrologic processes and because basaltic aquifers may be the principal water resources of volcanic islands [*Ingebritsen and Scholl*, 1993; *Scholl et al.*, 1996; *Descloitres et al.*, 1997; *Saar and Manga*, 1999; *Hurwitz et al.*, 2003a; *Hurwitz et al.*, 2003b; *Izuka and Gingerich*, 2003; *Mariner et al.*, 2003; *Nathenson and Thompson*, 2003; *Saar and Manga*, 2003; *Evans et al.*, 2004; *Revil et al.*, 2004; *Christiansen et al.*, 2005; *Join et al.*, 2005]. The hydrogeology of regions underlain by extensive flood basalts have also been investigated because of their importance as water resources [e.g., *Lindholm and Vaccaro*, 1988; *Kulkarni et al.*, 2000]. Also, basaltic aquifers have been studied to elucidate the mechanics of groundwater flow through fractures [e.g., *Leonardi et al.*, 1996; *Faybishenko et al.*, 2000]. Among the open questions relating to permeability in basaltic rocks and its influence on groundwater flow are how flowpaths relate to surface topography in regions with complex volcanic histories.

In the field of watershed hydrology, geologic setting and permeability have generally been assigned secondary importance relative to climatic factors. However, some studies have shown the importance of watershed geology in controlling the relative magnitudes of various hydrologic processes and the routing of water within a catchment. Hydrograph characteristics in basaltic landscapes are tied to the presence of groundwater systems [*Manga*, 1997; 1999; *Whiting and Moog*, 2001; *Tague and Grant*, 2004]. In Japanese catchments underlain by granite, differences in drainage density, landslide frequency, runoff generation, peak flows, and stream temperature were observed when compared to those underlain by more permeable sedimentary rocks [*Onda*, 1993; 1994]. At the hillslope scale, work in Georgia has shown that water routing and peak flow generation are controlled by bedrock topography rather than surface topography, as a result of contrasting permeabilities of the bedrock and soils [*McDonnell et al.*, 1996; *Freer et al.*, 2002]. Till thickness and the depth to underlying impermeable rock have been shown to strongly influence hydrologic regime in swamps of the Canadian Shield [*Devito et al.*, 1996]. Recent studies have

also revealed that bedrock storage of water can be significant even in relatively impermeable areas dominated by shallow subsurface flow [*Montgomery and Dietrich*, 2002; *McGuire et al.*, 2005; *Tromp-van Meerveld et al.*, 2006]. While the above studies make headway into understanding how permeability affects runoff generation, an integrated assessment of how permeability modulates watershed response climatically-imposed variability needs to be undertaken.

The question of how a landscape arrived at its present form is central to the field of geomorphology, and geomorphologists have historically used a region's geologic history and setting to underpin their interpretations of processes and features. *Thornbury* [1954] lists as the second fundamental concept of geomorphology that "[g]eologic structure is a dominant control factor in the evolution of landforms and is reflected in them." In this context, "structure" encompasses not only those aspects typically included in structural geology (e.g., folding, faulting), but also rock hardness, stratigraphy, and permeability. This concept arises from the formative work of W.M. *Davis* [1902] who argued that structure, process, and time are the major controls on landscape evolution. Classic geomorphology treatises illustrate different patterns of geologically-controlled drainage network forms, including radial, trellised, and rectangular [e.g., *Thornbury*, 1954]. Current foremost models of landscape evolution draw heavily on stream-power driven erosion [*Whipple and Tucker*, 1999; *Willett*, 1999], but often neglect to include geomorphic effects of groundwater flow that may be important in permeable landscapes. Drainage patterns, as well as the overall geomorphology of a landscape, may be strongly influenced by permeability, but the processes and rates of geomorphic evolution in permeable landscapes are poorly understood, as is the evolution of permeability over geologic time.

Answers to these open questions on the influence of permeability from the disciplines of hydrogeology, watershed hydrology, and geomorphology are also important for addressing broader research issues of current interest. These issues include climate change, prediction in ungauged basins, and the history of water on Mars.

There is growing recognition among the scientific community, policy makers and the general public that human activities are altering present and future climate, and that climate change will have significant impacts on humans and ecosystems [*IPCC*, 2001]. One area of concern is the effect of climate change on water resources, particularly in snow-dominated regions susceptible to warming-induced rain or melt [*Barnett et al.*, 2005]. In order to prepare effective mitigation strategies, it is important to understand the current functioning of hydrologic systems and their response to climatic variability. Permeable watersheds may respond differently to climate change than impermeable watersheds, because of the additional storage provided by groundwater systems.

In 2003, the International Association of Hydrological Sciences launched the decade on prediction in ungauged basins (PUB), recognizing the need for the hydrological sciences to address the large number of ungauged or poorly gauged basins throughout the world [*Sivapalan et al.*, 2003]. The initiative seeks to develop new process models and reduce uncertainties in prediction. Incorporating an improved understanding of permeability controls on hydrological processes may be a necessary step toward advancing predictive hydrology in many landscapes.

The quest to understand the history of Mars and the search for water on the Martian landscape is a massive multi-national, interdisciplinary scientific mission with implications for that planet and this one. New observations by the Mars rovers are adding to the evidence that Mars once had abundant groundwater and at least occasional surface water [*Squyres et al.*, 2006]. The planet, which is largely covered by basalt, has extensive valley networks of debated origin [*Bandfield et al.*, 2000; *Aharonson et al.*, 2002; *Hynek and Phillips*, 2003]. A better understanding of hydrologic processes on permeable basaltic landscapes on this planet would provide insight into the hydrologic and geomorphic history of Mars.

This work focuses on two units of analysis: watershed and landscape. A watershed is the topographically-defined area upslope of a point, and a landscape is defined in this document as a geographically contiguous region of broadly similar topography, geology, and climate. In geomorphology, both the watershed and landscape are common units of analysis, but in hydrology, the concept of a landscape is less commonly used. With the growing emphasis on prediction in ungauged watersheds, hydrologists are recognizing the utility of landscape scale analyses and are beginning to define hydrologic-landscape regions and other similar units [*Wolock et al.*, 2004].

1.2 Setting

This research is set in the particular context of the west slope of the central Oregon Cascades, focusing on the McKenzie River watershed (Figure 1.1). The Willamette River basin, of which the McKenzie River is a tributary, is home to over 70% of Oregon's population, and rivers originating in the Cascades supply drinking water to over three million Oregon residents. An improved understanding of the hydrogeology of the Cascades will benefit water resources managers in Oregon. Here I provide a general overview of the geology, climate, and hydrology of the study area, with more detailed descriptions given in the relevant subsequent chapters.

The Cascades volcanic arc is formed by the subduction of the Juan de Fuca plate under the North American plate. The Oregon Cascades are divided into two geologic provinces: High Cascades and Western Cascades. The High Cascades are the active portion of the arc and lie within an inferred graben structure. Volcanism associated with rift propagation and up to 3 km of subsidence began about 5 million years ago (Ma) and has produced largely basaltic and basaltic andesite lavas [*Conrey et al.*, 2002]. These lavas originated from numerous shield volcanoes and cinder cones and form a low-sloping platform that is interspersed with long-lived composite volcanoes that produce more compositionally diverse volcanic products. The Western Cascades are 10- to 40-million years old and composed of dacitic tuffs, andesitic lava flows, and

minor basaltic and rhyolitic volcanic rocks [*Conrey et al.*, 2002]. The Western Cascades have been extensively folded, faulted, and dissected, while the High Cascades are relatively undissected. The crest of the Cascade Range lies between 1500 and 2000 m, with High Cascade peak elevations reaching 3000 m, and Western Cascade peak elevations ~1800 m.

The Oregon Cascades experience a Mediterranean climate with strong orographic effects on temperature and precipitation. Examination of Oregon Climate Service data for 1971-2000 for two stations with contrasting elevations reveals these orographic effects on temperature. McKenzie Bridge, at an elevation of 451 m, has average January and July temperatures of 2.7°C and 20.1°C, respectively. In contrast, Santiam Junction, at 1167 m above sea level, has average January and July temperatures of -1.4°C and 15.4°C, respectively. Precipitation on the west slope of the Cascades ranges from 2 to 3.8 m [*Taylor and Hannan*, 1999]. Over 70% of annual precipitation falls between November and March, and little precipitation occurs between about June 15th and October 1st. During the winter, seasonal snowpacks form above 1200 m, a mixture of rain and snow falls between 400 and 1200 m, and rain dominates below 400 m.

Most of the major drainages on the west slope of the Cascades cut across both the High and Western Cascade geologic provinces, and their hydrology is influenced by the climate, geology, and topography of each region [*Grant*, 1997]. Based on a survey of United States Geological Survey (USGS) gauge records, High Cascades streams provide an estimated 55% of August streamflow to the Willamette River at Portland. Under natural conditions, without flow supplementation from flood control reservoirs in the Western Cascades, the portion of Willamette summer flow from the High Cascades would be even higher. In the winter, rapid runoff from the Western Cascades diminishes the importance of High Cascades water for sustaining discharge. On the east side of the Cascades, groundwater-fed streams contribute the majority of summer streamflow to the Deschutes basin [*Gannett et al.*, 2003].

The McKenzie River watershed has the highest proportion of High Cascades geology of any Willamette River tributary [*Tague and Grant*, 2004]. The McKenzie watershed also provides habitat for threatened and endangered fish species, superb recreational areas, electricity and flood control from federal and municipal dams, and drinking water for Oregon's second largest city. With an area of 3465 km^2, the watershed comprises less than 12% of the Willamette basin's area, but it provides almost 25% of the Willamette River's water during low flow periods [*PNWERC*, 2002]. Measurements I made and compiled on August 5-7, 2003 reveal that over 80% of the discharge in the McKenzie River at Vida was from High Cascade spring-fed streams, with an additional 11% released from storage of two flood control reservoirs (Figure 1.2).

1.3 Hydrogeologic investigations in the McKenzie River watershed and surrounding areas of the High Cascades

The first hydrogeologic report on the High Cascades of the McKenzie River watershed was by *Stearns* [1929], who took part in a pack train trip up the McKenzie River to Clear Lake during the summer of 1926. Stearns described the climate, geology, physiography, water falls, and springs of the upper McKenzie River valley. Using sparse gauging records and discharge data, Stearns estimated:

> "the flow from springs in the upper McKenzie Valley is about 925 second-feet [cubic feet per second], or about 670,000 acre-feet per year. Of this amount about 520 second-feet rises in four spring groups. All of these springs issue from basalt, and three of them discharge about 150 second-feet each. The size of the springs is evidence of the remarkable permeability of the basaltic flows of this region."

By the end of the 1920s, the basic hydrogeologic framework of the High Cascades and major sources of summer streamflow to the McKenzie River had been identified. Stearns later had a long career studying volcanoes and hydrology in Hawaii with the USGS [*Stearns*, 1942; 1985].

At the same time, water power resources of the McKenzie basin were being explored to supply electricity to the growing population in the Willamette Valley [*Jones and Stearns*, 1931]. Leaburg Dam was built on the lower McKenzie River in 1930, and the 1960s saw a flurry of dam construction by the U.S. Army Corps of Engineers for flood control and the Eugene Water and Electric Board (EWEB) for hydroelectricity generation. In 1963, EWEB completed the Carmen-Smith Hydroelectric Project with a series of dams and diversion tunnels on the upper McKenzie and Smith Rivers [*EWEB*, 2003]. As part of that construction project, short-term measurements of groundwater inflow to one tunnel and discharge of Bunchgrass Creek were collected [*Sanderson*, 1963]. A series of USGS gauges were established on the mainstem and tributaries of the McKenzie River beginning in 1910 (Figure 1.3).

In 1946, Ruth Hopson completed a Ph.D. dissertation on the natural history of the McKenzie River valley [*Hopson*, 1946]. Although her work largely focused on the life forms of the McKenzie River watershed, she recognized that geology and hydrology set the template for the plants, animals, and humans of the region:

> "Boulders clashing in rushing mountain torrents, fair-sized streams gushing forth as springs in the sides of mountains, creeks tumbling over precipices, white waters of glacial streams playing their daily crescendoes, and ringing clatter of the rock avalanches dashing down the steep mountain sides all produce sounds…sounds that reverberate from cliff to cliff and announce a region that is still vigorous in the stage of early youth [*Hopson*, 1946, p. 324-325]."

In 1948, the 64 km^2 H.J. Andrews Experimental Forest was established in the Lookout Creek watershed, within the McKenzie River basin. Now a National Science Foundation Long-Term Ecological Research site, the Andrews Forest has been the location of ground-breaking and long-term monitoring studies that have well characterized the forests and streams of the Western Cascade region. An extensive database of publications resulting from work at the Andrews Forest is available at http://www.fsl.orst.edu/lter/.

During the 1980s, geothermal resource exploration of the Cascades included the drilling of deep boreholes near Santiam Pass and the publication of several competing heat source models [*Ingebritsen et al.*, 1989; *Blackwell et al.*, 1990]. To date there has been no exploitation of the geothermal resources of the Oregon Cascades for heating or power production. Slightly later, the research focus shifted to hydrothermal systems, including hot springs [*Ingebritsen et al.*, 1994; *Ingebritsen et al.*, 2001]. Cascade hot springs are extensively used for recreation by visitors to Forest Service sites or private resorts. One feature noted in the geothermal and hydrothermal work was the isothermal zone extending from the surface to ~300 m, which was thought to be associated with high fluxes of groundwater [*Ingebritsen et al.*, 1989].

The documenting of excess chloride concentrations in the spring-fed streams of the Separation Creek watershed in 1999 combined with interferometric synthetic aperture radar data indicating uplift in an area west of the Three Sisters, sparked several years of intense investigation into spring geochemistry and its use as an indicator of ongoing magmatic intrusions and long-term intrusion rates [*Iverson*, 1999; *Wicks et al.*, 2002; *Evans et al.*, 2004].

Since the 1990s there has been a spate of hydrogeologic research in the Deschutes River basin, which lies to the east of the McKenzie River watershed. Michael Manga and his students have used time series analyses, mathematical models, and isotopic measurements to gain insight into High Cascades aquifers on the east side of the Cascade crest [*Manga*, 1996; 1997; 1998; *James et al.*, 1999; *Manga*, 1999; *James et al.*, 2000; *Manga and Kirchner*, 2004; *Saar and Manga*, 2004]. Peter Whiting and colleagues examined hydrology and channel morphology of spring-fed streams in the upper Deschutes basin [*Whiting and Stamm*, 1995; *Whiting and Moog*, 2001]. In addition, the USGS developed a regional groundwater model [*Gannett and Lite*, 2004], and a monograph on Deschutes River hydrology and geomorphology was published [*O'Connor and Grant*, 2003].

At the same time that the intensive work on the Deschutes basin was underway, Gordon Grant and colleagues began examining differences in hydrological regimes between the High and Western Cascades [*Grant*, 1997; *Tague and Grant*, 2004]. It is from the work of Tague and Grant [2004] that this research germinated, although this work has been influenced by the research on Deschutes hydrogeology and earlier work.

1.4 Structure of the dissertation

The objective of this research is to understand how landscape permeability controls groundwater flowpaths, discharge dynamics, and geomorphic evolution. The basaltic landscape of the Oregon High Cascades forms a natural laboratory to address these topics. This research asks specific questions about the High Cascades drainage system: where does the water come from; how do streams respond to climatic variability; and how does the High Cascade landscape evolve. This research also informs the understanding of processes and features of young basaltic landscapes throughout the world.

The three main parts of this research are linked by a common theme and setting. Each part explores how geologic history in basaltic landscapes influences hydrologic processes at a distinct time scale, making use of the High Cascades portion of the McKenzie River watershed as a field area (Figure 1.4). This common field setting allows the exploration of multiple, interlinked lines of research facilitating the development of a comprehensive understanding of the hydrology and geomorphic evolution of the McKenzie River watershed.

Chapter 2 address the open question of how groundwater flowpaths relate to surface topography in regions with complex volcanic histories, using a combination of discharge, temperature, and isotopic data collected from springs and information derived from topographic and geologic maps. These data allow aquifer sizes and locations, recharge elevations, transit times, and hydraulic conductivities to be

constrained. This aspect of the research considers the modern, steady-state, functioning of the groundwater systems, and takes a spatial approach to the analysis. This chapter is in press in Water Resources Research, and subsequent chapters reference it as *Jefferson et al.* [2006].

Chapter 3 investigates how the additional water storage afforded by groundwater systems in permeable rocks impacts streamflow responses to climate variability, using historical datasets of discharge, snow water equivalent, precipitation and temperature from two watersheds with contrasting rock ages. A variety of statistical time-series methods are applied to probe the datasets for differences in event, seasonal, inter-annual, and multi-decadal responses. These methods extend understanding of how groundwater influences the seasonal water budget and sensitivity to long-term changes in climate. This chapter is in preparation for submission to a journal targeting hydrologists and environmental scientists.

Chapter 4 examines the rates and processes of landscape evolution in permeable terrains, using extensive field reconnaissance, rock dating, and drainage density and relationships between local slopes and contributing areas. The observations and data allow the definition of three major stages in drainage development of the High Cascades. The analysis of the rates of landscape evolution is combined with a discussion of the processes responsible for reducing the permeability of basaltic landscapes over timescales of ~2 Ma. This chapter is in preparation for submission to a journal targeting geomorphologists and geologists.

Finally, in Chapter 5, directions for future research and management implications are presented. This chapter synthesizes the results of the previous chapters to provide a more holistic view of hydrology and geomorphic evolution of the High Cascades.

1.5 References cited

Aharonson, O., M. T. Zuber, D. H. Rothman, N. Schorghofer, and K. X. Whipple (2002), Drainage basins and channel incision on Mars, *PNAS*, *99*, 1780-1783.

Bandfield, J. L., V. E. Hamilton, and P. R. Christensen (2000), A global view of Martian surface compositions from MGS-TES, *Science*, *287*, 1626-1630.

Barnett, T. P., J. C. Adam, and D. P. Lettenmaier (2005), Potential impacts of warming climate on water availability in snow-dominated regions, *Nature*, *438*, 303-308.

Blackwell, D. D., J. L. Steele, M. K. Frohme, C. F. Murphey, G. R. Priest, and G. L. Black (1990), Heat flow in the Oregon Cascade Range and its correlation with regional gravity, Curie point depths, and geology, *Journal of Geophysical Research*, *95*, 19475-19493.

Christiansen, L. B., S. Hurwitz, M. O. Saar, S. E. Ingebritsen, and P. A. Hsieh (2005), Seasonal seismicity at western United States volcanic centers, *Earth and Planetary Science Letters*, *240*, 307-321.

Conrey, R. M., E. M. Taylor, J. M. Donnely-Nolan, and D. R. Sherrod (2002), North-central Oregon Cascades: exploring petrologic and tectonic intimacy in a propagating intra-arc rift, in *Field Guide to Geologic Processes in Cascadia*, edited by G. W. Moore, Special Paper 36, pp. 47-90, Oregon Department of Geology and Mineral Industries, Salem.

Davis, W. M. (1902), *Geographical Essays*, 777 pp., Ginn Publishing, Boston. Reprinted 1954, Dover, New York.

Descloitres, M., M. Ritz, B. Robineau, and M. Courteaud (1997), Electrical structure beneath the eastern collapsed flank of Piton de la Fournaise volcano, Reunion Island: Implications for the quest for groundwater, *Water Resources Research*, *33*, 13-19.

Devito, K. J., A. R. Hill, and N. Roulet (1996), Groundwater-surface water interactions in headwater forested wetlands of the Canadian shield, *Journal of Hydrology*, *181*, 127-147.

Evans, W. C., M. C. van Soest, R. H. Mariner, S. Hurwitz, S. E. Ingebritsen, C. W. J. Wicks, and M. E. Schmidt (2004), Magmatic intrusion west of Three Sisters, central Oregon, USA: the perspective from spring geochemistry, *Geology*, *32*, 69-72.

EWEB (2003), Initial consultation document for the Carmen-Smith Hydroelectric Project (FERC No. 2242), Final Report, Prepared by Stillwater Sciences, Arcata, Calif. for Eugene Water and Electric Board, Eugene, Ore.

Faybishenko, B., C. Doughty, M. Steiger, J. C. S. Long, T. R. Wood, J. S. Jacobsen, J. Lore, and P. T. Zawislanski (2000), Conceptual model of the geometry and physics of water flow in a fractured basalt vadose zone, *Water Resources Research*, *36*, 3499-3520.

Freer, J., J. J. McDonnell, K. J. Beven, N. E. Peters, D. A. Burns, R. P. Hooper, B. Aulenbach, and C. Kendall (2002), The role of bedrock topography on subsurface storm flow, *Water Resources Research*, *38*, 1269.

Freeze, R. A., and J. A. Cherry (1979), *Groundwater*, 604 pp., Prentice Hall, Englewood Cliffs, NJ.

Gannett, M. W., and K. E. J. Lite (2004), Simulation of regional groundwater flow in the upper Deschutes Basin, Oregon, *Water-Resour. Invest. Report 03-4195*, 84 pp, U.S. Geol. Surv., Washington.

Gannett, M. W., M. Manga, and K. E. J. Lite (2003), Groundwater hydrology of the Upper Deschutes Basin and its influence on streamflow, in *A Peculiar River: Geology, Geomorphology, and Hydrology of the Deschutes river*, edited by J. E. O'Connor and G. E. Grant, 7, pp. 31-49, American Geophysical Union, Washington.

Grant, G. E. (1997), A geomorphic basis for the hydrologic behavior of large river systems., in *River Quality: Dynamics and Restoration*, edited by A. Laenen and D. A. Dunnette, pp. 105-116, Lewis Publishers, Boca Raton.

Harmon, R. S., and C. M. Wicks (Eds.) (2006), *Perspectives on Karst Geomorphology, Hydrology, and Geochemistry: A Tribute Volume to Derek C. Ford and William B. White*, 366 pp., Geological Society of America, Boulder, Colo.

Hopson, R. E. (1946), The Study of a Valley -- The McKenzie River Region of Oregon, with Special Reference to the Educational Significance of its Natural History, PhD thesis, Cornell U., Ithaca, NY.

Hurwitz, S., F. Goff, C. J. Janik, W. C. Evans, D. A. Counce, M. L. Sorey, and S. E. Ingebritsen (2003a), Mixing of magmatic volatiles with groundwater and interaction with basalt on the summit of Kilauea Volcano, Hawaii, *Journal of Geophysical Research*, *108*, 2028, doi:2010.1029/2001JB001594.

Hurwitz, S., K. L. Kipp, S. E. Ingebritsen, and M. E. Reid (2003b), Groundwater flow, heat transport, and water table position within volcanic edifices: Implications for volcanic processes in the Cascade Range, *Journal of Geophysical Research-Solid Earth*, *108*.

Hynek, B. M., and R. J. Phillips (2003), New data reveal mature, integrated drainage systems on Mars indicative of past precipitation, *Geology*, *31*, 757-760.

Ingebritsen, S. E., D. L. Galloway, E. M. Colvard, M. L. Sorey, and R. H. Mariner (2001), Time-variation of hydrothermal discharge at selected sites in the western United States: implications for monitoring, *Journal of Volcanology and Geothermal Research*, *111*, 1-23.

Ingebritsen, S. E., R. H. Mariner, and D. R. Sherrod (1994), Hydrothermal systems of the Cascade Range, north-central Oregon, *Prof. Pap. 1044-L.*, 86 pp. pp, U.S. Geol. Surv., Washington, D.C.

Ingebritsen, S. E., and M. A. Scholl (1993), The hydrogeology of Kilauea volcano, *Geothermics*, *22*, 255-270.

Ingebritsen, S. E., D. R. Sherrod, and R. H. Mariner (1989), Heat flow and hydrothermal circulation in the Cascade Range, north-central Oregon, *Science*, *243*, 1458-1462.

IPCC (2001), Climate Change 2001: The Scientific Basis. Contribution of Working Group I to the Third Assessment Report of the Intergovernmental Panel on

Climate Change, edited by J. T. Houghton, et al., Cambridge University Press., Cambridge.

Iverson, J. T. (1999), An Investigation of the Chloride Anomaly in Separation Creek, Lane County, Oregon, Honors Bachelor of Science in Geology thesis, 52 pp, Oregon State University, Corvallis.

Izuka, S. K., and S. B. Gingerich (2003), A thick lens of fresh groundwater in the southern Lihue Basin, Kauai, Hawaii, USA, *Hydrogeology Journal*, *11*, 240-248.

James, E. R., M. Manga, and T. P. Rose (1999), CO2 degassing in the Oregon Cascades, *Geology*, *27*, 823-826.

James, E. R., M. Manga, T. P. Rose, and G. B. Hudson (2000), The use of temperature and isotopes of O,H,C and noble gases to determine the pattern and spatial extent of groundwater flow, *Journal of Hydrology*, *237*, 100-112.

Jefferson, A., G. E. Grant, and T. P. Rose (2006), The influence of volcanic history on groundwater patterns on the west slope of the Oregon High Cascades, *Water Resources Research*, *in press*, 2005WR004812.

Join, J.-L., J.-L. Folio, and B. Robineau (2005), Aquifers and groundwater within active shield volcanoes. Evolution of conceptual models in the Piton de la Fournaise volcano, *Journal of Volcanology and Geothermal Research*, *147*, 187-201.

Jones, B. E., and H. T. Stearns (1931), Water-Power Resources of the McKenzie River and its Tributaries, Oregon, *Water-Supply Pap. 637-C*, U.S. Geol. Surv., Washington, D.C.

Koltermann, C. E., and S. M. Gorelick (1996), Heterogeneity in sedimentary deposits: A review of structure-imitating, process-imitating, and descriptive approaches, *Water Resources Research*, *32*, 2617-2658.

Kulkarni, H., S. B. Deolankar, A. Lalwani, B. Joseph, and S. Pawar (2000), Hydrogeologic framework of the Deccan basalt groundwater systems, west-central India, *Hydrogeology Journal*, *8*, 368-378.

Leonardi, V., F. Arthaud, J. C. Grillot, V. Avetissian, and P. Bochnaghian (1996), Modelling of a fractured basaltic aquifer with respect to geologic setting, and climatic and hydraulic conditions: the case of perched basalts at Garni (Armenia), *Journal of Hydrology*, *179*, 87-109.

Lindholm, G. F., and J. J. Vaccaro (1988), Region 2, Columbia Lava Plateau, in *Hydrogeology*, edited by W. Back, et al., pp. 37-50, Geological Society of America, Boulder, Colo.

Manga, M. (1996), Hydrology of spring-dominated streams in the Oregon Cascades., *Water Resources Research*, *32*, 2435-2440.

Manga, M. (1997), A model for discharge in spring-dominated streams and implications for the transmissivity and recharge of quaternary volcanics in the Oregon Cascades, *Water Resources Research*, *33*, 1813-1822.

Manga, M. (1998), Advective heat transport by low-temperature discharge in the Oregon Cascades, *Geology*, *26*, 799-802.

Manga, M. (1999), On the timescales characterizing groundwater discharge at springs, *Journal of Hydrology*, *219*, 56-69.

Manga, M., and J. W. Kirchner (2004), Interpreting the temperature of water at cold springs and the importance of gravitational potential energy, *Water Resources Research*, *40*, W05110, doi:05110.01029/02003WR002905.

Mariner, R. H., W. C. Evans, T. S. Presser, and L. D. White (2003), Excess nitrogen in selected thermal and mineral springs of the Cascade Range in northern California, Oregon, and Washington: sedimentary or volcanic in origin?, *Journal of Volcanology and Geothermal Research*, *121*, 99-114.

McDonnell, J. J., J. Freer, R. Hooper, C. Kendall, D. Burns, and J. Peters (1996), New method developed for studying flow on hillslopes, *Eos*, *77*, 465-472.

McGuire, K. J., J. J. McDonnell, M. Weiler, C. Kendall, B. L. McGlynn, J. M. Welker, and J. Seibert (2005), The role of topography on catchment-scale water residence time, *Water Resources Research*, *41*, W05002, doi:05010.01029/02004WR003657.

Montgomery, D. R., and W. E. Dietrich (2002), Runoff generation in a steep, soil-mantled landscape, *Water Resources Research*, *38*, 1168, doi:1110.1029/2001WR000822.

Nathenson, M., and J. M. Thompson (2003), Slightly thermal springs and non-thermal springs at Mount Shasta, California: Chemistry and recharge elevations, *Journal of Volcanology and Geothermal Research*, *121*, 137-153.

O'Connor, J. E., and G. E. Grant (Eds.) (2003), *A Peculiar River: Geology, Geomorphology, and Hydrology of the Deschutes River, Oregon*, 219 pp., American Geophysical Union, Washington, D.C.

Onda, Y. (1993), Underlying rock type controls of hydrological processes and shallow landslide occurrence, in *Sediment Problems: Strategies for Monitoring, Prediction and Control*, edited by R. F. Hadley and T. Mizuyama, pp. 47-55, International Association of Hydrological Sciences, Wallingford, Oxfordshire.

Onda, Y. (1994), Contrasting hydrological characteristics, slope proceses and topography underlain by paleozoic sedimentary rocks and granite, *Transactions, Japanese Geomorphological Union*, *15A*, 49-65.

PNWERC (2002), *Willamette River Basin Planning Atlas: Trajectories of environmental and ecological change*, 178 pp., Oregon State University Press, Corvallis, OR.

Revil, A., A. Finizola, F. Sortina, and M. Ripepe (2004), Geophysical investigations at Stromboli volcano, Italy: implications for ground water flow and paroxysal activity, *Geophysical Journal International*, *157*, 426-440.

Saar, M. O., and M. Manga (1999), Permeability-porosity relationship in vesicular basalts, *Geophysical Research Letters*, *26*, 111-114.

Saar, M. O., and M. Manga (2003), Seismicity induced by seasonal groundwater recharge at Mt. Hood, Oregon, *Earth and Planetary Science Letters*, *214*, 605-618.

Saar, M. O., and M. Manga (2004), Depth dependence of permeability in the Oregon Cascades inferred from hydrogeologic, thermal, seismic, and magmatic modeling constraints, *Journal of Geophysical Research*, *109*, B04204, 04210.01029/02003JB002855.

Sanderson, R. B. (1963), Ground-water inflow into the Carmen-Smith diversion tunnel McKenzie River Basin, Oregon, 4 pp, U.S. Geological Survey, Washington.

Scholl, M. A., S. E. Ingebritsen, C. J. Janik, and J. P. Kauahikaua (1996), Use of precipitation and groundwater isotopes to interpret regional hydrology on a tropical volcanic island: Kilauea volcano area, Hawaii, *Water Resources Research*, *32*, 3525-3537.

Sivapalan, M., K. Takeuchi, S. W. Franks, V. K. Gupta, H. Karambiri, V. Lakshmi, X. Liang, J. J. McDonnell, E. M. Mendiondo, P. E. O'Connell, T. Oki, J. W. Pomeroy, D. Schertzer, S. Uhlenbrook, and E. Zehe (2003), IAHS decade on predictions in ungauged basis (PUB), 2003-2012: shaping an exciting future for the hydrological sciences, *Hydrological Sciences Journal*, *48*, 857-880.

Squyres, S. W., A. H. Knoll, R. E. Arvidson, B. C. Clark, J. P. Grotzinger, B. L. Joliff, S. M. McLennan, N. Tosca, J. F. Bell, III, W. M. Calvin, W. H. Farrand, T. D. Glotch, M. P. Golombek, K. E. Herkenhoff, J. R. Johnson, G. Klingelhofer, H. Y. McSween, and A. S. Yen (2006), Two years at Meridian Planum: results from the Opportunity rover, *Science*, *313*, 1403-1407.

Stearns, H. T. (1929), Geology and Water Resources of the Upper McKenzie Valley, Oregon, *Water Supply Paper 597-D*, U.S. Geol. Surv., Washington, D.C.

Stearns, H. T. (1942), Hydrology of volcanic terranes, in *Hydrology*, edited by O. E. Meinzer, pp. 678-703, McGraw-Hill, New York.

Stearns, H. T. (1985), *Geology of the State of Hawaii*, 2nd ed., 335 pp., Pacific Books, Palo Alto, Calif.

Tague, C., and G. E. Grant (2004), A geological framework for interpreting the low flow regimes of Cascade streams, Willamette River Basin, Oregon, *Water Resources Research*, *40*, W04303 04310.01029/02003WR002629.

Taylor, G. H., and C. Hannan (1999), *The Climate of Oregon: From Rain Forest to Desert*, 211 pp., Oregon State University Press, Corvallis.

Thornbury, W. D. (1954), *Principles of Geomorphology*, 618 pp., John Wiley, New York.

Tromp-van Meerveld, I., N. E. Peters, and J. J. McDonnell (2006), Effect of bedrock permeability on subsurface stormflow and the water balance of a trenched hillslope at the Panola Mountain Research Watershed, Georgia, *Hydrological Processes*, *in press*.

Whipple, K. X., and G. E. Tucker (1999), Dynamics of the stream-power river incision model: Implications for height limits of mountain ranges, landscape response timescales, and research needs, *Journal of Geophysical Research*, *104*, 17661-17674.

White, W. B. (2002), Karst hydrology: recent developments and open questions, *Engineering Geology*, *65*, 85-105.

Whiting, P. J., and D. B. Moog (2001), The geometric, sedimentologic, and hydrologic attributes of spring-dominated channels in volcanic areas, *Geomorphology*, *39*, 131-149.

Whiting, P. J., and J. Stamm (1995), The hydrology and form of spring-dominated channels, *Geomorphology*, *12*, 223-240.

Wicks, C. W. J., D. Dzurisin, S. E. Ingebritsen, W. Thatcher, Z. Lu, and J. T. Iverson (2002), Magmatic activity beneath the quiescent Three Sisters volcanic center, central Oregon Cascade Range, USA, *Geophysical Research Letters*, *29*, 1122, 1110.1029/2001GL014205.

Willett, S. D. (1999), Orogeny and orography: The effects of erosion on the structure of mountain belts, *Journal of Geophysical Research*, *104*, 28957-28981.

Wolock, D. M., T. C. Winter, and G. McMahon (2004), Delineation and evaluation of hydrologic-landscape regions in the United States using geographic information system tools and multivariate statistical analyses, *Environmental Management*, *34*, S71-S88.
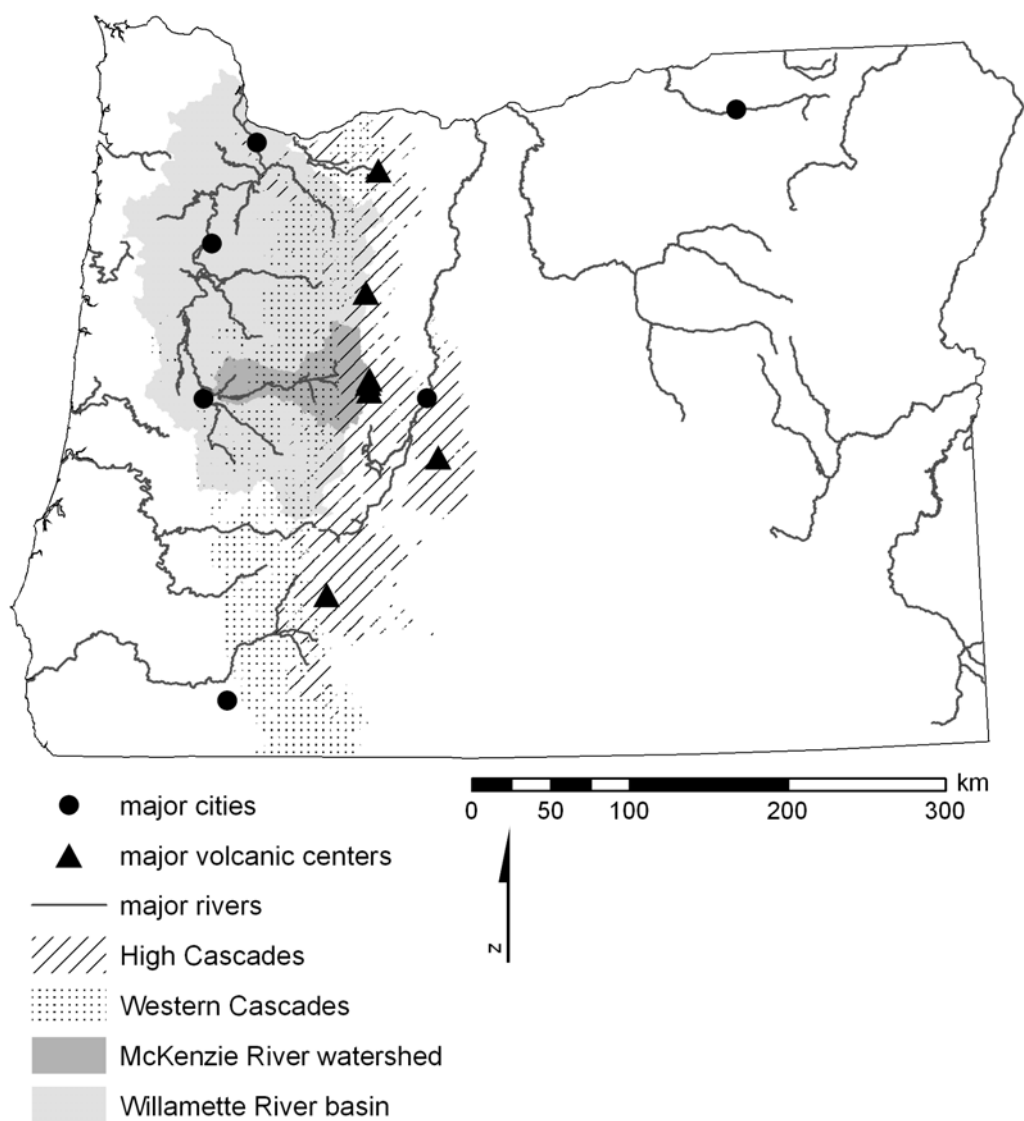
Figure 1.1. Map of Oregon showing Cascades geology and major rivers and cities. The High Cascades and Western Cascades are delineated based on the Quaternary-Tertiary boundary following the mapping of *Sherrod and Smith* [2000].
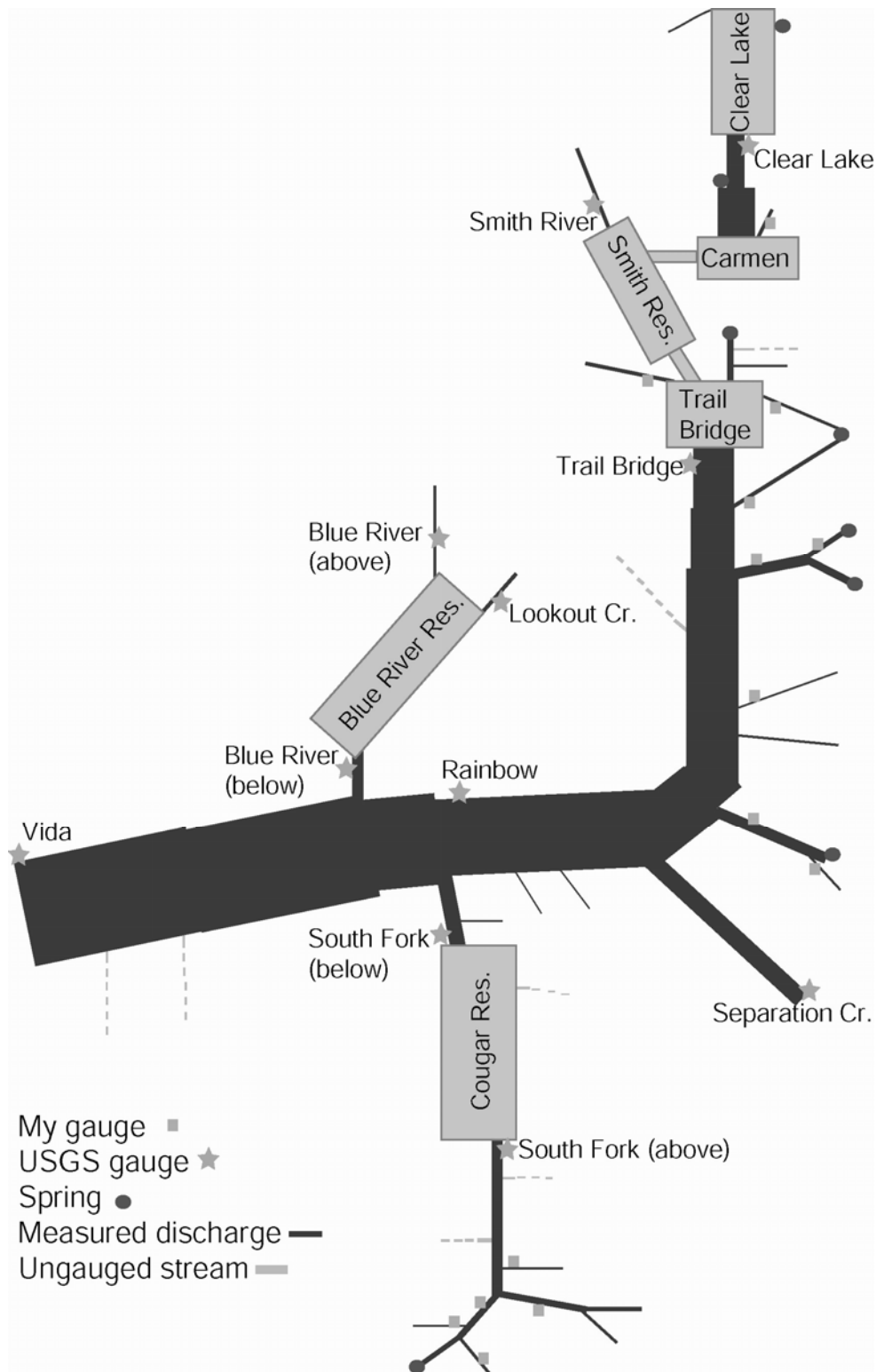
Figure 1.2. Diagram of the upper McKenzie River watershed illustrating relative magnitudes of discharge on August 5-7, 2003.
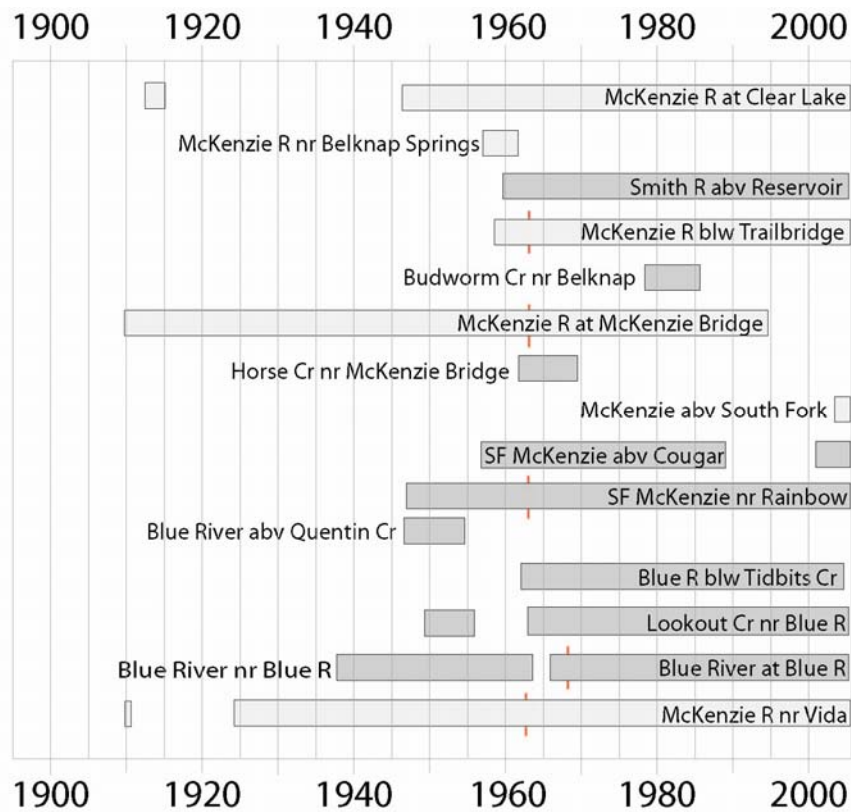
Figure 1.3. Timeline of USGS gauges in the upper McKenzie River watershed. Gauge records are arranged in a downstream fashion, mainstem gauges are indicated by light gray boxes, tributary gauge records are represented by dark gray boxes, and short vertical lines indicate the earliest influence of upstream dams.
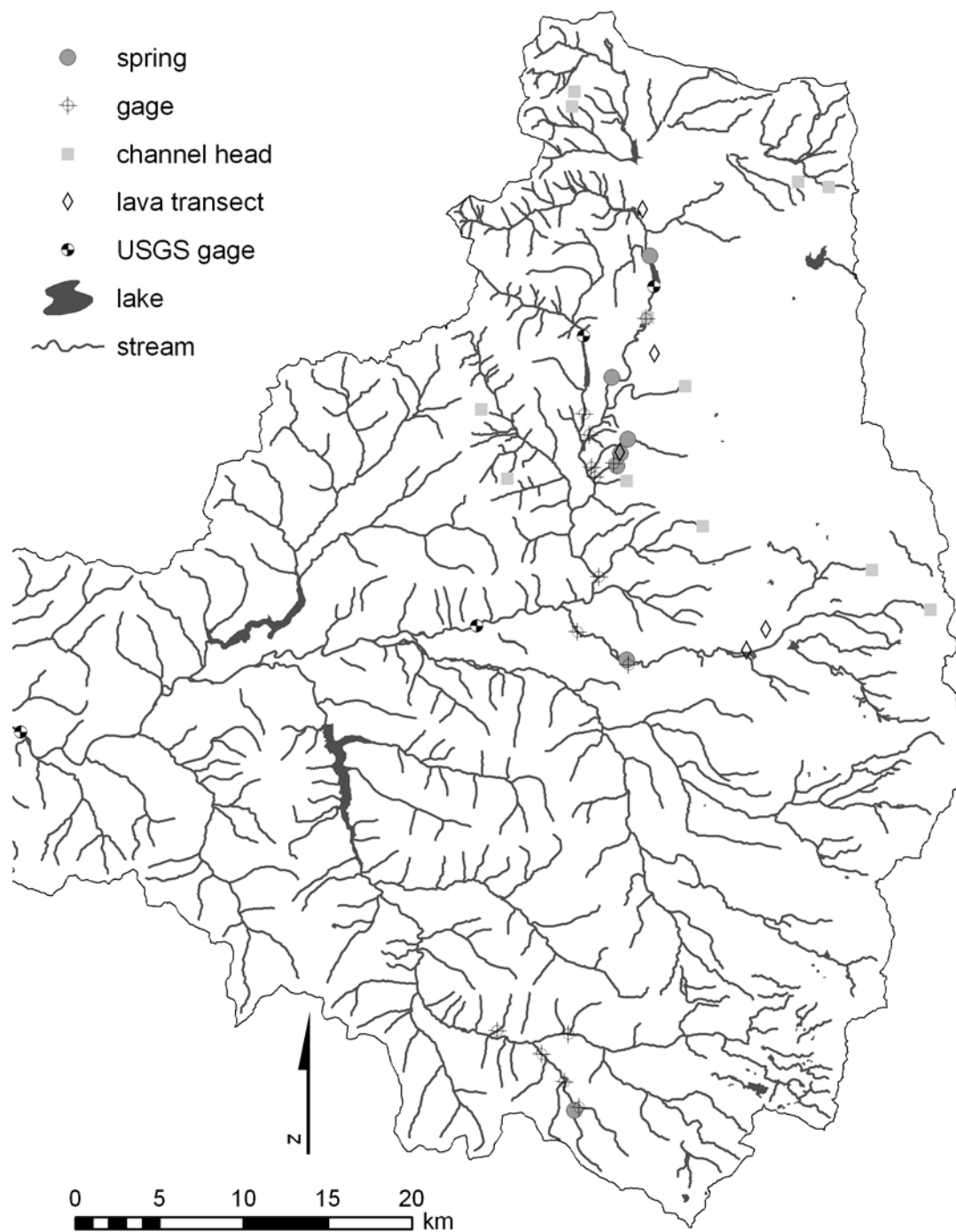
Figure 1.4. Map of the upper McKenzie River watershed showing all of the field sites used in this research. Selected USGS gauges are also shown.

THE INFLUENCE OF VOLCANIC HISTORY ON GROUNDWATER PATTERNS ON THE WEST SLOPE OF THE OREGON HIGH CASCADES

Anne Jefferson, Gordon E. Grant, Timothy P. Rose

2 The influence of volcanic history on groundwater patterns on the west slope of the Oregon High Cascades

2.1 Abstract

Spring systems on the west slope of the Oregon High Cascades exhibit complex relationships among modern topography, lava flow geometries, and groundwater flow patterns. Seven cold springs were continuously monitored for discharge and temperature in the 2004 water year, and periodically sampled for $\delta^{18}O$, δD, tritium, and dissolved noble gases. Anomalously high unit discharges suggest that topographically-defined watersheds may not correspond to aquifer boundaries, and oxygen isotope data reveal that mean recharge elevations for the springs are coincident with extensive Holocene lava fields. $^{3}He/^{4}He$ ratios in most of the springs are close to atmospheric, implying shallow flowpaths, and aquifer thicknesses are estimated to be 30-140 m. Estimates using $^{3}H/^{3}He$ data with exponential and gamma distributions yield mean transit times of ~3-14 years. Recharge areas and flow paths are likely controlled by the geographic extent of lava flows, and some groundwater may cross the Cascade crest.

2.2 Introduction

The Cascade Range, an active volcanic arc stretching from southern British Columbia to northern California, intercepts Pacific Ocean air masses moving east over the northwestern United States. These moisture-rich air masses supply abundant precipitation to the western slopes of the Cascades, yielding runoff to major river systems in the Pacific Northwest. The topography of the Cascade Range is shaped by competing forces of constructional volcanism and glacial and fluvial erosional processes. In regions where volcanic effusion rates exceed erosion rates, thick undissected platforms of layered lava and pyroclastic flows dominate the landscape. In central Oregon, coalescing Quaternary-age shield volcanoes produced a >1000 m

thick sequence of basaltic lava flows in the fault-bounded High Cascades [*Conrey et al.*, 2002]. These young lavas have extremely high permeabilities [*Saar and Manga*, 2004], and a significant portion of the precipitation in this area infiltrates to recharge groundwater flow systems. These groundwater systems emerge down gradient as large-volume spring-fed streams with higher summer flows and lower temperatures than the shallow subsurface flow fed streams draining the adjacent, older, less permeable Western Cascades terrain [*Tague and Grant*, 2004].

Understanding the movement of water in this young volcanic landscape gives us insight into the interplay between volcanic history and groundwater resources that can be applied to other mafic volcanic regions, such as Iceland, Central America, and the East African Rift zone. In addition, heightened interest in understanding the history of water and channel development on Mars is focusing on similar interactions between groundwater and volcanism [*Aharonson et al.*, 2002; *Head et al.*, 2003].

Furthermore, knowledge of Oregon Cascades hydrogeology is important for making water resource management decisions and predicting the response to potential changes in climate. Cascade rivers support salmon runs, generate hydropower, provide recreational opportunities, and supply drinking water to millions of people. In the summer, the majority of water from the Cascades is supplied by spring-fed streams from the young volcanic terrains of the High Cascades [*Gannett et al.*, 2003; *Jefferson et al.*, 2004]. As climate warms and snowpacks decrease according to current trends and predictions [*Hayhoe et al.*, 2004; *Mote et al.*, 2005], hydrological modeling suggests that spring-fed streams will be subject to declines in late summer discharge even as they become ever more important regional water resources [*Tague et al.*, in review].

Hydrogeologic investigations of High Cascades aquifer systems are complicated by several factors. Surface runoff is largely absent, drainage density is low (~0.4 km/km^2) and there are few wells to provide hydraulic conductivity and head data. Multiple,

overlapping volcanic centers with a several million year eruption history, punctuated by episodes of glaciation and erosion, preclude the application of models developed for shield volcanoes on ocean islands [e.g., *Izuka and Gingerich*, 2003; *Join et al.*, 2005]. Older lava flows were confined by topography that is now buried and obscured, resulting in hidden groundwater divides and flowpaths, but the size and inaccessibility of the area make geophysical methods for revealing aquifer structure impractical [e.g., *Descloitres et al.*, 1997; *Revil et al.*, 2004; *Join et al.*, 2005]. Flowpaths may include flow both in fractures and through the porous matrix (a dual porosity system), providing spring systems in this area with complex timescales of response to changes in recharge [*Manga*, 1999].

In this study we use springs as a window into the subsurface hydrology of the High Cascades and apply a variety of methods to investigate the source, quantity, and transit time of the water. Additionally, we examine the congruence of subsurface flowpaths and surface topography, and estimate hydraulic conductivities. We report discharge and temperature measurements, derive recharge elevations from stable isotopes, estimate flowpath depths and transit times with tritium and noble gases, and predict recharge areas using mass balance and lava flow geometry for seven groundwater systems in the McKenzie River watershed. Our intent is to both expand understanding of this important source of water in the Pacific Northwest and to explore interactions between volcanic and hydrogeologic processes.

2.3 Geologic and hydrologic context

The active portion of the Oregon Cascades volcanic arc, formed by the subduction of the Juan de Fuca plate under the North American plate, is a partially fault-bounded region known as the High Cascades. Rift related volcanism associated with nearly 3 km of subsidence within the High Cascades over the last 5 million years has resulted in the eruption of dominantly basaltic and basaltic andesite lavas [*Conrey et al.*, 2002]. These eruptions have generated a thick pile of relatively flat lying mafic lava flows

and cinders, punctuated by composite volcanoes such as the Three Sisters. The study area lies at the convergence of the Cascade volcanic arc, Basin and Range, and High Lava Plains (Figure 2.1a). The central Oregon Cascades has experienced the most extensive Quaternary mafic volcanism of any part of the arc [*Sherrod and Smith*, 1990]. The area has also been subject to three Pleistocene glaciations, which formed ice caps and valley glaciers [*Scott*, 1977], and whose deposits obscure some of the older volcanic rocks. To the west of the High Cascades lie the Western Cascades, a 10- to 40-million year-old mature continental arc, dominated by voluminous dacitic tuffs, andesitic lava flows and minor basaltic and rhyolitic volcanic rocks.

The geologic differences between the High Cascades and the Western Cascades result in distinct landscape forms and hydrologic functioning (Figure 2.1b). The High Cascades landscape has relatively gentle slopes, with little dissection, and it is underlain by young, high permeability rocks of relatively uniform composition. The Western Cascades landscape is steep, deeply dissected, and underlain by older, low permeability rocks of varying compositions. High Cascades stream networks are primarily spring-fed, whereas Western Cascade streams are runoff-dominated.

Of the numerous High Cascades volcanic centers, several bear special note in reference to the hydrology of the study area (Figure 2.1c). Scott Mountain is a late Pleistocene basaltic shield volcano with 32 km^2 of exposed lava and more extensive lava flows covered by till [*Conrey et al.*, 2002]. Eruptions from Belknap Crater covered 63 km^2 with lava between ~3000 and 1300 years before present (ybp), while the Sand Mountain-Nash Crater chain of 23 cinder cones and associated lava flows covered 68 km^2 between ~3800 and 2750 ybp [*Sherrod et al.*, 2004]. Sims Butte and Collier Cone have sent basaltic andesite lava down the Lost Creek glacial trough in the past 15,000 years [*Conrey et al.*, 2002]. South of the Three Sisters, volcanism on the west side of the crest has been quiet for >120,000 years, and glaciation and erosion have made determination of individual vents and associated flows more difficult

[*Sherrod*, 1991]. However, one of our major cold springs issues from these Quaternary lavas.

The McKenzie River watershed (Figure 2.1c) drains the west side of the High Cascades from Three Fingered Jack to south of the Three Sisters. In this watershed, seven springs with discharge >0.85 m^3/s have been identified. Six of these springs drain into tributaries of the McKenzie River above McKenzie Bridge, Oregon. At McKenzie Bridge, the McKenzie River has a topographic drainage area of 901 km^2, of which 507 km^2 are covered by Quaternary volcanic rocks. The remaining large spring is on a tributary to the South Fork of the McKenzie River. In most of the study area, a normal fault with >1 km offset separates the High Cascades from the Western Cascades [*Conrey et al.*, 2002]. The upper portion of the McKenzie River parallels this fault line.

In the High Cascades, >75% of the annual precipitation falls during the winter. Mid-latitude storms rise over the Cascades, resulting in a strong orographic effect. Above 1500 m, most precipitation falls as snow, which remains until the late spring. Below 1500 m, precipitation falls as both rain and snow, and snowpacks are transient. The west side receives ~2.00 to 3.80 m of rain and snow per year, compared with ~0.75 to 1.65 m of precipitation, predominantly snow, on the eastern slope [Taylor and Hannan, 1999]. The 2003 and 2004 water years had slightly below normal precipitation, with 89 and 93%, respectively, of the 1971-2000 mean annual precipitation.

Long-term streamflow records are sparse in the High Cascades, and most of the USGS gages in the McKenzie River watershed are along the main stem (Figure 2.1c). Generally, High Cascade streams exhibit muted winter peak flows and nearly constant summer base flows, with peak flows only 3-4 times higher than summer flows. In contrast, streams in other parts of western Oregon have peak flows >1000 times higher than base flows [*Tague and Grant*, 2004]. Geothermal spring systems are present

along faults on the western slope of the Cascades (Figure 2.2) [*Ingebritsen et al.*, 1994], but are volumetrically minor contributors to streamflow.

An array of isotopic studies, discharge measurements, and hydrogeologic models have been employed to gain insight into volcanic aquifers on the east side of the Cascade crest [*Manga*, 1996; 1997; 1998; 1999; *James et al.*, 2000; *Manga*, 2001; *Gannett et al.*, 2003; *Manga and Kirchner*, 2004], but different dynamics might apply to the western slope of the Cascades due to the greater precipitation flux, which could lead to shorter transit times or greater water storage than on the east side. Also, on the western slope, the mixture of rain and snow creates multiple pulses of recharge. Additionally, Quaternary lavas on the west side of the Cascades are bounded <15 km from the crest by higher elevation and lower permeability Western Cascades rocks, whereas on the east side, High Cascades lavas commingle with high permeability back-arc and Basin and Range volcanic rocks at comparable elevation. Thus, flowpaths are likely on the order of kilometers on the west side rather than tens of kilometers as on the east side [*James et al.*, 2000].

2.4 Methods

2.4.1 Study site selection and characterization

A survey of discharge measurements revealed that the majority of summer flow in the McKenzie River is sourced at springs, and seven of the largest springs were selected for detailed study. For the 2004 water year (10/1/2003 to 9/30/2004), we monitored discharge at Lost, Olallie North, Olallie South, Roaring, and Sweetwater springs (Figure 2.1c, Table 2.1). TruTrack WT-HR data loggers were used to measure water height at 15- to 60-minute intervals, and discharge was measured >10 times at each site using a Marsh-McBirney velocity meter via wading [*Carter and Davidian,* 1968]. Stage-discharge rating curves were developed to calculate mean annual discharge.

Beginning in July 2002, water temperature was measured hourly at each of the springs by Onset Hobo® Water Temp Pro data loggers, with ±0.2°C accuracy.

The other two large springs are Tamolitch and Great Springs. Gaging downstream of Tamolitch Spring was established in October 2003 by Stillwater Sciences. Great Spring feeds directly into Clear Lake, which is gaged by the USGS (gage # 14158500). Clear Lake has many springs and seeps along the lakeshore and bottom, of which Great Spring is the most easily accessible. Groundwater is the only source of August flow from Clear Lake, and it averages 8.5 m^3/s [*Herrett et al.*, 2004], of which Great Spring contributes 10% [*Stearns*, 1929].

We computed a simplified water balance for the 2004 water year for the topographic watersheds of the springs. Topographic watersheds were delineated from a 10-m DEM using ArcGIS9. Monthly values of precipitation in 2 km by 2 km grid cells were derived from the PRISM model [*Daly et al.*, 1994; *Daly et al.*, 2002] and summed. A runoff ratio, which is the fraction of precipitation that results in streamflow, of 0.68 was calculated for the McKenzie River near Vida, and was used as a regional value to constrain evapotranspiration. Evapotranspiration is recognized to vary with vegetation and altitude, but distributed data do not exist for the study area, so here we neglect spatial variability. We assumed that the 2409 km^2 drainage area of the McKenzie River above Vida is large enough that slight discrepancies between the topographically defined watershed and the groundwater recharge areas are probably insignificant to the calculated runoff ratio. Runoff ratios were also calculated for three smaller sub-basins of the McKenzie River that are gaged by the USGS. These basins had ratios ranging from 0.63 to 0.76, supporting the use of the runoff ratio at Vida as a reasonable regional value.

2.4.2 Sample collection and analysis

In order to determine source areas for the lava found at springs, rock samples were collected at four of the springs. Bulk rock samples were analyzed via X-ray fluorescence at Washington State University's GeoAnalytical Laboratory for 27 major and trace elements. These data were compared to each other and published rock chemistries.

Stable isotope data for 174 samples of springs, streams, lakes, and precipitation from the McKenzie River watershed were collected and analyzed between July 2002 and March 2005. Each of the seven major springs was sampled for stable isotopes at least three times, with two springs (Olallie North Spring and Lost Spring) sampled repeatedly (n = 22) to establish long-term trends in isotopic composition. Isotopic sample preparation was by the water-CO_2 equilibration method [*Epstein and Mayeda*, 1953] for oxygen isotopes, and by the zinc-reduction method for deuterium [*Coleman et al.*, 1982]. Analyses were completed on a VG dual inlet isotope ratio mass spectrometer at Lawrence Livermore National Laboratory. Isotopic values are reported in the standard δ-notation as per mil (‰) deviations from the VSMOW reference standard.

Water samples were collected at six of the major springs in August 2004 for helium and tritium analysis. Samples for helium analysis were collected in copper tubes, which were submerged in the spring pool, tapped to dislodge trapped air bubbles, and sealed with stainless steel pinch-off clamps. Samples for tritium analysis were collected in plastic bottles. Tritium and helium analyses were completed by the Noble Gas Isotope Lab at the University of Miami, following procedures described in [*Clarke et al.*, 1976]. All samples were collected as close as possible to the spring orifice, as noted by water bubbling or gushing from the rocks.

2.4.3 Recharge elevation estimation

In mountainous regions, precipitation becomes progressively depleted in heavy isotopes (^{2}H and ^{18}O) with increasing elevation, as first described by *Dansgaard* [1964]. In this study, the variation in stable isotope values of small springs as a function of altitude was used to estimate the average recharge elevations for large springs. Small springs are considered proxies for local recharge of precipitation at a given elevation [Rose et al., 1996]. Samples from 10 small springs (< 0.12 m^3/s discharge) were collected during the summers of 2003 and 2004. Additionally, data from 9 small springs and 1 well from the McKenzie River watershed, or drainages to the west, were reported by *Ingebritsen et al.* [1994], and data were used from 7 springs sampled by *Evans et al.* [2004] from the McKenzie watershed.

2.4.4 Helium calculations and transit time estimation

The time from when water enters an aquifer to when it exits at a spring is referred to as the transit time [*Etcheverry and Perrochet*, 2000]. Tritium (^{3}H) and tritogenic helium (^{3}He$_{trit}$) have been employed to date young groundwater (transit times less than ~50 years) in a variety of settings [*Aeschbach-Hertig et al.*, 1998; *James et al.*, 2000; *Rademacher et al.*, 2005]. Atmospheric tritium concentrations greatly increased as a result of nuclear weapons testing in the 1950s and 1960s, but by the 1990s, atmospheric tritium activities had approximately returned to pre-bomb levels. The constrainable time period and resolution are enhanced by measuring ^{3}H in combination with its daughter product, ^{3}He$_{trit}$.

All of the tritium in groundwater is derived from the atmosphere, but helium has multiple sources that complicate interpretation. In order to constrain the amount of ^{3}He$_{trit}$ in a water sample, it is necessary to determine the contributions from atmosphere-equilibrium solubility, dissolution of air bubbles during recharge (so called "excess air"), decay of U and Th in the crust, and mantle helium from magmatic

sources. Crustal and mantle sources of helium are referred to as terrigenic. Fortunately, atmospheric, crustal, and mantle sources have differing ratios of ^{3}He/^{4}He, and all neon is commonly assumed to be atmospherically derived, so these differences can be used to calculate the relative contribution of helium from each source [*Schlosser et al.*, 1989].

Following *Schlosser et al.* [1989], terrigenic helium (^{4}He$_{terr}$) is derived from

$$^4He_{terr} = {}^4He_{meas} - \left(\frac{^4He}{Ne}\right)_{atm} \cdot \left(Ne_{meas} - Ne_{eq}\right) - {}^4He_{eq} \tag{1}$$

where ^{4}He$_{meas}$ is the measured helium concentration, (^{4}He/Ne)$_{atm}$ is 0.2882 [*Hilton*, 1996], Ne$_{meas}$ is the measured neon concentration, Ne$_{eq}$ is the equilibrium dissolved neon concentration, and ^{4}He$_{eq}$ is the equilibrium dissolved helium concentration. Equilibrium solubilities of Ne and He were corrected for recharge temperature and altitude. Recharge temperature is assumed to be the same as the spring temperature corrected for gravitational potential energy dissipation [*Manga and Kirchner*, 2004], as discussed below, and mean recharge altitude is derived from δ^{18}O values of the springs as described above.

Total ^{3}He is calculated by multiplying the measured ^{4}He concentration by the measured ratio of ^{3}He to ^{4}He. The atmospheric ^{3}He component, which includes both equilibrium and excess helium, is determined using

$$^3He_{atm} = \left({}^4He_{meas} - {}^4He_{terr}\right) \cdot R_a - {}^4He_{eq} \cdot R_a \cdot \left(1 - \alpha\right) \tag{2}$$

where R$_a$ is the atmospheric ^{3}He/^{4}He ratio, 1.384*10^{-6} [*Clarke et al.*, 1976], and α = 0.983, the solubility isotope effect [*Schlosser et al.*, 1989]. Tritogenic helium is calculated as

$$^3He_{trit} = {}^4He_{meas} \cdot \left(\frac{^3He}{^4He}\right)_{meas} - {}^3He_{atm} - {}^4He_{terr} \cdot \left(\frac{^3He}{^4He}\right)_{terr} \tag{3}$$

where (^{3}He/^{4}He)$_{meas}$ is the measured helium isotope ratio and (^{3}He/^{4}He)$_{terr}$ is the terrigenic helium isotope ratio.

It is common to assume that either mantle or crustal sources of helium can be neglected in the terrigenic helium flux when using the tritium-helium method to date groundwater [e.g., *Schlosser et al.,* 1989; *James et al.,* 2000], because the terrigenic helium isotope ratio cannot be measured directly in environments where both mantle and crustal helium are expected to occur. Following *Saar et al.* [2005], we consider mantle helium in the Cascades to have an ^{3}He/^{4}He ratio normalized to the atmosphere (R/R$_a$) of 8.19 and crustal helium to have R/R$_a$ = 0.007. We solve equation (3) by varying (^{3}He/^{4}He)$_{terr}$ iteratively until the resultant ^{3}He/^{4}He ratio, including the atmospheric, terrigenic, and tritogenic components, equals the measured ^{3}He/^{4}He ratio of each sample.

Once tritogenic helium concentrations are obtained, ^{3}H/^{3}He mean transit time (T) is calculated using:

$$T = \frac{t_{1/2}}{\ln 2}\left[1 + \frac{^3He_{trit}}{^3H}\right],$$ (4)

where t$_{1/2}$ is the tritium half-life (12.43 years) and $^3He_{trit}$ and ^3H are expressed in tritium units [*Schlosser et al.*, 1989]. Uncertainty in the transit time estimates is the result of measurement uncertainty in the tritium concentrations and uncertainty in the correct recharge temperature and elevation.

Equation (4) inherently calculates transit times with a piston-flow model. *Manga* [1999] suggested that High Cascades aquifers are more appropriately modeled with an exponential transit time distribution, which incorporates distributed recharge and mixing of water of different ages at the spring orifice. The transit time distribution, g(t), for this model,

$$g(t) = \frac{1}{T}e^{t/T}$$ (5)

is a function of time (t), and the mean transit time (T). Work by *Kirchner et al.* [2001], suggests that many catchments do not exhibit behavior consistent with the exponential model. Their work supports a gamma transit time distribution,

$$g(t) = \frac{\tau^{\alpha-1}}{\beta^{\alpha}\Gamma(\alpha)} e^{-\tau/\beta} , \qquad (6)$$

where β is a scale parameter and α is a shape parameter. Mean transit time is $\alpha\beta$, and α ~ 0.5 has been found to fit solute tracer concentration curves for a number of catchments [*Kirchner et al.*, 2001].

These transit time distributions are implemented using the convolution integral,

$$c_{out}(t) = \int_{-\infty}^{t} c_{in}(\tau)g(t-\tau)e^{-\lambda(t-\tau)}d\tau , \qquad (7)$$

where c_{out} and c_{in} are the output and input time series, τ is an integration variable, and λ is the radioactive decay constant. The input time series is provided by precipitation-weighted tritium concentrations at Portland which began in 1963 [*IAEA/WMO*, 2005], and extended backwards to 1953 by regression with measurements made in Ottawa [*Michel*, 1989]. The convolution integral was used with both exponential and gamma transit time distributions and solved for yearly time-steps of 0 to 50 years. Exponential and gamma mean transit times for each spring were calculated using the 2004 output concentrations of ^{3}H and ^{3}He to calculate ^{3}H/^{3}He mean transit times and linearly interpolating between the two closest time-steps.

2.5 Results

2.5.1 Recharge areas

The seven major spring systems all have runoff ratios that diverge from the regional average (Figure 2.3). Five of the springs discharge more water than their topographic watersheds receive in precipitation, as shown by the position above the 1:1 line. In order to account for the high discharge values, these springs must be receiving water sourced outside their topographic watersheds. Conversely, the two springs that plot below the regional average are not receiving all of the precipitation that falls on their topographic watershed. Thus, there is a strong discordance between topographic

watersheds and groundwater recharge areas. These results suggest that modern topography is not the main constraint on groundwater catchments, despite relief of ~1000 m between the elevation of the springs and the Cascade crest. Given this finding, we used stable isotopes, water temperature, and rock chemistry to provide insights into recharge elevations and areas for the springs.

We derived a local meteoric water line of $\delta D = 8.3\ \delta^{18}O + 17$ ($r^2 = 0.95$, $n = 44$) based on isotopic sampling of springs, streams, and precipitation in the McKenzie River basin (Figure 2.4). Evaporative enrichment was only exhibited by late summer samples from small spring pools and lakes (not shown in Figure 2.4). Thus, evaporation does not appear to have significantly affected the isotopic composition of the snowpack, or that of infiltration through the unsaturated zone.

Repeated sampling (n=22) of Lost Spring and Olallie North Spring from July 2002 to March 2005 showed little variability in isotopic composition on a seasonal or interannual basis (Figure 2.5). The standard deviation for the Lost Spring data set was 0.08‰, and for Olallie North Spring it was 0.05‰. Both of these values are smaller than the analytical uncertainty of 0.1‰. Given an annual range of precipitation $\delta^{18}O$ of 8‰, based on a 3-year record from a Western Cascades site <10 km west of the upper McKenzie River [*McGuire et al.*, 2005], the lack of variability in the groundwater suggests complete mixing at the spring orifice or that transit times may be long enough to substantially mute input variability.

Small springs show a decrease in $\delta^{18}O$ of 0.16‰ per 100 m elevation gain, as shown in Figure 2.6 ($r^2 = 0.67$), which is slightly lower than temperate and worldwide averages of 0.20‰ per 100 m elevation gain [*Dansgaard*, 1964; *Bowen and Wilkinson*, 2002], but is within the 0.14 to 0.23‰ range of values reported for the Cascade Range [*Ingebritsen et al.*, 1994; *Rose et al.*, 1996; *James et al.*, 2000; *Nathenson and Thompson*, 2003].

The altitude-isotope line (Figure 2.6) was fitted by linear regression to the isotopic compositions and discharge elevations of the small springs. Even though small springs are assumed to recharge locally, there is some recharge elevation above their outlets. Local peaks were generally less than 150 m higher than the small springs, and the springs are likely recharging water at multiple elevations along the slopes. Unambiguous recharge elevations could not be definitively identified from the surrounding topography, so discharge elevations were used instead. Given the slope of the altitude-isotope line, uncertainty in recharge elevations associated with analytical error of isotope values is ± 60 m. Uncertainty associated with recharge elevations is probably on the same order of magnitude.

Projecting the mean isotopic composition of large springs (Table 2.1) onto the altitude-isotope line for small springs, recharge-weighted mean recharge elevations were found to be between 1000 and 1600 m (Figure 2.7). The elevation range for recharge to the springs corresponds with the majority of the area covered by Quaternary mafic lava.

Like $\delta^{18}O$, temperature has also been used as a proxy for recharge elevation, although its interpretation may be complicated by geothermal heating and the dissipation of gravitational potential energy. *Manga and Kirchner* [2004] suggest that such dissipation is a significant heat source for springs in volcanic regions, citing energy balance calculations and examples from Mt. Shasta in California and the east side of the Oregon High Cascades. Given their findings, we compared spring temperatures to the mean annual surface temperature of their isotopically-inferred recharge elevations. Mean annual and mean May temperature data were obtained for 10 stations on the west slope of the Cascades in the vicinity of the study area from the Oregon Climate Service, H.J. Andrews Experimental Forest, and Natural Resources Conservation Service SNOTEL network. A best-fit line for mean annual temperature was -5.7°C/km + 13.6 (r^2=0.80), and May temperatures, during the principal snowmelt and groundwater recharge period, were higher than mean annual temperatures. Measured

temperatures at six of seven springs were equal to or lower than mean annual surface temperatures for the mean recharge elevations. When the correction for gravitational potential energy (2.3°C/km, *Manga and Kirchner* [2004]) is applied, all springs are 0.9-3.4°C colder than their recharge elevations. Measured temperature at Lost Spring is warmer than predicted for its mean recharge elevation, but colder when corrected for gravitational potential energy. As discussed below, temperature at this spring may be influenced by mixing with geothermal water. Therefore, geothermal heating appears to be insignificant in most cases, and we suggest that springs are probably deriving their water from a range of elevations and associated recharge temperatures.

We propose that the geometry of lava flows may have a dominant control on aquifer geometry. Basaltic lava flows have highly permeable rubble zones surrounding a dense, low permeability interior [*Kilburn*, 2000]. Most water flow occurs within the rubble zones, but fractures allow transmission of water through flow interiors and vertically between lava flows [*Kiernan et al.*, 2003]. Rubble zones at contacts between lava flows result in highly anisotropic aquifers, with the direction of highest permeability oriented parallel to the lava flow direction [*Davis*, 1969]. These high permeability regions are not laterally continuous between adjacent lava flows, potentially segregating groundwater flowpaths by the spatial extent of a particular lava lobe. Volcanic dikes and lower permeability strata can also compartmentalize groundwater flow [*Izuka and Gingerich*, 2003]. In the Cascades, most lava flows originate near the crest and flow primarily east or west, filling in lows in the pre-existing topography. In many places, young lava flows abut older, more weathered, and potentially less permeable rocks. Thus, determining the source vent of a lava flow from which a spring issues allows the identification of probable recharge areas that may lie outside the spring's topographic watershed.

Published geologic maps clearly link lava at the Great, Tamolitch, and Lost springs to their source vents (Figure 1c). Great Spring rises from Sand Mountain lava [*Sherrod et al.*, 2004], Tamolitch Spring emerges from Belknap Crater lava [*Stearns*, 1929], and

Lost Spring springs from Sims Butte lava [*Lund*, 1977], so no rocks were collected or analyzed at these locations. The area around Sweetwater, Olallie North, and Olallie South springs has not been mapped in detail. A map of the Oregon Cascades shows the area around Sweetwater and Olallie South springs as unconsolidated sediments or sedimentary rocks [*Sherrod and Smith*, 2000]. Nonetheless, upon reconnaissance, we found vesicular lava flows exposed and sampled them at the orifices of Sweetwater and Olallie North springs. Olallie South Spring emerges from beneath a talus pile, so the ridge above the spring and a down-slope area were sampled instead.

Trace elements can be particularly diagnostic for identifying rocks from the same lava flow or vent. Strontium and Nb are two trace elements commonly used to distinguish lavas in the Oregon Cascades [*Conrey et al.*, 2002]. Samples at Sweetwater and Olallie North have very similar Sr and Nb concentrations (Table 2.2), indicating that the rocks are likely part of the same lava flow. The sample down-slope of Olallie South has a different major element composition but similar Sr and Nb concentrations compared to the Sweetwater and Olallie North samples. The sample from the ridge above Olallie South is clearly from a different source. These interpretations are supported by comparisons of major-element variations including SiO_2, TiO_2, and the Mg# (molar ratio of Mg to Mg plus Fe). Sweetwater and Olallie North have identical Mg numbers of 0.60, while the down-slope sample equals 0.59 and the ridge sample equals 0.57. The ridge sample also has more SiO_2 and less TiO_2 than the other samples (Table 2.2). The chemical compositions of the Sweetwater and Olallie North samples are very similar to that of a sample from near the summit of Scott Mountain. This sample (#99-37) has 683 ppm Sr, 13.2 ppm Nb, 50.47 wt% SiO_2, and 1.60 wt% TiO_2, all of which closely correspond to the Sweetwater and Olallie North Samples [*Conrey et al.*, 2002].

Based on the rock chemistry (Table 2.2), we interpret the Sweetwater and Olallie North samples as being part of the same Scott Mountain lava flow, and the sample down-slope of Olallie South as also originating from Scott Mountain. This suggests

that the Scott Mountain area is a likely source of recharge to Sweetwater and Olallie North springs. The ridge above Olallie South is not composed of Scott Mountain lava, and it is mapped as older Quaternary basaltic andesite not linked to any identified vent [*Sherrod and Smith*, 2000]. Olallie South Spring may be fed by a source other than or in addition to Scott Mountain.

Spring water temperature and $\delta^{18}O$ data impart additional information about relationships between source areas for Sweetwater, Olallie North, and Olallie South springs. Sweetwater Spring and Olallie North Spring are located 952 m apart, but both emerge from Scott Mountain lava and their mean $\delta^{18}O$ and temperature are within analytical uncertainty of each other (Table 2.1). We conclude that Sweetwater and Olallie North springs are likely sourced in the same area. In contrast, Olallie South Spring, which is located 785 m south of Olallie North Spring, has water that is warmer by 0.6°C and isotopically heavier than Olallie North Spring. We conclude that Olallie South has a different, lower elevation recharge area than Olallie North and Sweetwater springs.

Roaring River is fed by Roaring Spring and a second 0.73 m^3/s spring located ~300 m north. As these two springs have temperature and $\delta^{18}O$ within analytical uncertainty of each other, we infer that they share the same water source. Roaring Spring issues from basaltic andesite that may have originated near Irish Mountain, but cannot be definitely linked to Irish Mountain based on published rock chemistry data. The orifice of Roaring Spring spans ~50 m along a nearly horizontal line, but samples from lava both above and below the height of the Roaring Spring orifice are within analytical uncertainty for many elements, and have very similar Sr and Nb concentrations (Table 2.2). Based on the rock chemistry, then, we conclude that the groundwater does not reach the land surface at Roaring Spring via a contact between lava flows. Instead the water may be discharging through a fracture network within a single flow.

In the Lost Creek glacial trough, a spring with unusual discharge dynamics seems to share the same recharge area with the larger, perennial Lost Spring. Ephemeral White Branch Spring ($0 \leq Q \leq 2$ m^3/s) is located 750 m up-valley, but has the same mean δ^{18}O and temperature as Lost Spring. Both springs emerge from Sims Butte lava, and the seasonally fluctuating water table may sometimes be below White Branch Spring while always providing flow to Lost Spring.

2.5.2 Flowpath depths and helium sources

In order to aid comparison of helium isotope ratios reported in this paper with those collected from other hot and cold springs in the region, helium isotope ratios were adjusted following the air-saturated water corrections of *Hilton* [1996] despite the possibility that the highly atmospheric signature of the spring water may dilute the magmatic helium signal [*Saar et al.*, 2005]. For the springs sampled in this study, measured R/R$_a$ values range from 0.93 to 2.14, and corrected ratios (R$_c$/R$_a$) range from 0.74 to 3.19 (Table 2.3). The helium isotope ratios are similar to those of cold springs on the east side of the Cascades, which range from 0.95 to 5.19 R$_c$/Ra [*James et al.*, 2000; *Saar et al.*, 2005]. Three geothermal springs in the McKenzie River watershed have ^{3}He/^{4}He ratios of 3.3 to 5.2 R$_c$/Ra, and cold springs feeding Separation Creek, a tributary to the McKenzie River have the highest ratios reported in the Cascades, ranging from 2.4 to 8.6 R$_c$/Ra [*Evans et al.*, 2004]. The high helium isotope ratios in the Separation Creek springs are the result of magmatic degassing from an intrusion underlying the area [*Evans et al.*, 2004]. We infer that R/R$_a$ values >1 in our study area are related to magmatic gas emissions.

Olallie South, Tamolitch, and Roaring springs have helium isotope ratios close to that of the atmosphere and have little ^{3}He from terrigenic sources (crustal and magmatic). These springs likely follow shallow flowpaths where they encounter a low terrigenic helium flux in their short transit time. Underlying these shallow flowpaths, there may be deep geothermal water that incorporates the terrigenic helium, shielding the cold

springs from encountering it (Figure 2.2). The Ne/^{4}He ratio for Olallie North suggests that entrapment of an air bubble during sampling yielded spurious results. ^{3}He$_{trit}$ for Olallie North was estimated from interpolation between Olallie South Spring and Great Spring values, based on their ^{3}H measurements.

Lost Spring has the largest discharge and largest mantle component of any of the sampled springs. These results conform to the model of regional groundwater systems with longer transit times and higher ^{3}He/^{4}He ratios than more localized aquifers [*James et al.*, 2000; *Nathenson and Thompson*, 2003]. Perhaps more importantly, the aquifer feeding Lost Spring crosses the White Branch Fault Zone [*Conrey et al.*, 2002], where a water-supply well is slightly thermal, with an elevated chloride concentration (56 mg/L) and R_c/R_a value (6.8) [*Evans et al.*, 2004]. We suggest that, in the vicinity of the fault zone, groundwater with near-atmospheric helium ratios mixes with a small amount of thermal water with a magmatic helium isotope signature. This results in the helium isotope ratios sampled down-gradient at Lost Spring. This interpretation is supported by the low ^{14}C values for the well and Lost Spring [*Evans et al.*, 2004] and may also explain the anomalously warm temperature of Lost Spring as compared to that of its recharge elevation. These results suggest that fault zones play a key role in mixing deep geothermal water with shallow groundwater systems.

2.5.3 Transit time

Using the tritium-tritogenic helium data, mean transit times for the spring aquifers were estimated in three ways (Table 2.3). Transit times calculated using the ratio of ^{3}H/^{3}He (equation (4)), range from 4.1 years for Roaring Spring to 26.0 years for Great Spring. Transit times derived using the exponential (equation (5)) and gamma (equation (6)) distributions are shorter, ranging from 4.4 to 13.3 years and from 3.2 to 13.6 years respectively. Uncertainty surrounding each estimate is ~1 year.

The simple exponential and gamma distributions, which apply to flow through porous media, may not reflect the complex hydrogeology of the study area. If there is significant flow through interconnected fractures or zones of stagnant water, tracer-based transit time estimates may not reflect the water's true transit time and multiple tracers may provide divergent estimates [*Mazor and Nativ*, 1992; *Maloszewski et al.*, 2004]. Other models that include dual porosity systems [e.g., *Maloszewski and Zuber*, 1985] might better represent the physical conditions. However, these models require more complete information about fracture geometry and matrix characteristics than are available for the study area. [*Cook et al.*, 2005] showed that it may be possible to constrain fracture and matrix parameters by measuring multiple tracers in vertically nested piezometers. However, mixing of multiple flow lines occurs at the springs, so no tracer profiles can be derived, nor fracture parameters determined, in the High Cascades. Many studies have simplified matters by treating the aquifer as a porous matrix and ignoring the fractures [*Aeschbach-Hertig et al.*, 1998; *Manga*, 1999]. In such models, the aquifer is represented by a single hydraulic conductivity reflecting contributions from both fractures and matrix. This is the approach taken here.

The exponential and gamma models produce similar results, with Great Spring having slightly longer transit times and the other springs having slightly shorter transit times in the gamma model than in the exponential model. Without repeated sampling, it is impossible to determine which model is more appropriate for the spring systems studied, so we choose to bracket the transit times using the shortest and longest times from the two models for each spring. Thus, transit time to Great Spring averages 12.9 – 14.4 years; Olallie North averages 8.4 – 10.3 years; Olallie South averages 6.8 – 8.9 years; Roaring averages 2.9 – 4.4 years; and Tamolitch averages 5.2 – 7.2 years. For these five springs, the mean transit time is 7.2 years when weighted by discharge.

The long mean transit time for Lost Spring, 54.5 years using the ^{3}H/^{3}He ratio, cannot be explained using the exponential or gamma models. It is probably the result of mixing between groundwater with shorter transit times and deeper, tritium-dead

groundwater. This interpretation is consistent with the temperature and helium data discussed above.

2.6 Discussion

2.6.1 Recharge areas

While there are too many possible permutations to fully constrain recharge area geometry without hydraulic head data, isotopic and geologic data allow estimates of the likely size and flowpath of each aquifer. Isotopically-determined recharge elevations highlight a band across each topographic watershed, from which a mean precipitation value is derived from PRISM data. Spring discharge is multiplied by the regional runoff ratio (0.68) and divided by the mean precipitation to calculate the recharge area for each spring. Overall, the six springs require a recharge area that is 95% of the size of their combined topographic watersheds. However, there are large discrepancies between the estimated size of the recharge area and the size of the topographic watershed for each individual spring (Table 2. 1).

For a portion of the upper McKenzie River watershed in which five major springs are located (453 km^2, Figure 2.1b), recharge for the springs requires 66% of the area. Most of the remaining area provides water for small runoff-dominated streams and accretion along the McKenzie River channel, while the rest likely drains east of the Cascades crest. A regional groundwater model for the Deschutes River basin, lying east of the McKenzie River basin, requires 22.6 m^3/s of water from the west side of the Cascades crest in order to account for all of the groundwater discharge in that arid environment [*Gannett and Lite*, 2004]. The McKenzie River basin likely supplies <3 m^3/s of water to the east side.

In addition to estimating the area of the groundwater recharge zones, we constrained their locations based on geology and mean recharge elevation (Figure 2.8). Great

Spring is likely sourced on and around Sand Mountain, both within and outside of its topographic watershed. Tamolitch Spring is probably fed by groundwater recharge and flow through Belknap Crater lava, in the southern portion of its watershed, with the rest of the area likely providing the ~6 m^3/s of groundwater that accretes in the McKenzie River channel between Clear Lake and Tamolitch Spring. Scott Mountain appears to be a major area of groundwater recharge. Sweetwater and Olallie North springs are probably sourced in the northern and eastern portions of Scott Mountain, while Olallie South Spring may derive its water from lower elevation Scott Mountain lava, within and to the south of its topographic watershed. The likely recharge area for Lost Spring is less clear, although there are a few clear point sources of recharge where streams and lakes drain into the Collier Cone lava. The occurrence of these point sources suggests that the southern portion of the Lost Spring topographic watershed may be the source of the spring's water. The area bounded on the north by Sims Butte and Collier Cone lava supplies more than enough water to account for the spring's discharge. The northern portion of the watershed may drain to the more northerly springs and may also provide water to the Deschutes basin. Roaring Spring is probably sourced along the Cascade Crest, but glacial and erosional processes in the >120,000 years since lava emplacement obscure lava geometries and confound specific interpretations of the recharge area.

2.6.2 Aquifer properties

The Quaternary lavas of the High Cascades are exposed over large areas of the landscape surface and, where not exposed, are buried only by shallow soils or glacial deposits. These lavas form a stack of mostly high permeability rock more than 1000 m in thickness, as documented in deep bore holes in the study region [*Conrey et al.*, 2002]. Thermal profiles in the bores holes are isothermal within the uppermost several hundred meters of the saturated zone, which has been attributed to the high transmissivity of groundwater through these aquifers. Analysis of thermal, as well as

other data, suggests that hydraulic conductivities are on the order of 10^{-6} m/s at 500 m [*Saar and Manga*, 2004].

Driller's logs for 6 wells drilled in late Quaternary lavas in the study region showed an average rise of 11 m between the depth where water was first encountered and the subsequent static water level [*OWRD*, 2005]. Only one well had a static water level at the same depth as it was first discovered. One well became artesian when drillers reached a depth of 17 m. These drill logs suggest that much of the High Cascades aquifer system behaves as a confined aquifer.

The volume of mobile water in an aquifer is the product of the mean transit time and spring discharge (Q). Using 7.2 years as the mean transit time and a total discharge of 17.07 m^3/s from the seven springs, combined mobile water volume is ~4 km^3. The aquifer thickness can then be calculated by dividing the aquifer volume by its porosity and mass-balanced recharge area. We assume an effective porosity of 15%, following *Ingebritsen et al.* [1994], and calculate aquifer thicknesses ranging from ~30 m for Roaring Spring to ~120 m for Great Spring. Seepage velocities were calculated from the effective porosity multiplied by the distance between the spring and the mean recharge elevation band divided by the mean transit time. Seepage velocities range between $1*10^{-6}$ and $7*10^{-6}$ m/s (0.1 to 0.6 m/day).

Assuming groundwater flow through a homogeneous, isotropic porous material, we use Darcy's law,

$$K = \frac{Q}{bw}\frac{dl}{dh}, \qquad\qquad (8)$$

to determine the hydraulic conductivity of our investigated volcanic aquifers in the High Cascades. Here K is hydraulic conductivity, dl is the distance between the spring and its mean recharge elevation band, dh is the elevation difference between mean recharge and the spring, w is the width of the lava flow from which the spring emerges in a cross-section near the spring, and b is the aquifer thickness. Calculated hydraulic conductivities are $3*10^{-4} \le K \le 1*10^{-2}$ m/s. These results bracket an estimated

hydraulic conductivity on the order of 10^{-3} m/s for springs in the Deschutes River basin, directly to the east of the study area, derived from a linearized Boussinesq equation for unconfined aquifers [*Manga*, 1996]. They also bracket an estimated hydraulic conductivity of $2*10^{-3}$ m/s for a spring near Lassen, part of the California Cascades, made using the Boussinesq equation in combination with spring-fed stream recession analysis and mean transit time from ^{3}H/^{3}He [*Manga*, 1999]. Basalt flows on Kilauea, Hawaii, also have very similar hydraulic conductivities [*Ingebritsen and Scholl*, 1993].

2.7 Conclusions

In young volcanic arcs that receive large amounts of annual precipitation, high recharge rates coupled with volcanic aquifers that have high near-surface hydraulic conductivity lead to extensive groundwater systems. The aquifers are locally constrained by the geographic extent of permeable lava flows, with recharge areas and flow paths that are not fully bounded by modern topography. Flowpaths are generally shallow and water discharging at large, cold springs has had limited contact with geothermal systems. A combination of hydrologic, isotopic, and geologic data illuminate these groundwater systems by providing data on aquifer sizes and locations, recharge elevations, transit times, and other aquifer characteristics. Our observations on the west slope of the Oregon High Cascades emphasize the importance of volcanic history in controlling the patterns of groundwater flow in young mafic landscapes.

2.8 Acknowledgements

2.9 References cited

Aeschbach-Hertig, W., P. Schlosser, M. Stute, H.J. Simpson, A. Ludin, and J.F. Clark (1998), A ^{3}H/^{3}He study of ground water flow in a fractured bedrock aquifer, *Ground Water*, *36*(4), 661-670.

Aharonson, O., M.T. Zuber, D.H. Rothman, N. Schorghofer, and K.X. Whipple (2002), Drainage basins and channel incision on Mars, *Proc. Natl. Acad. Sci.*,, *99*(4), 1780-1783.

Bowen, G.J., and B. Wilkinson (2002), Spatial distribution of δ^{18}O in meteoric precipitation, *Geology*, *30* (4), 315-318.

Carter, R.W., and J. Davidian (1968), General Procedure for Gaging Streams, *Techniques of Water-Resources Investigations of the United States Geological Survey*, Book 3 Chap. A6, U.S. Geol. Surv., Washington, DC.

Clarke, W.B., W.J. Jenkins, and Z. Top (1976), Determination of tritium by mass-spectrometric measurement of ^{3}He, *Int. J. of Applied Radiation and Isotopes*, *27*, 515-522.

Coleman, M.L., T.J. Sheperd, J.J. Durham, J.E. Rouse, and G.R. Moore (1982), Reduction of water with zinc for hydrogen isotope analysis, *Analytical Chemistry*, *54*, 993-995.

Conrey, R.M, D.R. Sherrod, P. Hooper, and D. Swanson (1997), Diverse primitive magmas in the Cascade arc, Northern Oregon and Southern Washington, *The Canadian Mineralogist, 35*, 367-396.

Conrey, R.M., E.M. Taylor, J.M. Donnely-Nolan, and D.R. Sherrod (2002), North-central Oregon Cascades: exploring petrologic and tectonic intimacy in a propagating intra-arc rift, in *Field Guide to Geologic Processes in Cascadia*, edited by G.W. Moore, pp. 47-90, Oregon Department of Geology and Mineral Industries, Salem, Ore.

Cook, P.G., A.J. Love, N.I. Robinson, and C.T. Simmons (2005), Groundwater ages in fractured rock aquifers, *J. Hydrol.*, *308*(1-4), 284-301.

Craig, H. (1961), Isotopic variations in meteoric waters, *Science*, *133*, 1702-170.

Daly, C., R.P. Nielson, and D.L. Phillips (1994), A statistical-topographic model for mapping climatological precipitation over mountanious terrain, *J. Appl. Meteorology*, *33*, 140-158.

Daly, C., W.P. Gibson, G.H. Taylor, G.L. Johnson, and P. Pasteris (2002), A knowledge-based approach to the statistical mapping of climate, *Climate Res.*, *22*, 99-113.

Dansgaard, W. (1964), Stable isotopes in precipitation, *Tellus*, *16*(4), 436-468.

Davis, S.N. (1969), Porosity and permeability of natural materials, in *Flow Through Porous Media*, edited by R.J.M. De Wiest, pp. 53-89, Academic Press, New York, NY.

Descloitres, M., M. Ritz, B. Robineau, and M. Courteaud (1997), Electrical structure beneath the eastern collapsed flank of Piton de la Fournaise volcano, Reunion Island: Implications for the quest for groundwater, *Water Resour. Res.*, *33*(1), 13-19.

Epstein, S., and T. Mayeda (1953), Variation of [18]O content of water from natural sources, *Geochim. Cosmochim. Acta, 4*, 213-224.

Etcheverry, D. and P. Perrochet (2000), Direct simulation of groundwater transit-time distributions using the reservoir theory, *Hydrogeology J., 8*, 200-208.

Evans, W.C., M.C. van Soest, R.H. Mariner, S. Hurwitz, S.E. Ingebritsen, C.W.J. Wicks, and M.E. Schmidt (2004), Magmatic intrusion west of Three Sisters, central Oregon, USA: the perspective from spring geochemistry, *Geology, 32* (1), 69-72.

Gannett, M.W., and K.E.J. Lite (2004), Simulation of regional groundwater flow in the upper Deschutes Basin, Oregon, *U.S. Geol. Surv. Water Res. Invest. Report, 03-4195*.

Gannett, M.W., M. Manga, and K.E.J. Lite (2003), Groundwater hydrology of the Upper Deschutes Basin and its influence on streamflow, in *A Peculiar River: Geology, Geomorphology, and Hydrology of the Deschutes River, Oregon, Water Sci. Appl. Ser.,* vol. 7, edited by J.E. O'Connor, and G.E. Grant, pp. 31-49, AGU, Washington, DC.

Hayhoe, K., D.R. Cayan, C.B. Field, P.C. Frumhoff, E.P. Maurer, N.L. Miller, S.C. Moser, S.H. Schneider, K.N. Cahill, E.E. Cleland, L. Dale, R. Draek, R.M. Hanemann, L.S. Kalkstein, J. Lenihan, C.K. Lunch, R.P. Neilson, S.C. Sheridan, and J.H. Verville (2004), Emissions pathways, climate change, and impacts on California, *Proc. Natl. Acad. Sci.*, *101*(34), 12422-12427.

Head, J.W., L. Wilson, and K.L. Mitchell, Generation of recent massive water floods at Cerberus Fossae, Mars by dike emplacement, cryospheric cracking, and confined aquifer groundwater release, *Geophys. Res. Lett., 30* (11), 1577, doi: 10.1029/2003GL017135, 2003.

Herrett, T.A., G.W. Hess, J.G. House, G.P. Ruppert, and M.-L. Courts (2004), Water Resources Data for Oregon, Water Year 2004, *Water Data Report OR-04-1*, 968 pp., U.S. Geol. Surv., Washington, DC.

Hilton, D.R. (1996), The helium and carbon systematics of a continental geothermal system: results from monitoring studies at Long Valley Caldera (California, U.S.A.), *Chem. Geol., 127*, 269-295.

IAEA/WMO (2005), The GNIP Database, Global Network of Isotopes in Precipitation http://isohis.iaea.org/, Int. At. Energy Agency, Vienna.

Ingebritsen, S.E. and M.A. Scholl (1993), The hydrogeology of Kilauea volcano, *Geothermics, 22*, 255-270.

Ingebritsen, S.E., R.H. Mariner, and D.R. Sherrod (1994), Hydrothermal systems of the Cascade Range, north-central Oregon, *Prof. Pap. 1044-L*, 86 pp., U.S. Geol. Surv., Washington, DC.

Izuka, S.K., and S.B. Gingerich (2003), A thick lens of fresh groundwater in the southern Lihue Basin, Kauai, Hawaii, USA, *Hydrogeology J.*, *11*, 240-248.

James, E.R., M. Manga, T.P. Rose, and G.B. Hudson (2000), The use of temperature and isotopes of O,H,C and noble gases to determine the pattern and spatial extent of groundwater flow, *J. Hydrol.*, *237*(1-2), 100-112.

Jefferson, A., G.E. Grant, S.L. Lewis, and C. Tague (2004), Geology broadly predicts summer streamflow in volcanic terrains: lessons from the Oregon Cascades, *Eos Trans. AGU*, *85*(47), Fall Meet. Suppl. Abstract H33C-0475.

Join, J.-L., J.-L. Folio, and B. Robineau (2005), Aquifers and groundwater within active shield volcanoes. Evolution of conceptual models in the Piton de la Fournaise volcano, *J. Volcanology and Geothermal Research*, *147*(1-2), 187-201.

Kiernan, K., C. Wood, and G. Middleton (2003), Aquifer structure and contamination risk in lava flows: insights from Iceland and Australia, *Environmental Geology*, *43*, 852-865.

Kilburn, C.R.J. (2000), Lava flows and flow fields, in *Encyclopedia of Volcanoes*, edited by H. Sigurdsson, pp. 291-305, Academic Press, San Diego, Calif.

Kirchner, J.W., X. Feng, and C. Neal (2001), Fractal stream chemistry and its implications for contaminant transport in catchments, *Nature, 403*, 524-527.

Lund, E.H. (1977), Geology and hydrology of the Lost Creek glacial trough, *The Ore Bin*, *39*(9), 141-156.

Maloszewski, P. and A. Zuber (1985), On the theory of tracer experiments in fissured rocks with a porous matrix, *J. Hydrol.*, *79*, 333-358.

Maloszewski, P., W. Stichler, and A. Zuber (2004), Interpretation of environmental tracers in groundwater systems with stagnant water zones, *Isotopes in Env. and Health Stud., 40,* 21-33.

Manga, M. (1996), Hydrology of spring-dominated streams in the Oregon Cascades., *Water Resour. Res*, *32*(8), 2435-2440.

Manga, M. (1997), A model for discharge in spring-dominated streams and implications for the transmissivity and recharge of quaternary volcanics in the Oregon Cascades, *Water Resour. Res*, *33*(8), 1813-1822.

Manga, M. (1998), Advective heat transport by low-temperature discharge in the Oregon Cascades, *Geology*, *26*(9), 799-802.

Manga, M. (1999), On the timescales characterizing groundwater discharge at springs, *J. Hydrol.*, *219*, 56-69.

Manga, M., and J.W. Kirchner (2004), Interpreting the temperature of water at cold springs and the importance of gravitational potential energy, *Water Resour. Res*, *40*, W05110, doi:10.1029/2003WR002905.

Mazor, E. and R. Nativ (1992), Hydraulic calculation of groundwater flow velocity and age: examination of the basic premises, *J. Hydrol, 138,* 211-22.

McGuire, K.J., J.J. McDonnell, M. Weiler, C. Kendall, B.L. McGlynn, J.M. Welker, and J. Seibert (2005), The role of topography on catchment-scale water residence time, *Water Resour. Res, 41*, W05002, doi:10.1029/2004WR003657.

Michel, R.L. (1989), Tritium deposition in the continental United States: 1953-1983, *U.S. Geol. Surv. Water Res. Invest. Report 89-4072*.

Mote, P.W., A.F. Hamlet, M. Clark, and D.P. Lettenmaier (2005), Declining mountain snowpack in western North America, *Bull. Am. Meteorological Soc.*, *86*(1), 39-49.

Nathenson, M., and J.M. Thompson (2003), Slightly thermal springs and non-thermal springs at Mount Shasta, California: Chemistry and recharge elevations, *J. Volcanology and Geothermal Research*, *121*, 137-153.

OWRD (2005), Well Log Database http://apps2.wrd.state.or.us/apps/gw/well_log/Default.aspx/, Oregon Water Resources Department, Salem, Ore.

Rademacher, L.K., J.F. Clark, D.W. Clow, and G.B. Hudson (2005), Old groundwater influence on stream hydrochemistry and catchment response times in a small Sierra Nevada catchment: Saheghen Creek, California, *Water Resour. Res*, *41*, W02004, doi:10.1029/2003WR002805.

Revil, A., A. Finizola, F. Sortina, and M. Ripepe (2004), Geophysical investigations at Stromboli volcano, Italy: implications for ground water flow and paroxysal activity, *Geophys. J. Int.*, *157*, 426-440.

Rose, T.P., M.L. Davisson, and R.E. Criss (1996), Isotope hydrology of voluminous cold springs in fractured rock from an active volcanic region, northeastern California, *J. Hydrol.*, *179*, 207-236.

Saar, M.O., and M. Manga (2004), Depth dependence of permeability in the Oregon Cascades inferred from hydrogeologic, thermal, seismic, and magmatic modeling constraints, *J. Geophys. Res.*, *109*, B04204, 10.1029/2003JB002855.

Saar, M.O., M.C. Castro, C.M. Hall, M. Manga, and T.P. Rose (2005), Quantifying magmatic, crustal, and atmospheric helium contributions to volcanic aquifers using all stable noble gases: Implications for magmatism and groundwater flow, *Geochem. Geophys. Geosys.*, *6*, Q03008, doi:10.1029/2004GC000828.

Schlosser, P., M. Stute, C. Sonntag, and K.O. Munnich (1989), Tritogenic [3]He in shallow groundwater, *Earth Planetary Sci. Lett.*, *94*, 245-256.

Scott, W.E. (1977), Quaternary glaciation and volcanism, Metolius River area, Oregon, *Geol. Soc. Am. Bull.*, *88*, 113-124.

Sherrod, D.R. (1991), Geologic map of a part of the Cascade Range between latitudes 43°-44°, Central Oregon, *U.S. Geol. Surv. Misc. Invest. Ser. I-1891*.

Sherrod, D.R., and J. G. Smith, J.G. (1990), Quaternary extrusion rates of the Cascade Range, northwestern United States and southern British Columbia, *J. Geophys. Res., 95*, 19465-19474.

Sherrod, D.R., and J.G. Smith (2000), Geologic Map of Upper Eocene to Holocene Volcanic and Related Rocks of the Cascade Range, Oregon, *U.S. Geol. Surv. Geol. Invest. Ser. I-2569*.

Sherrod, D.R., E.M. Taylor, M.L. Ferns, W.E. Scott, R.M. Conrey, and G.A. Smith (2004), Geologic Map of the Bend 30- x 60-Minute Quadrangle, Central Oregon, *U.S. Geol. Surv. Geol. Invest. Ser. I-2683*.

Stearns, H.T. (1929), Geology and Water Resources of the Upper McKenzie Valley, Oregon, *U.S. Geol. Surv. Water Supply Pap. 597-D*.

Tague, C., and G.E. Grant (2004), A geological framework for interpreting the low flow regimes of Cascade streams, Willamette River Basin, Oregon, *Water Resour. Res*, *40*, W04303 10.1029/2003WR002629.

Tague, C., G.E. Grant, M. Farrell, and A. Jefferson, Deep groundwater mediates streamflow response to climate warming in the Oregon Cascades, *Climatic Change*, in review.

Tague, C., M. Farrell, and G.E. Grant (2006), Hydrogeologic controls on summer stream temperatures in the McKenzie River basin, Oregon, *Hydrol. Processes*, in press.

Taylor, G.H., and C. Hannan (1999), *The Climate of Oregon: From Rain Forest to Desert*, 211 pp., Oregon State University Press, Corvallis, Ore.

Table 2.1. Attributes of springs

	Great	Lost	Olallie North	Olallie South	Roaring	Sweetwater	Tamolitch
Topographic watershed area (km²)	3.88	197	2.96	15.9	9.03	14.8	127
Spring elevation (m)	918	585	715	630	1100	725	725
Mean discharge (m³/s)	0.85[†]	6	1.7	2.3	1.9	1.6	4.1[‡]
Mean temperature (°C)	4.9	6.3	4.5	5.1	4.5	4.6	5.4
Temperature standard deviation (°C)	0.12	0.54	0.03	0.01	0.07	0.12	0.09
Number of days with temperature data	519	643	778	853	800	243	98
Mean $\delta^{18}O$ (‰)	-12.8	-12.9	-12.6	-12.3	-13	-12.7	-12.6
$\delta^{18}O$ standard deviation (‰)	0.46	0.10	0.05	0.03	0.05	0.05	0.11
Number of $\delta^{18}O$ samples	11	23	22	6	6	3	6
Mean recharge elevation (m)	1372	1472	1247	1072	1528	1353	1278
Estimated recharge area (km²)	20.2	114	30.7	50.5	48.1	32.4	74.1
GPE dissipation corrected temperature (°C)	3.9	4.3	3.3	4.1	3.5	3.2	4.1

[†][Stearns, 1929]
[‡]Data provided by Stillwater Sciences

Table 2.2. XRF analyses of samples collected in the vicinity of springs

	Sweetwater Spring	Olallie North	Down-slope of Olallie South	Ridge above Olallie South	Roaring (above spring)	Roaring (below spring)
Sample #	AJ-05-4	AJ-04-3	AJ-05-3	AJ-05-5	AJ-04-6	AJ-04-5
Normalized Major Elements (Weight %)						
SiO_2	50.5	50.4	50.13	51.91	55.06	54.89
TiO_2	1.688	1.672	1.665	1.403	1.104	1.113
Al_2O_3	17.05	17.1	17.08	17.77	18.21	18.23
FeO*	9.16	9.05	9.52	9.06	7.86	7.91
MnO	0.156	0.156	0.163	0.163	0.141	0.142
MgO	7.56	7.62	7.7	6.65	4.82	4.85
CaO	9.12	9.08	9.11	8.55	7.52	7.64
Na_2O	3.34	3.47	3.33	3.46	4.12	4.09
K_2O	1.02	1.04	0.91	0.66	0.85	0.83
P_2O_5	0.403	0.407	0.388	0.377	0.316	0.32
Unnormalized Trace Elements (ppm)						
Ni	133	136	144	136	73	70
Cr	220	223	229	217	99	98
Sc	27	27	28	26	21	20
V	205	203	199	204	171	172
Ba	382	395	370	366	386	393
Rb	11	8	9	6	10	9
Sr	667	662	646	502	611	617
Zr	158	148	154	158	109	109
Y	26	24	26	29	20	21
Nb	13.1	13.7	12.3	10.1	6	5.8
Ga	17	16	18	19	20	19
Cu	49	60	62	56	60	55
Zn	81	80	83	92	82	83
Pb	2	7	3	5	6	5
La	17	14	19	18	11	15
Ce	35	40	43	39	29	24
Th	2	2	1	1	3	1
Nd	21	28	23	23	18	16

Table 2.3. Tritium-helium data, helium sources, and residence time estimates

	Great	Lost	Olallie North	Olallie South	Roaring	Tamolitch
^{3}H (TU)	3.83	3.57	4.18	4.38	4.67	4.61
^{4}He$_{meas}$ (cm^3/g STP)	$1.14*10^{-7}$	$1.10*10^{-7}$	$3.37*10^{-7}$	$6.74*10^{-8}$	$7.29*10^{-8}$	$6.41*10^{-8}$
Ne$_{meas}$ (cm^3/g STP)	$2.55*10^{-7}$	$2.33*10^{-7}$	$5.20*10^{-7}$	$2.13*10^{-7}$	$2.78*10^{-7}$	$2.27*10^{-7}$
(^{3}He/^{4}He)$_{meas}$/R$_a$	1.16	2.14	0.93	1.14	0.96	1.08
(^{3}He/^{4}He)corr/R$_a$	1.32	3.19	0.90	1.48	0.74	1.38
^{3}H/^{3}He mean transit time (yrs)	26.0	54.5	20.3 ‡	16.5	4.1 †	11.4
Lower Uncertainty Limit	25.5	54.0	19.8	16.1	3.4	10.9
Upper Uncertainty Limit	26.5	55.1	20.7	16.9	4.1	11.7
Exponential mean transit time (yrs)	13.3		10.1	8.7	4.4	7.1
Lower Uncertainty Limit	12.9		9.9	8.6	4.0	7.0
Upper Uncertainty Limit	13.7		10.3	8.9	4.4	7.2
Gamma mean transit time (yrs)	13.6		8.7	7.0	3.2	5.4
Lower Uncertainty Limit	12.9		8.4	6.8	2.9	5.2
Upper Uncertainty Limit	14.4		8.9	7.1	3.2	5.4

‡ Entrapment of an air bubble during sampling yielded spurious results. ^{3}He$_{trit}$ was estimated from interpolation between Olallie South Spring and Great Spring values, based on their ^{3}H measurements.
† Calculated (^{3}He/^{4}He)$_{terr}$ yielded a negative age, (^{3}He/^{4}He)$_{terr}$ of 0.007 (crustal endmember) was used to calculate ^{3}He$_{trit}$.

Figure 2.1. (a) Extent of High Cascade and Western Cascade volcanic rocks in Oregon [*Sherrod and Smith,* 2000], with the McKenzie River watershed (black outline) and some adjacent physiographic regions for reference. (b) Topography of the upper portion of the McKenzie River watershed showing Western Cascade geology (shading), locations of springs (stars), the cross-section illustrated in Figure 2.2 (light line), and the area discussed in Section 5.1 (black outline). (c) Locations of hydrologic and geologic features referred to in text. The McKenzie River watershed forms the map boundary. In the vicinity of Irish Mountain, depicted lava is undifferentiated 120,000-780,000 basalt and basaltic andesite. Geology is based on [*Sherrod and Smith*, 2000; *Sherrod et al.*, 2004]. Lost Spring's watershed is calculated below the spring, where the stream channel is single-thread.

Figure 2.1.

58
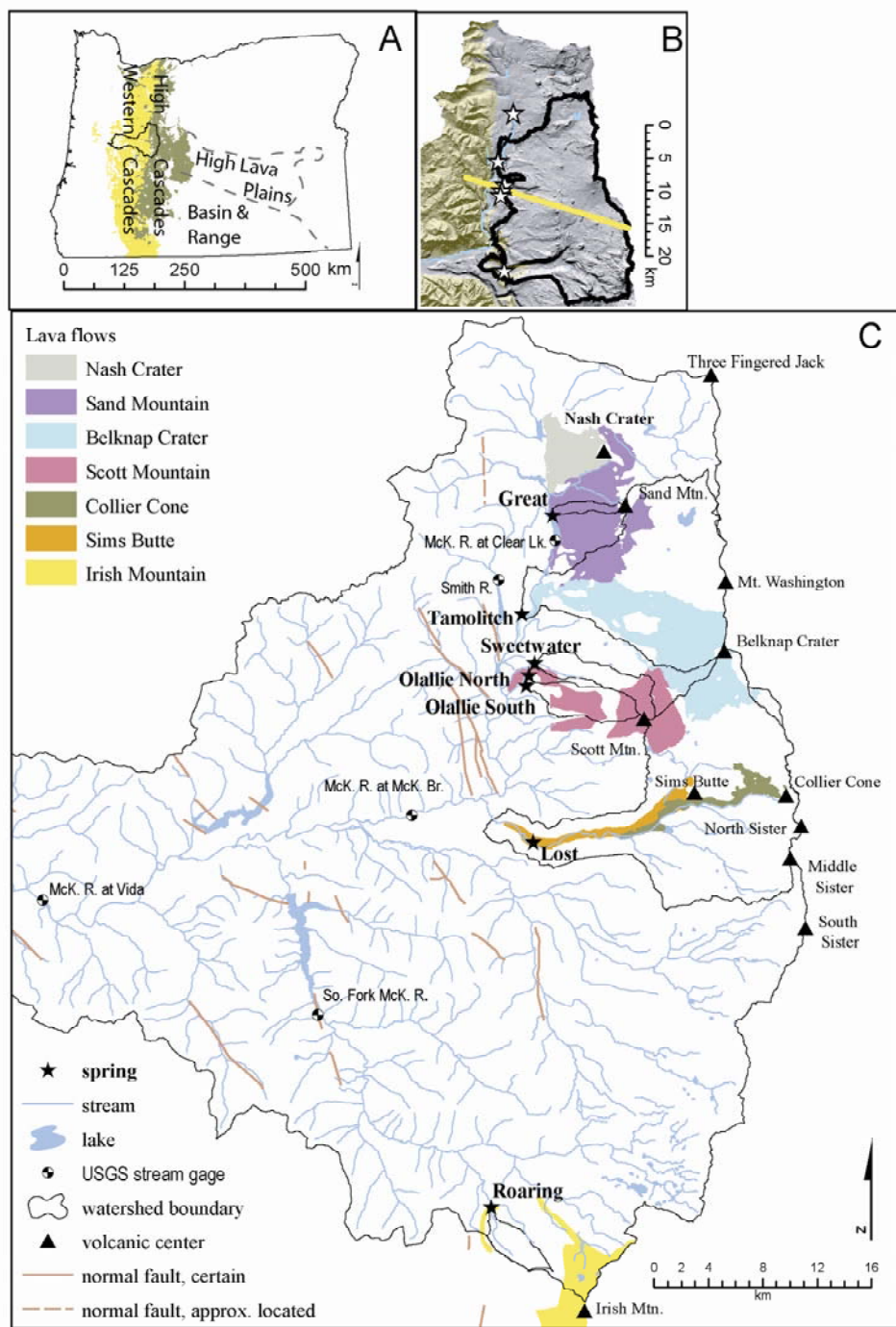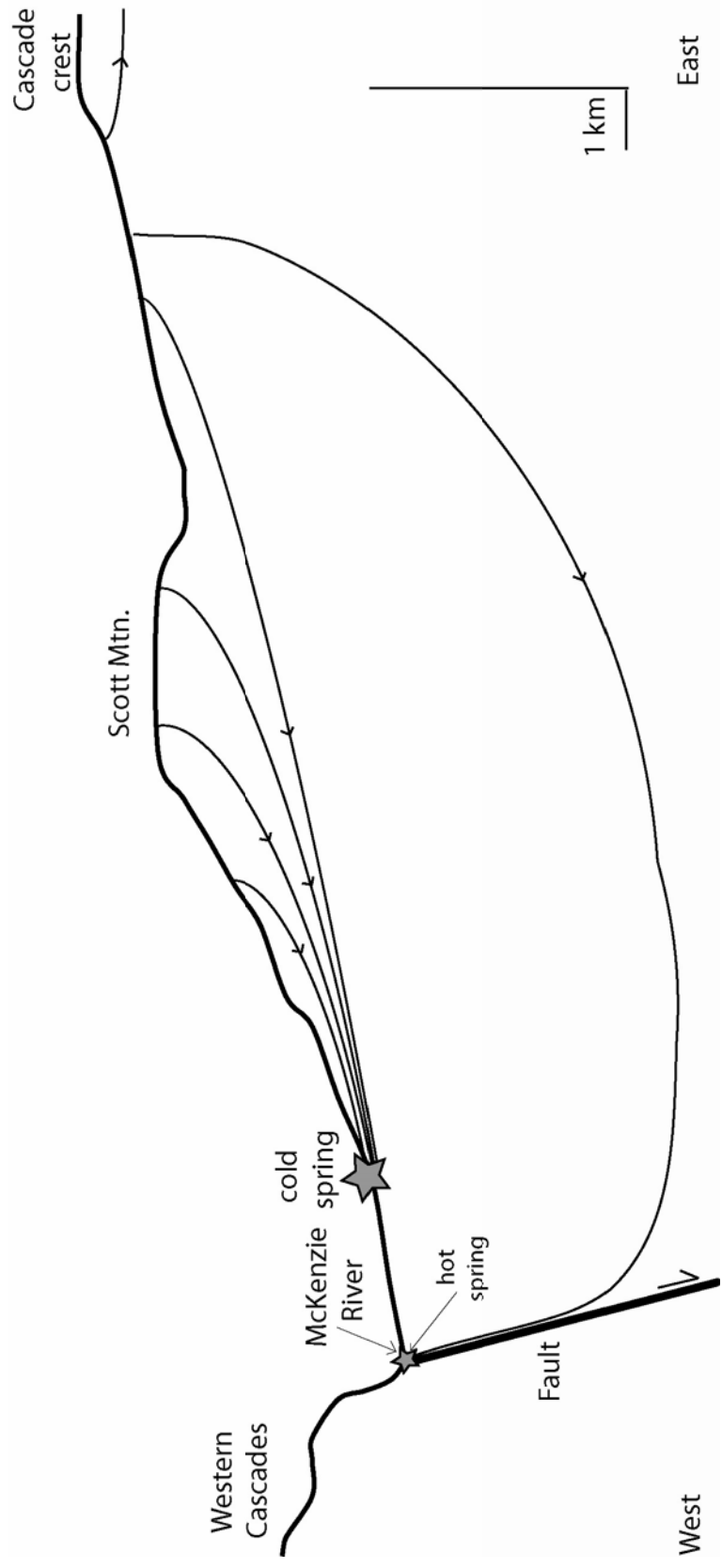
Figure 2.2. Cross-section from the Cascade crest to the Western Cascades along the line in Figure 2.1b. Actual topography is shown, but flowpaths are conceptual. Hot springs occur where deep groundwater flowpaths are interrupted by faults [*Ingebritsen et al.*, 1994], while cold springs are the result of shallower flowpaths.
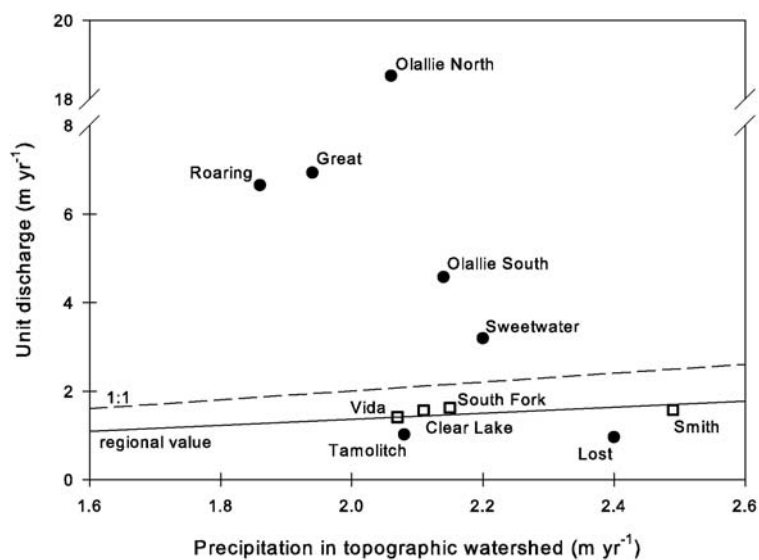
Figure 2.3. Relationship between unit discharge and precipitation for springs (black circles) and USGS gages (open squares) for water year 2004. The regional value line represents the runoff ratio for the McKenzie River at Vida (0.68). USGS gages aggregate both spring-fed and runoff-dominated streams.
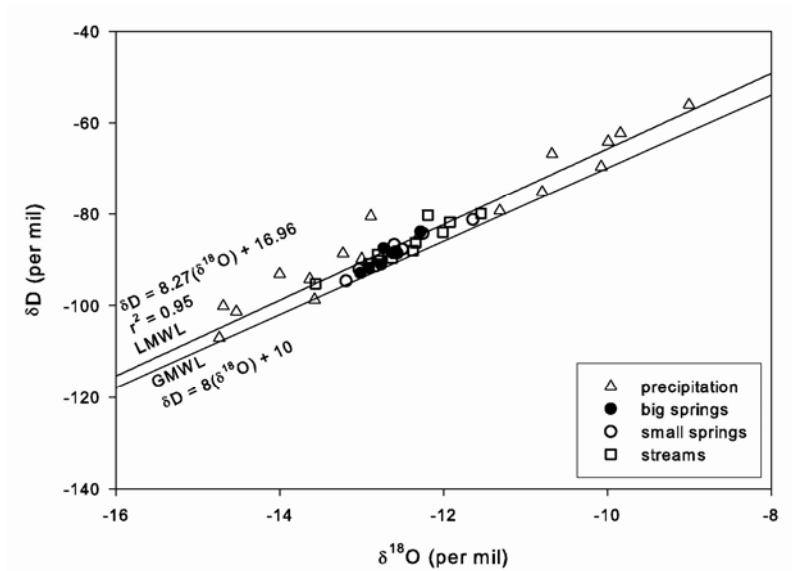
Figure 2.4. Relationship between $\delta^{18}O$ and δD for springs, streams, and precipitation in the McKenzie River watershed for samples collected in this study. GMWL is the global meteoric water line [*Craig*, 1961], and LMWL is the local meteoric water line, representing the best fit through the data. Points represent averages of all data for each site.
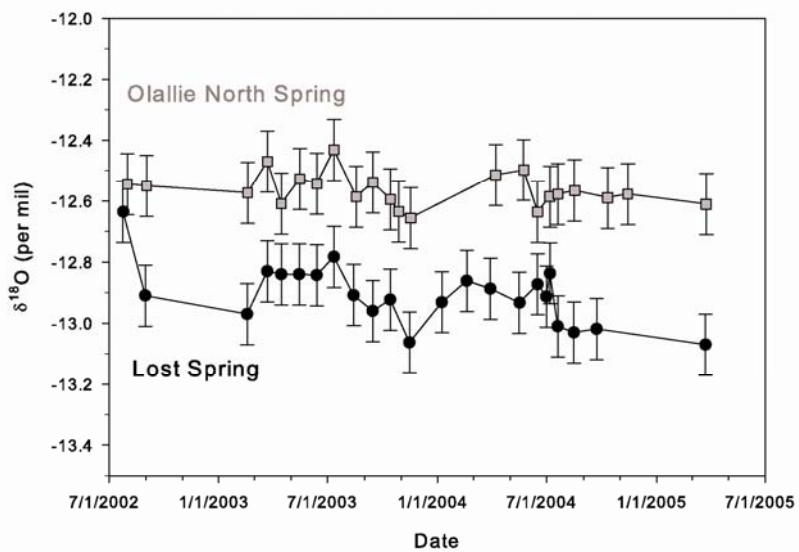
Figure 2.5. Time series of $\delta^{18}O$ data for two large springs, with analytical error bars of 0.1‰. The annual range in precipitation $\delta^{18}O$ for a nearby watershed was 8‰ for the years 2000-2002 [*McGuire et al.*, 2005].
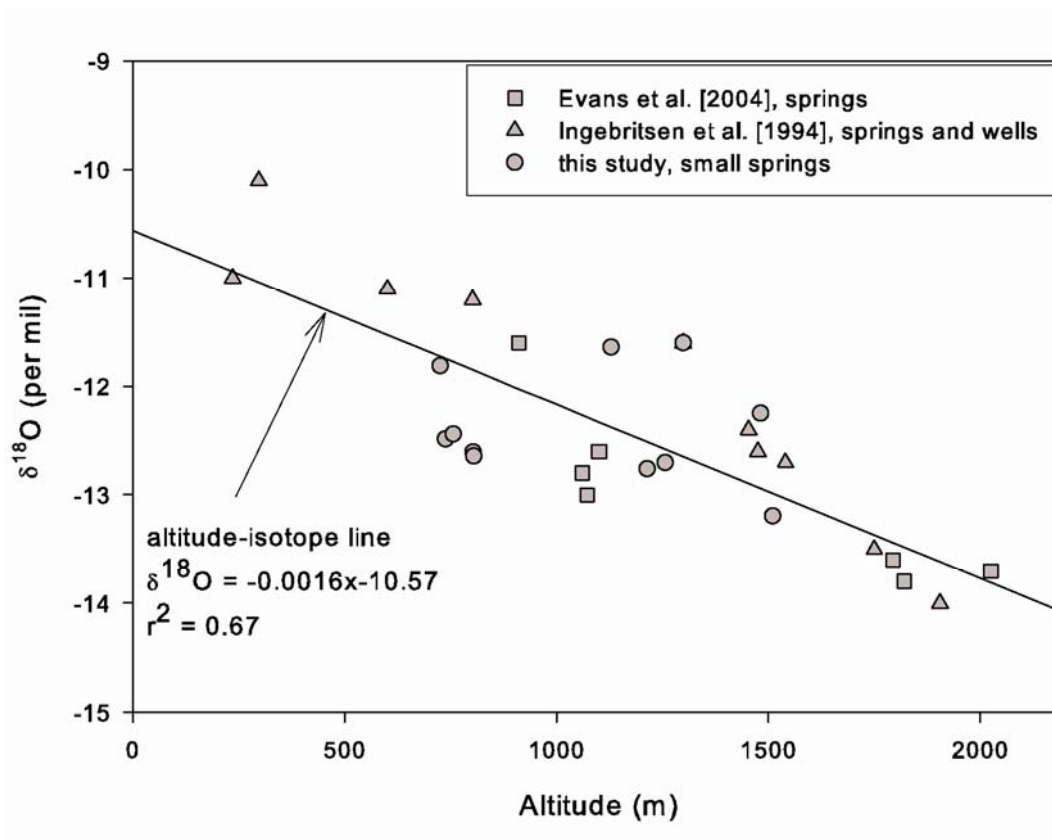
Figure 2.6. Relationship between altitude and $\delta^{18}O$ for small springs and wells, within and west of the study area. Altitude-isotope line is a regression through small spring data from this study, along with data from Ingebritsen *et al.* [1994] and Evans *et al.* [2004] for small springs and wells.
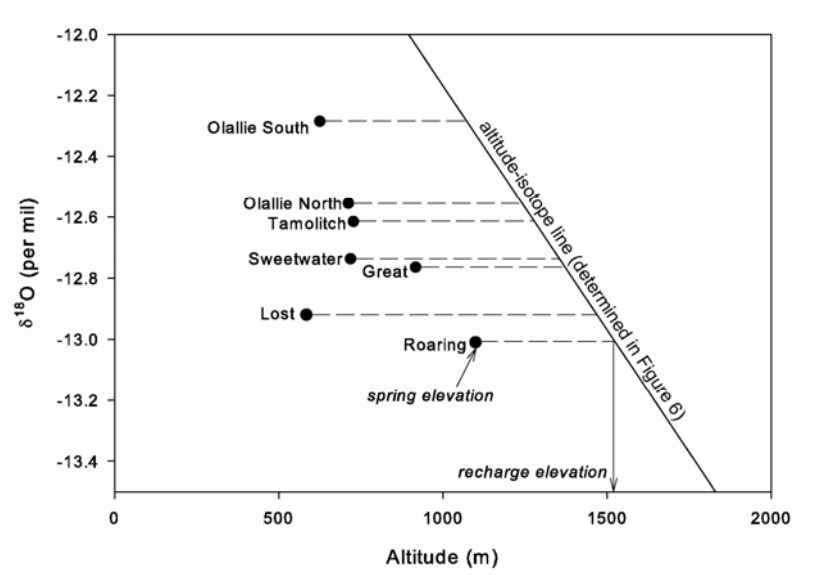
Figure 2.7. Calculation of mean recharge elevations, based on the altitude-isotope line determined in Figure 2.6 and average $\delta^{18}O$ of the large springs. Recharge elevations are determined by extrapolating the average $\delta^{18}O$ of each spring to the altitude-isotope line, and dropping a perpendicular to the x-axis.

Figure 2.8. Surface topography, inferred groundwater flowpaths, and recharge areas, based on geology and estimated recharge elevation and area. Cascade crest forms eastern edge of the map.
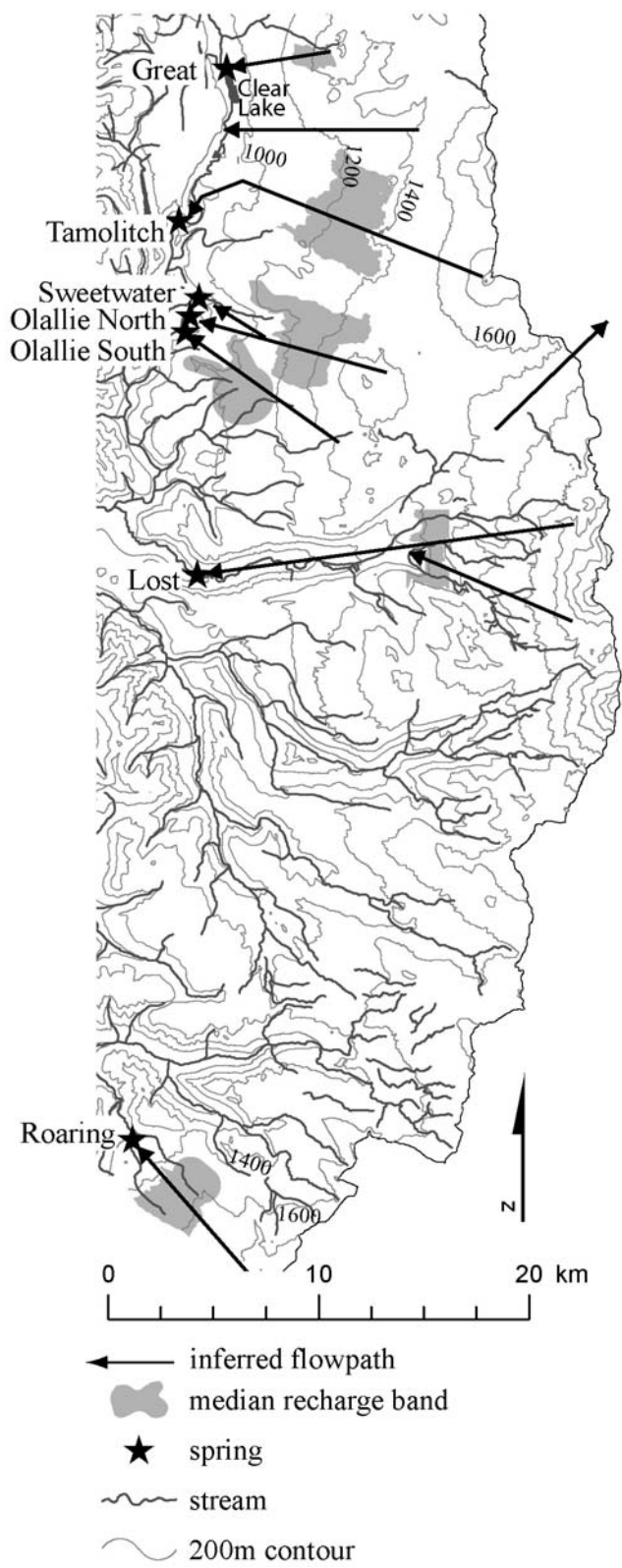
Figure 2.8.

3 Hydrogeologic controls on streamflow sensitivity to climate variation

3.1 Abstract

Climate models for the Northwest predict warmer temperatures, resulting in reduced snowpacks and summer streamflow. We examine how groundwater, snowmelt, and regional climate patterns control discharge at multiple time scales, using historical records from two watersheds with contrasting geologic properties and drainage efficiencies. In the groundwater-dominated watershed, aquifer storage and the associated slow summer recession are responsible for sustaining discharge even when the seasonal or annual water balance is negative, while in the runoff-dominated watershed subsurface storage is exhausted every summer. There is a significant 1-year cross-correlation between precipitation and discharge in the groundwater-dominated watershed (r=0.52), but climatic factors override geology in controlling the inter-annual variability of streamflow. Warmer winters and earlier snowmelt over the past ~60 years have shifted the hydrograph, resulting in summer recessions lasting 2 weeks longer and autumn minimum discharges 27% lower. The slow recession of groundwater-dominated streams makes them more sensitive than runoff-dominated streams to changes in snowmelt amount and timing.

3.2 Introduction

The Cascade Range mountains provide critical water supply for agriculture, municipalities, and ecosystems in the Pacific Northwest region of the United States. Recent analyses show that this region is sensitive to current and projected climate warming trends, specifically reduced snow accumulation and earlier spring melt, leading to a decline in summer streamflow. Temperature trends over the past half-century indicate warmer winters across the western United States [*Folland et al.*, 2001] and particularly in the Pacific Northwest [*Mote*, 2003]. These data are corroborated by ample proxy evidence of recent temperature increases in the Pacific

Northwest [*Cayan et al.*, 2001; *Regonda et al.*, 2005; *Stewart et al.*, 2005]. Snowpacks in western North America have declined over the past 50 years, primarily due to an increase in winter temperature [*Mote et al.*, 2005]. In accordance with earlier spring snowmelt, streamflow timing is earlier by one to four weeks than during the middle of the 20th century [*Stewart et al.*, 2005]. Climate models predict continued winter warming of 0.2 to 0.6°C per decade in the Pacific Northwest [*Washington et al.*, 2000; *Mote et al.*, 2003]. By 2050, Cascade snowpacks are projected to be less than half of what they are today [*Leung et al.*, 2004], potentially leading to major water shortages during the low-flow summer season. Regional-scale analyses identify climatic gradients as primary controls on changing streamflow regimes, but the potential for other hydrologic factors, notably groundwater, to influence this response has received much less attention.

In many watersheds, snowpack is the dominant water storage compartment, and snowmelt is quickly translated into streamflow. In the western United States, where there is little summer rainfall, the snowmelt peak is often the year's highest discharge event, and marks the beginning of a long decline in streamflow through the summer months. In watersheds where the bedrock is basalt, limestone or fractured rock, groundwater systems can mediate the translation of water from snowpack to streamflow by providing an additional storage compartment and damping variations in precipitation and recharge.

Our objective is to develop an understanding of how discharge is controlled at the event, seasonal, and inter-annual scales by the interactions among groundwater storage, snowmelt dynamics, and regional climate signals. The over-arching goal is to better predict hydrologic responses to future climate change in groundwater-dominated watersheds of the western United States. The focus of our research is an analysis of the historical discharge, precipitation, and snowpack records from two adjacent watersheds on the west slope of the Oregon Cascades. One watershed has an extensive groundwater system (McKenzie River at Clear Lake), while the other

watershed is runoff-dominated with little groundwater storage (Smith River). Results from the study watersheds should be broadly applicable to geologically similar watersheds in the Oregon Cascades and northern California.

Summer and autumn discharges are particularly important because they occur during periods of low flows, high water demand, and critical temperatures and flows for salmonids and other species. Decreases in summer streamflows restrict junior water rights users, constrain hydropower generation, and make in-stream flow targets difficult to meet. Lowered summer discharge can also exacerbate stream temperatures warmed by hot summers [*Webb et al.*, 2003], and some species are very temperature-sensitive [*Selong et al.*, 2001], such as the threatened bull-trout that inhabits the McKenzie River watershed. Decreased minimum flows have also been linked to drought stress and mortality in riparian vegetation [*Naiman et al.*, 1998].

Most watersheds on the western slopes of the Oregon Cascades encompass elevations that receive winter precipitation as a mixture of rain and snow. These watersheds have complex winter hydrographs that are dependent on the distribution of rain and snow during individual events, which in turn is controlled by storm temperatures and catchment hypsometry. Snow cover typically accumulates at temperatures close to the melting point, and thus is at risk from climate warming because temperature affects both the rate of snowmelt and the phase of precipitation. With a projected 2°C winter warming by mid-century, 9200 km^2 of currently snow-covered area in the Pacific Northwest would receive winter rainfall instead [*Nolin and Daly*, 2006].

Spatial patterns of summer streamflow in the Oregon Cascades exhibit significant differences between the geologically-distinct High and Western Cascade provinces [*Tague and Grant*, 2004]. A key control on these differences is the partitioning of water to slow-draining basaltic aquifers in the High Cascades, versus shallow subsurface storm flow through the upper few meters of soil and bedrock in the Western Cascades. *Saar and Manga* [2004] estimated a groundwater recharge rate of

100 cm/yr for the High Cascades, while Ingebritsen and others [1994] estimated a recharge rate of 3 cm/yr for the Western Cascades bedrock aquifers. High Cascades aquifers volumes are ~7 times greater than annual discharge [*Jefferson et al.*, 2006]. Groundwater discharge to High Cascades streams also has a moderating effect on water temperatures, resulting in lower diurnal variability and colder summer temperatures [*Tague et al.*, 2006].

Tague et al. [in review] used the hydro-ecological model RHESSys to examine the influence of geology on streamflow response to 1.5°C and 2.8°C warming scenarios. Their study included the High Cascades watershed used in this project, McKenzie River at Clear Lake. Their model showed that warmer temperatures resulted in greater reductions in August discharge and annual minimum flows for the High Cascades than the Western Cascade watershed, both in terms of absolute volumes and normalized by drainage area. The Western Cascade stream, however, showed greater relative reductions in these summer streamflow metrics. Model results illustrate that differences between the responses of the two sites were primarily due to differences in groundwater flow, as manifested in drainage efficiency of the watersheds. Spatial differences in recharge characteristics and the timing of snow accumulation and melt were shown to be important, but secondary, in terms of explaining responses at the two sites. Further, they found that in the 2.8°C warming scenario, August discharge of the McKenzie River at Clear Lake was reduced 23% from current mean values.

This study complements the previous model-based analysis through in-depth analysis of meteorological and streamflow records in order to more fully characterize climate-snowmelt-groundwater interactions for the Oregon Cascade region. To build insight, we present analyses of discharge dynamics at the event, seasonal, inter-annual, and decadal time scales, utilizing time-series analyses and correlations between parameters. While we explore dynamics during all seasons, we particularly focus on late summer streamflow because of its importance for water resources. Through these analyses, we identify the primary and secondary controls on discharge variability at

each time scale. This will facilitate model development that appropriately factors in the influence of geologic setting and in order to better predict the effects of future climate variability and change.

3.3 Study watersheds

The two study watersheds adjoin each other in the upper McKenzie River watershed on the west side of the Oregon Cascades (Figure 3.1). The McKenzie River at Clear Lake is located at N 44° 22', W 122° 0'. The watershed upstream from that point (the Clear Lake watershed) covers 239 km^2 and ranges in elevation from 918 to 2051 m, with an average elevation of 1215 m. The Smith River above Smith River Reservoir is located at N 44° 20', W 122° 02', with an area of 42 km^2 and elevations ranging from 803 to 1753 m; average elevation is 1216 m. The Smith River is tributary to the McKenzie River 16 river km downstream of Clear Lake and 6 km downstream of the Smith River gauge. The McKenzie River provides water and electricity for the second largest city in Oregon, supports a major recreational economy, and sustains superb salmonid habitat. The McKenzie River is a major tributary to the Willamette River, one of the largest rivers in the United States.

The study watersheds lie within the Cascades volcanic arc, which includes two distinct geologic provinces: the High Cascades and the Western Cascades. The High Cascades are known for their active composite volcanoes and extensive Quaternary basaltic lavas, while the Western Cascades are the products of Tertiary arc volcanism, and have been extensively folded, faulted, and weathered [*Priest et al.*, 1983]. High Cascade lava flows have high permeability, resulting in extensive groundwater systems, low slopes, and low drainage densities [*Jefferson et al.*, 2006; Chapter 4], whereas the Western Cascades are deeply dissected with well-developed drainage-networks and shallow subsurface storm flow [*Harr*, 1977]. We use the mapping of *Sherrod and Smith* [2000] to define the High Cascades as including all Quaternary igneous rocks and glacial till, while the Western Cascades includes all Tertiary

igneous rocks. The Clear Lake watershed is 66% High Cascades, 25% Western Cascades, and 9% lakes and alluvium. The Smith River watershed is composed entirely of Western Cascades geology.

The study watersheds are largely forested, although cover is patchy on the youngest lava flows in the Clear Lake watershed. Forests include stands of Douglas fir (*Pseudotsuga menziesii*), noble fir (*Abies procera*), Pacific silver fir (*Abies amabilis*), and western hemlock (*Tsuga heterophylla*). Wet and dry meadows are also found throughout the watersheds.

Daily discharge data for the study watersheds are available from the U.S. Geological Survey streamflow gages. For the McKenzie River at Clear Lake, data are available for the 1913-1915 water years (water years begin October 1) and continuously since October 1947 (gage # 14158500) [*Herrett et al.*, 2005]. Summer flow in the McKenzie River at Clear Lake consists largely of discharge from springs along the lakeshore. Additional wet season discharge includes direct precipitation onto the 0.6 km^2 lake, seasonal runoff from Fish Lake, and perennial runoff-dominated flow from Ikenick Creek. Based on occasional discharge measurements from August 2003 to September 2005, Ikenick Creek is a very minor contributor of summer flow to the McKenzie River at Clear, ranging from 3% on June 6, 2005 to 0.03% on September 20, 2005. Runoff from the creeks is probably much more significant during snowmelt periods. For Smith River (gage # 14158790), USGS daily discharge data are continuously available since October 1960 [*Herrett et al.*, 2005]. Smith River is runoff-dominated with no lakes or mapped springs.

There are two Natural Resources Conservation Service snowpack telemetry (SNOTEL) sites within the Clear Lake watershed that collect real-time, automated measurements of snow water equivalent (SWE), precipitation, and temperature [*http://www.wcc.nrcs.usda.gov/snow/*]. The Hogg Pass SNOTEL is located at 1451 m and Santiam Junction SNOTEL is at 1143 m. A third SNOTEL site, Jump Off Joe

(1067 m), lies <5 km west of the study watersheds [*http://www.wcc.nrcs.usda.gov/snow/*]. Approximately 20% of the Clear Lake watershed has an elevation higher than Hogg Pass, 63% is higher than Santiam Junction, and 83% is higher than Jump Off Joe. For Smith River, 12%, 64%, and 83% of the watershed area lies above the three SNOTEL stations respectively.

Annual precipitation ranges from 1000 to 3200 mm, and 70% falls between November and March, based on the historical data from the SNOTEL stations. The watersheds receive a mixture of rain and snow at all elevations. At Hogg Pass, 56% of annual precipitation accumulates as snow, whereas at Santiam Junction it is 37%, and at Jump Off Joe it is 25%. From 400 to 1200 m elevation in the Cascades, snowpacks may accumulate and melt several times in the winter season and rain-on-snow events are common [*Harr*, 1981]. Above this elevation, a seasonal snowpack of 2 to >7 m accumulates through the winter months and melts over the period March through June. In forested areas of the Cascades, up to 60% of falling snow can be intercepted by the forest canopy, but is later released by melt drip or falling snow masses. Sublimation accounts for only a minor component of ablation [*Storck et al.*, 2002]. Peak snow accumulation occurs around April 1st at Hogg Pass, and around March 1st at Santiam Junction and Jump Off Joe. The highest monthly stream discharge at both Clear Lake and Smith River have historically occurred in May, due to snowmelt, but peak flow events may be triggered by rain or rain-on-snow earlier in the water year.

3.4 Data compilation and analysis

We compiled daily time series datasets for discharge, precipitation, snow water equivalent, and temperature from the available USGS and SNOTEL records. Varying record lengths, as described below, were used for the analyses. Quality control on SNOTEL records was performed by the Oregon Climate Service [*Daly, pers. comm.,* 2005]. The Santiam Junction and Jump Off Joe SNOTEL sites precipitation and SWE records extend from water year 1979 through 2005, while for Hogg Pass precipitation

and SWE records are from water years 1980 through 2005. Temperature records for Hogg Pass and Jump Off Joe span water years 1985-2003. For Santiam Junction, temperature records span 1983-2003. Reported minimum and maximum daily temperatures were averaged to generate a single daily value for temperature.

In order to understand the relationship between climatological and hydrological variables in space and time, we performed Pearson's correlations, autocorrelations, and cross-correlations. Annual values of 49 parameters were derived from the discharge, precipitation, snow water equivalent, and temperature time series (Table 3.1). Pearson's product moment correlations were calculated for 41 parameters. Daily values of discharge, precipitation, SWE, and recharge (rain + snowmelt) for 1979-2005 were normalized using daily means, and auto- and cross-correlations were computed following *Box and Jenkins* [1976]. A similar analysis was conducted for annual time-series. Autocorrelation and cross-correlation procedures generate correlation coefficients for data pairs separated by variable time lags. Autocorrelation is a measure of correlation between values in a single series, while cross-correlation is a measure of correlation between values in two different series. The number of data pairs used to generate an auto- or cross-correlation coefficient varies with the lag, so for our purposes we considered $r < 0.25$ as insignificant.

Monthly values of the Niño 3.4 Index of sea surface temperature [*Trenberth and Stepaniak*, 2001] and the Southern Oscillation Index of surface pressure [*Ropelewski and Jones*, 1987] over the period 1978-2004 were used to explore correlations between El Niño/Southern Oscillation (ENSO) with annual discharge and snow water equivalent. We also correlated discharge and SWE with the Pacific Decadal Oscillation (PDO) data set from the University of Washington [*Mantua et al.*, 1997].

A simple water balance for the Clear Lake watershed was constructed for the 2001-2004 water years to examine the magnitudes and seasonal variations in water fluxes and stores. Discharge was calculated at the USGS gage, and precipitation, SWE, and

rain plus snowmelt at the areally weighted average basin elevation (1215 m) were derived by linear interpolation from values at Jump Off Joe and Hogg Pass. We also tested the linear interpolations of seasonal precipitation and rain plus melt against observed values at Santiam Junction. Basin-averaged evapotranspiration (ET) was calculated in RHESSys, a physically-based hydro-ecological model previously calibrated for the Clear Lake watershed [*Tague et al.*, in review]. ET estimates in RHESSys account for canopy transpiration, evaporation of canopy interception, litter/soil evaporation and snow sublimation losses. ET losses are calculated using Penman or Penman-Monteith approaches. Additional details on the RHESSys modeling approach are available in *Tague and Band* [2004].

Predictive models of September-November minimum discharge using available climatic and hydrologic measurements were developed using stepwise regression in SAS 9.1 (Table 3.1). Separate models were developed for the Clear Lake and Smith River watersheds. The models were based on data from the 1979-2005 water years, and stepwise selection of parameters proceeded until all variables in the model were significant at the 0.05 level and no other variables met the 0.05 significance level for entry into the model. Colinearity was minimized by manual elimination of strongly correlated variables.

3.5 Event and seasonal scale variability

The groundwater-dominated Clear Lake watershed exhibits a muted hydrograph response relative to the adjacent Western Cascade, runoff-dominated Smith River watershed (Figure 3.2). Base flows are higher, and peak flows are less frequent, smaller, and somewhat delayed relative to Smith River. Peak flows are generated by rain-on-snow, snowmelt, and rain events, with rain-on-snow events typically having sharp, isolated peaks. For example, on January 7-9, 2002 (event A in Figure 3.2), 53 mm of precipitation fell at Santiam Junction yielding an additional 44 mm of melt. The McKenzie River at Clear Lake had a peak flow 2 times greater than the pre-event

flow, while Smith River peak flow was 6 times greater than before the event. Snowmelt events are generally sustained, building gradually to their peak flows, often with intermediate peaks. For example, between April 1st and 23rd, 2002 (event B), 188 mm of precipitation fell at Santiam Junction and 564 mm of snow melted. The peak flow of the McKenzie River at Clear Lake was 4 times greater than the pre-event discharge, while at Smith River it was 8 times greater. Flows twice as large as the pre-event discharge were sustained for 14 days in the McKenzie River at Clear Lake and 6 days in the Smith River. The magnitude of response to rain events depends largely on the antecedent wetness in the watershed. For example, ~60 mm rain events in October 21, 2000 and May 15-16, 2001 (events C and D) produced very different hydrographs.

Annual unit discharge of the McKenzie River at Clear Lake and the Smith River are comparable, but the September unit discharge at Clear Lake is over six times higher than at Smith River, as illustrated in Figure 3.2. The ratio of May to September monthly discharge at Clear Lake is only 3.3, while for the Smith River it is 39.8. *Tague and Grant* [2004] provide an extended discussion of the low flow characteristics of High and Western Cascade streams and attribute the slow summer recession of High Cascade streams to their groundwater inputs.

Clear Lake and Smith River have very different autocorrelation structures (Figure 3.3a). The auto-correlation coefficient for Clear Lake remains above 0.25 for 89 days, whereas at Smith River r > 0.25 occurs only for 5 days, and it lasts only for 2 days when calculated for a recharge time series derived from rain and snowmelt at Hogg Pass. These results suggest that all stream systems have somewhat damped discharge variation relative to the input variation as estimated from a single SNOTEL site. Damping of the input signal reflects the distribution of response times of shallow subsurface and groundwater flow and in the channel network. The prevalence of longer response times associated with groundwater systems of the Clear Lake watershed result in substantial smoothing of the hydrograph and sustained high

autocorrelation values, relative to the faster shallow subsurface flow, runoff-dominated Smith River.

The maximum cross-correlation between discharge of Clear Lake and Smith River occurs at a one-day lag (Figure 3.3b), as do the peak cross-correlations of Clear Lake discharge and recharge at Santiam Junction and Jump Off Joe. These results suggest that the Clear Lake watershed experiences a minimal lag in discharge relative to the recharge time series or a runoff-dominated stream. This result is in stark contrast to the results of Manga (1999), who found a lag of 47-137 days for four snowmelt-dominated spring-fed streams on the east side of the Oregon Cascades using the delay from annual peak flow in runoff-dominated streams to annual peak flow in neighboring spring-fed streams. Manga (1999), however, used measurements directly from springs. *Tague et al.* [in review] show that discharge from Clear Lake includes both spring and shallow subsurface flow contributions. Thus, short lag times reflect the "fast" shallow subsurface component of the Clear Lake system. *Tague and Grant* [2004] also report greater lags in their analysis of Western versus High Cascade streams. However, their analysis used center of mass rather than peak of cross-correlations in order to emphasize seasonal rather than event responses.

There are also moderate cross-correlations between Clear Lake discharge and SWE at the 3 SNOTEL sites. The peak cross-correlations occur at 74 to 82 day lags, which represents the average time from snowfall to snowmelt plus the travel time of the snowmelt response signal through the watershed. Elevational differences are also apparent in the cross-correlation signal. For short lags, there is a moderate positive correlation between Hogg Pass SWE and discharge, because snow at high elevations may reflect rain at lower elevations, which, in turn, can lead to increasing discharge. There is no correlation between Santiam Junction or Jump-Off Joe SWE and Clear Lake discharge at short lags.

3.6 Water budget

For the four year period of 2001-2004, discharge plus ET equaled 101% of precipitation in the Clear Lake watershed (Figure 3.4). On the annual time-scale, ET was 26% of precipitation, which is almost exactly the same as the ET portion of a 30-year water balance calculated for Smith River watershed [*Jefferson and Grant*, 2003] and within the range of values reported for Western Cascade forests [*Jones and Post*, 2004]. The good match of the annual inputs and outputs and the concordance of ET estimates with regional values lend support to the seasonal water balance calculations. The interpolations based on linear regression from Hogg Pass and Jump Off Joe over-predict the control (Santiam Junction) record. We expected this because Santiam Junction lies in the rain shadow of the Western Cascades and often becomes snow-free earlier than Jump Off Joe. The purpose of interpolating precipitation and rain plus melt was to predict basin-averaged fluxes, and PRISM models show variation within the watershed based on both elevation and location [*Daly et al.*, 1997; *Daly et al.*, 2002].

We divided the year into three seasons based on the status of the snowpack. November through March constitutes the snow accumulation season; April through June is the snow ablation season; and July through October is the snow-free season. In the snow accumulation season, 35% of precipitation is stored as snowpack, 47% is accounted for as discharge, and 4% is lost to ET. The remaining 15%, ~200 mm, probably goes to replenishing the soil moisture supply and groundwater storage. In the snow ablation season, ET loss accounts for 49% of incoming precipitation and discharge is 138% of incoming precipitation. Abundant snowmelt, during the snow ablation season, supplies enough water to account for discharge and to provide ~125 mm to groundwater storage. In the snow-free season, discharge and ET are 260% of precipitation, and groundwater storage diminishes to sustain streamflow and supply water to vegetation.

Slight imbalances in water budgets are expected on an annual basis, because of fluctuating aquifer storage. Annual imbalances range from -5% to +10%, when discharge plus ET is compared to precipitation. Snowpack storage had varying importance between 2001 and 2005, depending on the size of the snowpack, timing of the melt, and the amount of spring rain. In 2002, snowmelt was 137% of April through June discharge, but in 2005, it was only 29% due to a warm dry winter combined with a wet spring.

3.7 Inter-annual variability

Generally, discharge, precipitation and SWE vary together throughout the period of record and among the 3 SNOTEL sites (Table 3.2). Mean annual discharges at Clear Lake and Smith River are strongly correlated with annual precipitation at all three sites (r>0.88), but only at Hogg Pass is there a strong correlation between accumulated snow water equivalent (SWE) and mean discharge (r=0.74 for Clear Lake). August discharge at Clear Lake was more strongly correlated with all but two of the precipitation and SWE parameters than was August discharge at Smith River, suggesting that summer streamflow in the groundwater-fed watershed is more strongly linked to hydroclimatic conditions than summer streamflow in the runoff-dominated watershed. Winter temperature was most strongly correlated with accumulated SWE at Jump Off Joe (r=-0.71), which lies within the transient snow zone and is strongly affected by temperature-induced phase changes in precipitation. The amount of peak SWE and the date at which it is reached are only weakly correlated for any individual site (r<0.55).

There is an inter-annual memory in the Clear Lake watershed as a result of the High Cascades groundwater system. Discharge at Clear Lake is moderately cross-correlated with the previous year's precipitation (r=0.52 for Hogg Pass), which is higher than the 1-year discharge autocorrelation (r=0.45). Both of the above correlations for Clear Lake discharge are higher than those for Smith River discharge with that of the

previous year or the 1-year lagged autocorrelation of precipitation, which are not statistically significant. At 2 year lags and beyond all auto- and cross-correlations are not statistically significant.

We examined and quantified the relationships between two major climate indices that have been correlated with streamflow in the Pacific Northwest: El Niño/Southern Oscillation Index and the Pacific Decadal Oscillation [*Beebee and Manga*, 2004]. Correlations between SWE and the monthly Niño 3.4 index for 1977-2000 were highest for the month of December, and were stronger for the lower elevation SNOTEL sites. Hogg Pass SWE had a correlation of -0.54 with December Niño 3.4, while the correlation at Santiam Junction was -0.60, and that at Jump Off Joe was -0.63. These finding suggest that the temperature shifts associated with the ENSO cycle are more important than the precipitation signal in determining snow accumulation in the transient snow zone. There were no significant correlations with annual or August discharge in either watershed. These results indicate that ENSO, as explained by the Niño 3.4 index, is a moderate predictor of SWE, but not of discharge. We also explored correlations using the SOI but found that the correlations were much lower than for the Niño 3.4 index. Using the PDO index, we found that there were no significant correlations with annual discharge, August discharge or station SWE.

Our results contrast with those of *Beebee and Manga* [2004] who found inverse correlations between annual discharge, peak runoff and ENSO for eight snowmelt dominated watersheds in central and eastern Oregon. However, our study area has a higher proportion of rain versus snow than the watersheds they studied, and it is also substantially more humid. They also used the SOI averaged over June-September and Niño 3.4 averaged over September-November. We used individual monthly values of the indices rather than seasonal aggregates to better understand the time lags between discharge and the climate indices. We found lower correlations for seasonally averaged values of both SOI and Niño 3.4. Like *Beebee and Manga* [2004], we found no significant correlation with PDO.

3.8 Autumn minimum discharge

The presence of groundwater also strongly influences the lowest flows of the year. Annual minimum discharge occurred between September and November during 52 of 64 years of the Clear Lake record and 41 of 45 years of the Smith River record. In the remaining years, annual minimum discharge occurred later in the winter, probably as a result of snowy or dry autumns that didn't recharge the stream and prolonged the recession. For consistency of analyses, we determined the minimum daily discharge between September 1 and November 30, henceforth called autumn minimum discharge. Autumn minimum discharge varied by a factor of 2.6-2.7 between 1960 and 2005 in both watersheds, but the magnitude of flow, on a unit area basis, is ~9 times greater in the Clear Lake watershed than the Smith River watershed. As discussed above, the greater autumn minimum flows in the groundwater-dominated watershed are the result of a slower summer recession. Clear Lake autumn minimum flows are also more strongly influenced by inter-annual fluctuations in precipitation (Figure 3.5). We propose that subsurface storage is nearly exhausted in the Smith River watershed every year, whereas autumn minimum flows in the Clear Lake watershed are sensitive to aquifer levels, which in turn are controlled by the current and previous year's precipitation inputs. Using the previous year's December-August mean discharge at Clear Lake as a proxy for precipitation, the Pearson correlation with Clear Lake autumn minimum discharge is 0.5.

Stepwise multiple linear regression was performed on the series of 1979-2005 autumn minimum discharges of Clear Lake and Smith River, using 18 potential predictor variables for each watershed (Table 3.1). Stepwise multiple linear regression for Smith River yielded a model using the accumulated snow water equivalent at Santiam Junction (S_{SJ}, mm) that explains 38.1% of the variation in the dataset. No other variables met the 0.05 significance level for entry into the model. The low association between Smith River autumn minimum discharge and hydroclimatic variables

supports our contention that subsurface storage in the watershed is nearly exhausted each year, and thus, insensitive to climatic variability.

In contrast to the results for Smith River, the best model for Clear Lake autumn minimum discharge uses four variables to explain 93.4% of the variation in the dataset. The predictive variables are mean discharge from December-August (Q_{Mean}, m^3/s), the previous year's autumn minimum discharge ($Q_{PrevMin}$, m^3/s), S_{SJ}, and the day of the calendar year on which autumn minimum discharge occurs (A). The regression equation is:

$$Q_{min} = 0.288*Q_{mean} + 0.00175*S_{SJ} + 0.292* Q_{PrevMin} - 0.0197*A + 4.73. \quad (1)$$

The high correlation between precipitation and mean discharge suggests that the discharge term represents the year's precipitation. The snow term is probably related to the timing of snowmelt and recharge to the aquifers. The previous minimum discharge term represents the inter-annual memory in the groundwater system and the state of the aquifer in the prior year. The autumn minimum flow date term represents the timing of the first major autumn rains that bring an end to the summer recession. Thus, autumn minimum flows are shown to be a function of subsurface storage, the year's precipitation, timing of snowmelt, and timing of the fall rains. Even when A is not included, the other 3 variables explain 90% of the variation in the historical record, enabling autumn minimum flows to be predicted by the end of August, using

$$Q_{min} = 0.312*Q_{mean} + 0.00174*S_{SJ} + 0.260* Q_{PrevMin} - 1.28. \quad (2)$$

3.9 Long-term trends

The only SNOTEL-derived snow or precipitation parameter to exhibit a statistically significant relationship with time was the date of last snow cover at Santiam Junction. There was a weak (r=-0.39) trend toward earlier loss of snow cover at this site, not exhibited at either the lower or the higher elevation sites. Santiam Junction may be particularly susceptible to warming-induced earlier snow cover loss, because it lies near the lower limits of seasonal snow cover. Future warming may result in much

more transient snow cover interspersed with winter rain. Hogg Pass and Jump Off Joe summer temperatures also exhibit statistically significant correlations with time, with r=0.37 and r=0.48, respectively.

Investigation of long-term trends in climatic and hydrograph parameters suggests that inter-annual variability masks potential trends in precipitation and SWE data derived from the <30 year SNOTEL record. The discharge record for Clear Lake is continuous since 1948 and also has data for 1913-1915. This longer dataset suggests that there are some long-term trends as described below, although the record is still dominated by inter-annual variability.

The hydrograph temporal centroid is the day of the water year when half of the annual discharge has occurred, and has been used as an indicator of climate change throughout the mountainous western U.S. [*Stewart et al.*, 2005]. We found that the temporal centroid is significantly correlated with temperature and SWE-derived variables, but not precipitation. Thus, early dates of the temporal centroid are indicative of warm years with winter rain or early snowmelt, regardless of the total precipitation or discharge. A regression between temporal centroid and water year using the 1913-2005 Clear Lake dataset suggests that the temporal centroid has moved earlier in the year by 24 days since 1913 (Figure 3.6). The three early year data points exert strong leverage on the these results, as this trend is statistically significant at the 95% confidence level, but a regression line fit through 1948 to 2005 data, which has a very similar slope (-0.25) to that of the longer regression (-0.27), is not statistically significant at the same confidence level (p=0.12). Using the regression equation from the 1913-2005 analysis, the temporal centroid moved forward by 14 days between 1948 and 2002, which is consistent with the findings of *Stewart et al.* [2005], who reported temporal centroids moving forward 1-4 weeks for the same period. There was no significant trend for Smith River, but that dataset begins in October 1960.

Warmer winters and earlier spring snowmelt also seem to be affecting the autumn minimum discharge from Clear Lake, resulting in a downward trend over time (Figure 3.7). The trend is statistically significant when calculated both with and without the 1913 to 1915 period. As discussed above, there is a significant correlation between autumn minimum discharge and annual precipitation. In order to utilize the whole record length, we used December-August mean discharge as a proxy for precipitation. Regression lines fit through the Q_{min}/Q_{mean} ratio versus calendar year also show statistically significant downward trends from 1948 to the present and 1913 to the present. Based on the regressions, autumn minimum discharge has declined by 27% since 1948 and Q_{min}/Q_{mean} has declined by ~6%. These trends suggest that as climate warms, autumn minimum flows of the McKenzie River at Clear Lake will continue to decrease. Extrapolating the regressions suggests that by 2050, autumn minimum discharge will be 38% lower than in 1948. There were no significant long-term trends in the Smith River dataset, which may reflect the shorter record length, but is consistent with our contention that the watershed is insensitive to climatic variability because subsurface storage in exhausted each summer.

3.10 Discussion

The different behaviors of groundwater- and runoff-dominated watersheds on event, seasonal, and inter-annual scales are clearly revealed by the analysis of historical records in the Clear Lake and Smith River watersheds. These contrasting behaviors allow us to identify the primary and secondary controls on watershed response at each time scale (Table 3.3). These different behaviors have implications for how the watersheds have responded to warming winters in the past 45 years and how they will respond to future climate warming.

At the event scale, discharge is controlled primarily by the magnitude and intensity of the rain or snowmelt and secondarily by the geology of the watershed. The recharge signal is spatially and temporally varying, because of topographic effects on both

precipitation and temperature. Particularly important to determining discharge is the location of the transition between snow and rain during a precipitation event and the average temperature during a melt event. The bedrock hydraulic conductivity determines whether most recharge is quickly routed to streams, resulting in a flashy hydrograph, such as that of Smith River, or whether most recharge reaches a deeper aquifer where the signal becomes damped and lagged, as in the Clear Lake watershed.

At the seasonal scale, variations in discharge are primarily controlled by the watershed geology, and secondarily by winter and spring temperature. For aquifers with seasonal recharge, damping of the hydrograph is a function of aquifer length, storativity, transmissivity and the periodicity of the recharge [*Townley*, 1995]. The aquifer characteristics of the Clear Lake watershed produce significant damping of the discharge time series relative to the recharge time series. This damping results in the sustained release of groundwater during the summer drought, even though the seasonal water balance is negative. In contrast, the shallow subsurface flow system of the Smith River watershed rapidly transmits pressure waves from recharge to produce changes in streamflow [*Torres et al.*, 1998]. This results in a flashy winter hydrograph and rapid summer recession.

In the Clear Lake watershed, the streamflow seasonality, as measured by the ratio of discharge in the highest flow month to that in September, is related to the partitioning of precipitation between rain and snow and the timing of the snowmelt. Years with higher snow to rain ratios have lower winter flows and relatively more recharge in the spring, resulting in more water to sustain summer discharge. Years with colder spring temperatures have delayed snowmelt, resulting in a later onset of the summer recession and higher discharge during the autumn minimum flow period. Both of these scenarios result in less month-to-month variability in discharge.

At the annual scale, mean discharge is controlled by the current year's precipitation. Although we have shown that the previous year's precipitation has some influence on

mean discharge at Clear Lake, the coefficient of variation for mean annual discharge (25%) is only slightly lower than that for Smith River (27%). This suggests that the groundwater system does not have a significant moderating effect on overall inter-annual flow variability. Drought and high water years show up with approximately the same frequency and severity in both groundwater- and runoff-dominated watersheds. However, the coefficient of variation is smaller for August discharge at Clear Lake (32%) than at Smith River (36%). This suggests that during the summer recession, groundwater can have a more important moderating effect on inter-annual variability. Conversely, at the tail end of the summer recession groundwater increases the effects of inter-annual variability. The coefficient of variation for Clear Lake autumn minimum discharge is 26%, while for Smith River it is 22%. This corresponds with our hypothesis that subsurface storage is nearly exhausted every year in the runoff-dominated Smith River watershed, resulting in less inter-annual variability.

Based on the patterns of the past several decades, we can begin to forecast what the next few decades will likely bring to streams in the Oregon Cascades. The correlations between accumulated SWE and winter temperature and ENSO indices, combined with the long-term decrease in the snow-covered season at Santiam Junction, suggest that there is very strong elevation sensitivity in SWE parameters. In particular, it seems that areas at the transition between transient and seasonal snowpacks are most sensitive to warmer winters. If winters continue to warm, we project that the elevation of the transient snow zone will shift upward and substantial portions of the previously snow-dominated Cascades will experience a higher frequency of winter rain events. For these watersheds, that in the future have more transient and less seasonal snow, winter discharge will increase and the snowmelt peak will become less important. Thus, the watersheds most sensitive to warming will be those with much of their area between 1100-1300 m. For watersheds already dominated by transient snow (<1100 m), the proportion of winter rain will increase, but the hydrograph will likely be less affected than for higher elevation watersheds. For the highest elevation watersheds (>1500 m), seasonal snow cover will persist but the snowmelt peak will occur earlier

in the spring. In the Willamette River watershed, 14% of the Cascade Range lies in elevation range between 1100 and 1300 m, and 91% lies below 1500 m. Approximately 37% of the area of the Clear Lake watershed lies within the 1100-1300 m range, as does 43% of the Smith River watershed.

The historical record suggests that the annual hydrograph has already shifted and that autumn minimum discharge in groundwater-dominated watersheds is already declining as snowmelt occurs earlier (Figure 3.8). Since the late 1940's the peak discharge month for Clear Lake has shifted from May to April, as a function of earlier snowmelt. This leads to longer summer recession periods, and ultimately lower autumn minimum discharges in groundwater-dominated watersheds. If future warming proceeds as predicted by regional climate models, the summer recession will further lengthen and minimum flows will decline even more. We expect that, in runoff-dominated watersheds, longer recession periods will exhaust subsurface storage sooner, but that the effect on autumn minimum discharge will be smaller than in groundwater-dominated watersheds. This conclusion is supported by the modeling results of *Tague et al.* [in review].

3.11 Conclusions

Analyses of the historical datasets for two watersheds in the Oregon Cascades clearly highlight the importance of groundwater systems in sustaining summer streamflow. Discharge and evapotranspiration in the groundwater-dominated watershed account for 260% of incoming precipitation between July and October, so groundwater storage and the associated slow recession are responsible for sustaining discharge even when the seasonal or annual water balance is negative. While groundwater significantly influences the shape of the annual hydrograph, climatic factors control the inter-annual variability of streamflow. Even though Cascades aquifers store multiple years worth of water [*Jefferson et al.*, 2006], and there is a one year memory associated with the groundwater system, these effects are not enough to dampen inter-annual variability in

streamflow in groundwater-dominated streams, as evidenced by comparable coefficients of variation between the two study watersheds.

Warmer winters and earlier snowmelt over the past ~60 years have shifted the hydrograph for the McKenzie River at Clear Lake, resulting in an earlier temporal centroid (14 days), longer summer recessions and lowered autumn minimum discharges (27%). Projections of future climate suggest that this trend will continue over the next 50 years. The slow summer recession of groundwater-dominated streams makes them more sensitive to changes in snowmelt amount and timing than are runoff-dominated streams. Groundwater-dominated watersheds that are transitioning between transient and seasonal snow regimes will be the most affected by projected climatic change, particularly in terms of late summer and fall streamflow. In the Oregon Cascades, the region of maximum sensitivity seems to be between 1100 and 1300 m, based on historical trends and projected changes over the next 50 years.

Our results suggest that water resource managers in the mountainous western United States must identify groundwater-dominated watersheds and those that are perched at the transient/seasonal snow transition, and that they should be prepared for significant changes to the annual hydrograph in those areas. Downstream water users and hydroelectric dam operators will have to adjust their usage schedules or face shortfalls. Aquatic species, such as salmonids, will be subject to diminishing flows and possibly increasing water temperatures.

3.12 Acknowledgements

3.13 References cited

Beebee, R., and M. Manga (2004), Variation in the relationship between snowmelt runoff in Oregon and ENSO and PDO, *Journal of the American Water Resources Association*, *40*, 1011-1024.

Box, G. E. P., and G. Jenkins (1976), *Time Series Analysis: Forecasting and Control*, 575 pp., Holden-Day, Boca Raton, Fla.

Cayan, D. R., S. A. Kammerdiener, M. D. Dettinger, J. M. Caprio, and D. H. Peterson (2001), Changes in the onset of spring in the western United States, *Bulletin of the American Meteorological Society*, *82*, 399-415.

Daly, C., W. P. Gibson, G. H. Taylor, G. L. Johnson, and P. Pasteris (2002), A knowledge-based approach to the statistical mapping of climate, *Climate Research*, *22*, 99-113.

Daly, C., G. Taylor, and W. Gibson (1997), The PRISM approach to mapping precipitation and temperature, paper presented at 10th Conf. on Applied Climatology, American Meteorological Society, Reno, NV.

Folland, C. K., T. R. Karl, and coauthors (2001), Observed climate variability and change, in *Climate Change 2001: The Scientific Basis. Contribution of Working Group I to the Third Assessment Report of the Intergovernmental Panel on Climate Change*, edited by J. T. Houghton, et al., pp. 99-181, Cambridge Univ. Press, Cambridge.

Harr, R. D. (1977), Water flux in soil and subsoil on a steep forested slope, *Journal of Hydrology*, *33*, 37-58.

Harr, R. D. (1981), Some characteristics and consequences of snowmelt during rainfall in western Oregon, *Journal of Hydrology*, *53*, 277-304.

Herrett, T. A., G. W. Hess, M. A. Stewart, G. P. Ruppert, and M.-L. Courts (2005), Water Resources Data for Oregon, Water Year 2005, *Water Data Report OR-05-1*, 942 pp, U.S. Geol. Surv., Washington, D.C.

Ingebritsen, S. E., R. H. Mariner, and D. R. Sherrod (1994), Hydrothermal systems of the Cascade Range, north-central Oregon, *Prof. Pap. 1044-L.*, 86 pp. pp, U.S. Geol. Surv., Washington, D.C.

Jefferson, A., and G. E. Grant (2003), Recharge areas and discharge of groundwater in a young volcanic landscape, McKenzie River, Oregon, *Geological Society of America Annual Meeting Abstracts with Programs*, *35*, 151-151.

Jefferson, A., G. E. Grant, and T. P. Rose (2006), The influence of volcanic history on groundwater patterns on the west slope of the Oregon High Cascades, *Water Resources Research*, *in press*, 2005WR004812.

Jones, J. A., and D. A. Post (2004), Seasonal and successional streamflow response to forest cutting and regrowth in the northwest and eastern United States, *Water Resources Research*, *40*, W05203, doi:05210.01029/02003WR002952.

Leung, L. R., Y. Qian, X. Bian, W. Washington, J. Han, and J. O. Roads (2004), Mid-century ensemble regional climate change scenarios for the western United States, *Climatic Change*, *62*, 75-113.

Mantua, N. J., S. R. Hare, Y. Zhang, J. M. Wallace, and R. C. Francis (1997), A Pacific interdecadal climate oscillation with impacts on salmon production, *Bulletin of the American Meteorological Society, 78*, 1069-1079.

Mote, P. W. (2003), Trends in snow water equivalent in the Pacific Northwest and their climatic causes, *Geophysical Research Letters*, *30*, 1601, doi:1610.1029/2003GL017258.

Mote, P. W., A. F. Hamlet, M. Clark, and D. P. Lettenmaier (2005), Declining mountain snowpack in western North America, *Bulletin of the American Meteorological Society*, *86*, 39-49.

Mote, P. W., E. Parson, A. F. Hamlet, W. S. Keeton, D. P. Lettenmaier, N. J. Mantua, E. L. Miles, D. Peterson, D. L. Peterson, R. Slaughter, and A. K. Snover (2003), Preparing for climatic change: the water, salmon, and forests of the Pacific Northwest, *Climatic Change*, *61*, 45-88.

Naiman, R. J., K. L. Fetherston, S. J. McKay, and J. Chen (1998), Riparian forests, in *River Ecology and Management: Lessons from the Pacific Northwest*, edited by R. J. Naiman and R. E. Bilby, pp. 289-323, Springer, New York City.

Nolin, A. W., and C. Daly (2006), Mapping "at-risk" snow in the Pacific Northwest, U.S.A., *Journal of Hydrometeorology, in press*.

Priest, G. R., N. M. Woller, G. L. Black, and S. H. Evans (1983), Overview of the geology of the central Oregon Cascade Range, in *Geology and Geothermal Resources of the Central Oregon Cascade Range*, edited by G. R. Priest and B. F. Vogt, 15, pp. 3-28, Oregon Department of Geology and Mineral Industries, Salem, Ore.

Regonda, S. K., B. Rajagopalan, M. Clark, and J. Pitlick (2005), Seasonal cycle shifts in hydroclimatology over the western United States, *Journal of Climate*, *18*, 372-384.

Ropelewski, C. F., and P. D. Jones (1987), An extension of the Tahiti-Darwin Southern Oscillation Index, *Monthly Weather Review*, *115*, 2161-2165.

Saar, M. O., and M. Manga (2004), Depth dependence of permeability in the Oregon Cascades inferred from hydrogeologic, thermal, seismic, and magmatic modeling constraints, *Journal of Geophysical Research, 109*, B04204, 04210.01029/02003JB002855.

Selong, J. H., T. E. McMahon, A. V. Zale, and F. T. Barrows (2001), Effects of temperature on growth and survival of bull trout, with application of an improved method for determining thermal tolerance in fishes, *Transactions of the American Fisheries Society*, *130*, 1026-1037.

Sherrod, D. R., and J. G. Smith (2000), Geologic Map of Upper Eocene to Holocene Volcanic and Related Rocks of the Cascade Range, Oregon, *Geol. Invest. Ser. I-2569*, U.S. Geol. Surv., Washington, D.C.

Stewart, I. T., D. R. Cayan, and M. D. Dettinger (2005), Changes toward earlier streamflow timing across western North America, *Journal of Climate*, *18*, 1136-1155.

Storck, P., D. P. Lettenmaier, and S. M. Bolton (2002), Measurement of snow interception and canopy effects on snow accumulation and melt in a

mountainous maritime climate, Oregon, United States, *Water Resources Research*, *38*, 1223, doi:1210.1029/2002WR001281.

Tague, C., M. Farrell, G. E. Grant, S. L. Lewis, and S. Rey (2006), Hydrogeologic controls on summer stream temperatures in the McKenzie River basin, Oregon, *Hydrological Processes*, *in press*.

Tague, C., and G. E. Grant (2004), A geological framework for interpreting the low flow regimes of Cascade streams, Willamette River Basin, Oregon, *Water Resources Research*, *40*, W04303 04310.01029/02003WR002629.

Tague, C., G. E. Grant, M. Farrell, J. Choate, and A. Jefferson (in review), Deep groundwater mediates streamflow response to climate warming in the Oregon Cascades, *Climatic Change*.

Tague, C. L., and L. E. Band (2004), RHESSys: regional hydro-ecologic simulation system--an object-oriented approach to spatially distributed modeling of carbon, water, and nutrient cycling, *Earth Interactions*, *8*, Paper No. 19, p. 11-42.

Torres, R., W. E. Dietrich, D. R. Montgomery, S. P. Anderson, and K. Loague (1998), Unsaturated zone processes and the hydrologic response of a steep, unchanneled catchment, *Water Resources Research*, *34*, 1865-1879.

Townley, L. R. (1995), The response of aquifers to periodic forcing, *Advances in Water Resources*, *18*, 125-146.

Trenberth, K. E., and D. P. Stepaniak (2001), Indices of El Niño evolution, *Journal of Climate*, *14*, 1697-1701.

Washington, W. M., J. W. Weatherly, G. A. Meehl, A. J. Semtener, T. W. Bettge, A. P. Craig, W. G. Strant, J. Arblaster, V. B. Wayland, R. James, and Y. Zhang (2000), Parallel Climate Model (PCM) control and transient simulations, *Climate Dynamics*, *16*, 755-774.

Webb, B. W., P. D. Clack, and D. E. Walling (2003), Water-air temperature relationships in a Devon river system and the role of flow, *Hydrological Processes*, *17*, 3069-3084.

Table 3.1. Parameters derived from hydrological and climatic data. The P column indicates parameters for which Pearson's product moment correlations were calculated. DOWY stands for day of water year, and DOY stands for day of calendar year. The R column indicates parameters which were used in regression model of autumn minimum discharge for the Clear Lake (C) and Smith River (S) watersheds.

Station	Parameter	Units	P	R
	Water Year	year	P	
Clear Lake	Mean discharge for water year	m^3/s	P	
Clear Lake	Mean discharge for December-August	m^3/s		C
Clear Lake	Mean August discharge	m^3/s	P	
Clear Lake	Autumn minimum discharge	m^3/s	P	C
Clear Lake	Date of autumn minimum discharge	DOY		
Clear Lake	Temporal center of mass	DOWY	P	
Clear Lake	Mean discharge for previous December-August	m^3/s		C
Clear Lake	Autumn minimum discharge of previous year	DOY		C
Smith River	Mean discharge for water year	m^3/s	P	
Smith River	Mean discharge for December-August	m^3/s		S
Smith River	Mean August discharge	m^3/s	P	
Smith River	Autumn minimum discharge	m^3/s	P	S
Smith River	Date of autumn minimum discharge	DOWY		
Smith River	Temporal center of mass	DOWY	P	
Smith River	Mean discharge for previous December-August	m^3/s		S
Smith River	Autumn minimum discharge of previous year	DOY		S
Hogg Pass	Total precipitation in water year	mm	P	CS
Hogg Pass	Accumulated precipitation on April 1	mm	P	
Hogg Pass	Accumulated SWE	mm	P	CS
Hogg Pass	SWE present on April 1	mm	P	CS
Hogg Pass	Date of Peak SWE	DOWY	P	CS
Hogg Pass	Peak SWE	mm	P	
Hogg Pass	Last date with SWE	DOWY	P	
Hogg Pass	Temporal center of mass of rain plus melt	DOWY	P	CS
Hogg Pass	Average winter temperature (November-March)	°C	P	
Hogg Pass	Average spring temperature (April-June)	°C	P	
Hogg Pass	Average summer temperature (July-October)	°C	P	
Santiam Junction	Total precipitation in water year	mm	P	CS
Santiam Junction	Accumulated precipitation on April 1	mm	P	CS
Santiam Junction	Accumulated SWE	mm	P	CS
Santiam Junction	SWE present on April 1	mm	P	CS
Santiam Junction	Date of Peak SWE	DOWY	P	CS
Santiam Junction	Peak SWE	mm	P	
Santiam Junction	Last date with SWE	DOWY	P	
Santiam Junction	Temporal center of mass of rain plus melt	DOWY	P	CS
Santiam Junction	Average winter temperature (November-March)	°C	P	
Santiam Junction	Average spring temperature (April-June)	°C	P	
Santiam Junction	Average summer temperature (July-October)	°C	P	

Table 3.1 (Continued).

Station	Parameter	Units	P	R
Jump Off Joe	Total precipitation in water year	mm	P	CS
Jump Off Joe	Accumulated precipitation on April 1	mm	P	
Jump Off Joe	Accumulated SWE	mm	P	CS
Jump Off Joe	SWE present on April 1	mm	P	CS
Jump Off Joe	Date of Peak SWE	DOWY	P	CS
Jump Off Joe	Peak SWE	mm	P	
Jump Off Joe	Last date with SWE	DOWY	P	
Jump Off Joe	Average winter temperature (November-March)	°C	P	
Jump Off Joe	Average spring temperature (April-June)	°C	P	
Jump Off Joe	Average summer temperature (July-October)	°C	P	

Table 3.2. Correlation coefficients for selected variables. Bold terms are statistically significant at the 95% confidence level. Mean, August, and autumn min. are daily discharges. CT is the temporal center of the hydrograph. SWE and Precip. are cumulative values for the water year. Peak day is the day of peak SWE accumulation, and Peak SWE is the amount. Winter temperature is average daily median temperature for November through March, and spring temperature is the average daily median temperature for April through June.

		Clear Lake				Smith River			
		WY Mean	August	Autumn Min.	CT	WY Mean	August	Autumn Min.	CT
Clear Lake	Mean	**1.00**							
	August	**0.88**	**1.00**						
	Autumn Min.	**0.93**	**0.92**	**1.00**					
	CT	-0.10	0.28	0.04	**1.00**				
Smith River	Mean	**0.94**	**0.86**	**0.84**	-0.04	**1.00**			
	August	**0.50**	**0.76**	**0.59**	**0.43**	**0.86**	**1.00**		
	Autumn Min.	**0.56**	**0.74**	**0.74**	**0.41**	**0.49**	**0.62**	**1.00**	
	CT	-0.26	0.05	-0.14	**0.89**	-0.23	0.23	0.21	**1.00**
Hogg Pass	SWE	**0.74**	**0.77**	**0.69**	0.25	**0.80**	**0.44**	**0.47**	0.00
	Precip.	**0.91**	**0.75**	**0.81**	-0.19	**0.95**	**0.44**	**0.40**	**-0.34**
	Peak Day	0.14	0.25	0.17	0.15	0.21	**0.39**	0.11	0.21
	Peak SWE	**0.67**	**0.79**	**0.68**	**0.39**	**0.74**	**0.53**	**0.56**	0.11
	Winter T	-0.08	-0.33	-0.20	**-0.60**	-0.18	**-0.51**	**-0.43**	**-0.50**
	Spring T	-0.33	**-0.52**	**-0.47**	**-0.45**	-0.38	**-0.55**	**-0.52**	-0.34
Santiam Junction	SWE	**0.57**	**0.76**	**0.68**	**0.48**	**0.61**	**0.58**	**0.62**	0.27
	Precip.	**0.88**	**0.82**	**0.85**	-0.01	**0.95**	**0.55**	**0.51**	-0.22
	Peak Day	0.21	**0.34**	0.28	0.23	0.24	0.18	**0.43**	0.05
	Peak SWE	**0.51**	**0.73**	**0.60**	**0.51**	**0.57**	**0.60**	**0.60**	0.30
	Winter T	-0.09	-0.32	-0.23	**-0.58**	-0.20	**-0.40**	-0.36	**-0.52**
	Spring T	**-0.46**	**-0.64**	**-0.60**	-0.35	**-0.47**	**-0.56**	**-0.67**	-0.27
Jump Off Joe	SWE	0.36	0.55	0.44	**0.64**	0.38	0.36	0.48	**0.49**
	Precip.	**0.93**	**0.82**	**0.88**	-0.10	**0.93**	**0.51**	**0.50**	-0.26
	Peak Day	0.14	0.29	0.26	0.28	0.05	0.23	**0.36**	0.26
	Peak SWE	**0.34**	**0.54**	**0.40**	**0.69**	**0.39**	**0.43**	**0.50**	**0.53**
	Winter T	-0.11	-0.34	-0.26	**-0.55**	-0.14	-0.32	**-0.42**	**-0.53**
	Spring T	-0.15	-0.30	-0.26	-0.36	-0.23	-0.35	-0.31	-0.34

Table 3.2 (continued).

		Hogg Pass						Santiam Junction						Jump Off Joe					
		SWE	Precip.	Peak Day	Peak SWE	Winter T	Spring T	SWE	Precip.	Peak Day	Peak SWE	Winter T	Spring T	SWE	Precip.	Peak Day	Peak SWE	Winter T	Spring T
Hogg Pass	SWE	1.00																	
	Precip.	0.74	1.00																
	Peak Day	-0.06	0.13	1.00															
	Peak SWE	0.92	0.66	0.05	1.00														
	Winter T	-0.34	-0.14	-0.43	-0.61	1.00													
	Spring T	-0.40	-0.35	-0.62	-0.44	0.46	1.00												
Santiam Junction	SWE	0.81	0.53	0.02	0.90	-0.59	-0.42	1.00											
	Precip.	0.77	0.95	0.13	0.75	-0.27	-0.39	0.68	1.00										
	Peak Day	0.33	0.18	0.07	0.55	-0.44	0.05	0.45	0.24	1.00									
	Peak SWE	0.75	0.48	0.05	0.91	-0.74	-0.35	0.94	0.64	0.55	1.00								
	Winter T	-0.34	-0.17	-0.35	-0.60	0.95	0.55	-0.60	-0.33	-0.41	-0.73	1.00							
	Spring T	-0.38	-0.41	-0.64	-0.42	0.31	0.94	-0.38	-0.45	-0.06	-0.26	0.38	1.00						
Jump Off Joe	SWE	0.67	0.33	-0.05	0.75	-0.59	-0.37	0.88	0.48	0.29	0.80	-0.59	-0.28	1.00					
	Precip.	0.69	0.95	0.14	0.64	-0.16	-0.36	0.57	0.97	0.15	0.51	-0.21	-0.45	0.39	1.00				
	Peak Day	0.06	0.05	0.24	0.25	-0.30	-0.15	0.35	0.06	0.43	0.32	-0.21	-0.27	0.29	0.02	1.00			
	Peak SWE	0.68	0.33	-0.07	0.77	-0.67	-0.39	0.86	0.47	0.29	0.84	-0.64	-0.23	0.96	0.36	0.27	1.00		
	Winter T	-0.27	-0.08	-0.42	-0.50	0.81	0.40	-0.65	-0.23	-0.48	-0.69	0.80	0.31	-0.71	-0.13	-0.44	-0.71	1.00	
	Spring T	-0.23	-0.22	-0.61	-0.24	0.41	0.93	-0.25	-0.25	0.10	-0.19	0.54	0.85	-0.26	-0.21	-0.01	-0.29	0.44	1.00

Table 3.3. Controls on discharge variability for Cascades watersheds.

Scale	Primary Control	Secondary Control
Event	Precipitation	Geology
Seasonal	Geology	Winter-spring temperature
Annual	Precipitation	Geology (minor)
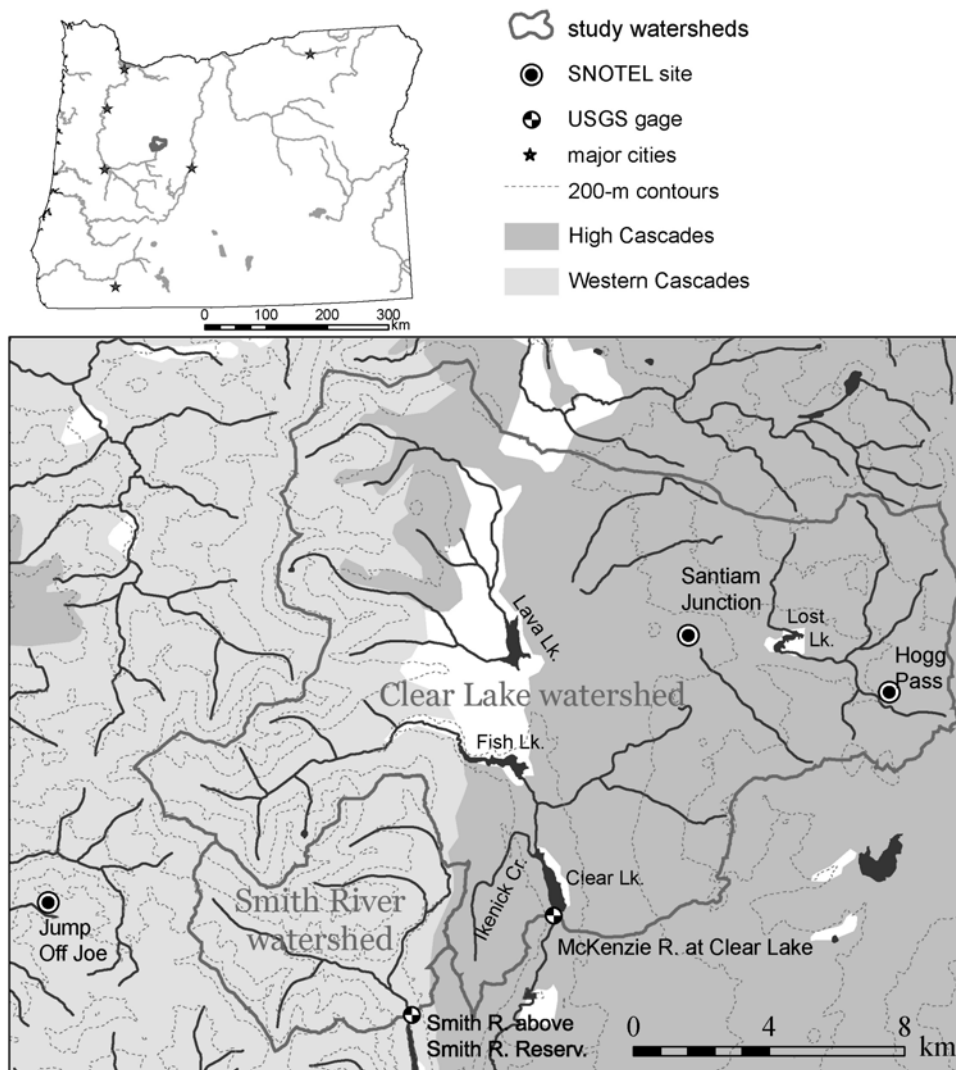
Figure 3.1: Map showing the study watersheds relative to their location in Oregon and to Cascades topography and geology.
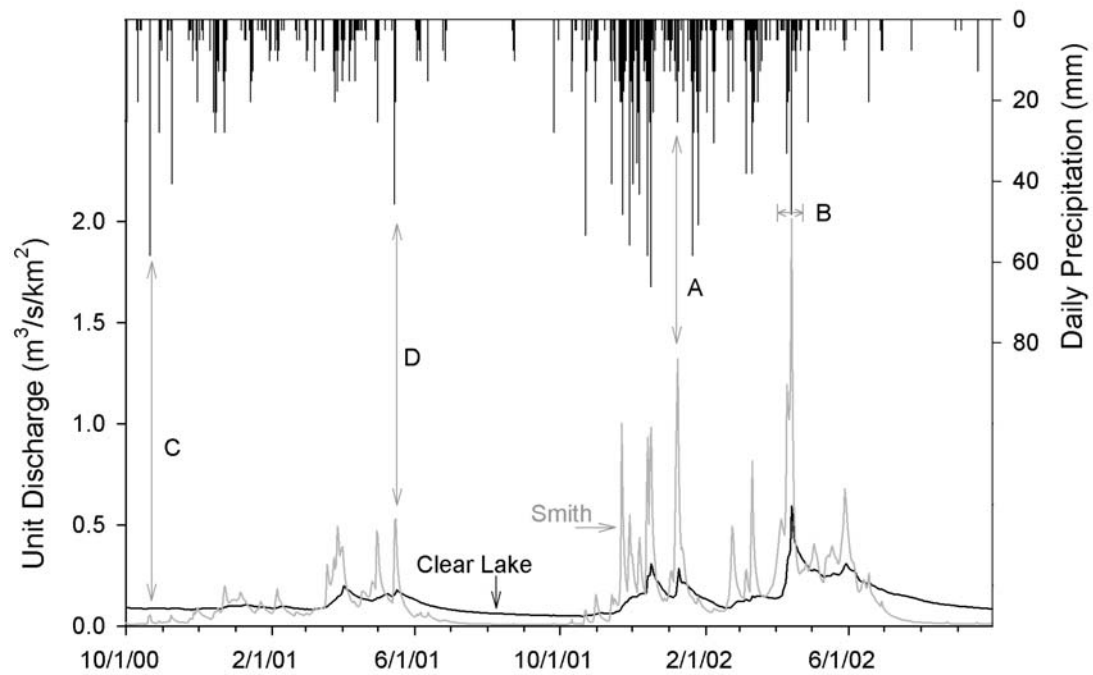
Figure 3.2. Water years 2001-2002 Santiam Junction precipitation and unit discharge hydrographs for the McKenzie River at the outlet of Clear Lake and Smith River above Smith River Reservoir. Event A corresponds to January 7-9, 2002; event B corresponds to April 1-23, 2002; event C corresponds to October 21, 2000; and event D corresponds to May 15-16, 2001. Events are discussed in the text.
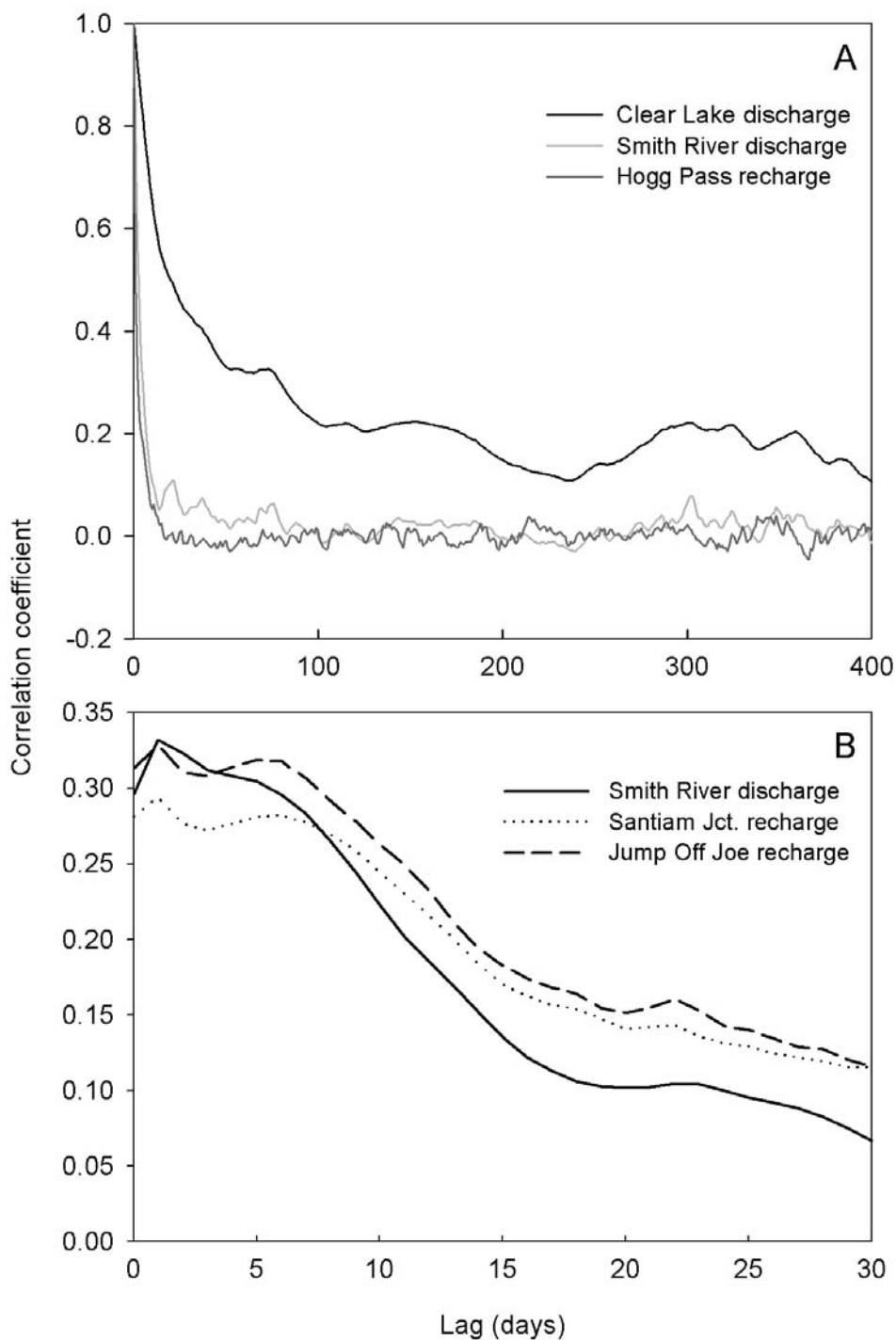
Figure 3.3. Auto- and cross-correlations of time-series data. (a) Auto-correlation time series for Clear Lake discharge, Smith River discharge, and Hogg Pass recharge (rain plus snowmelt). (b) Cross-correlation time series for Clear Lake discharge versus Smith River discharge, Santiam Junction recharge, and Jump Off Joe recharge.
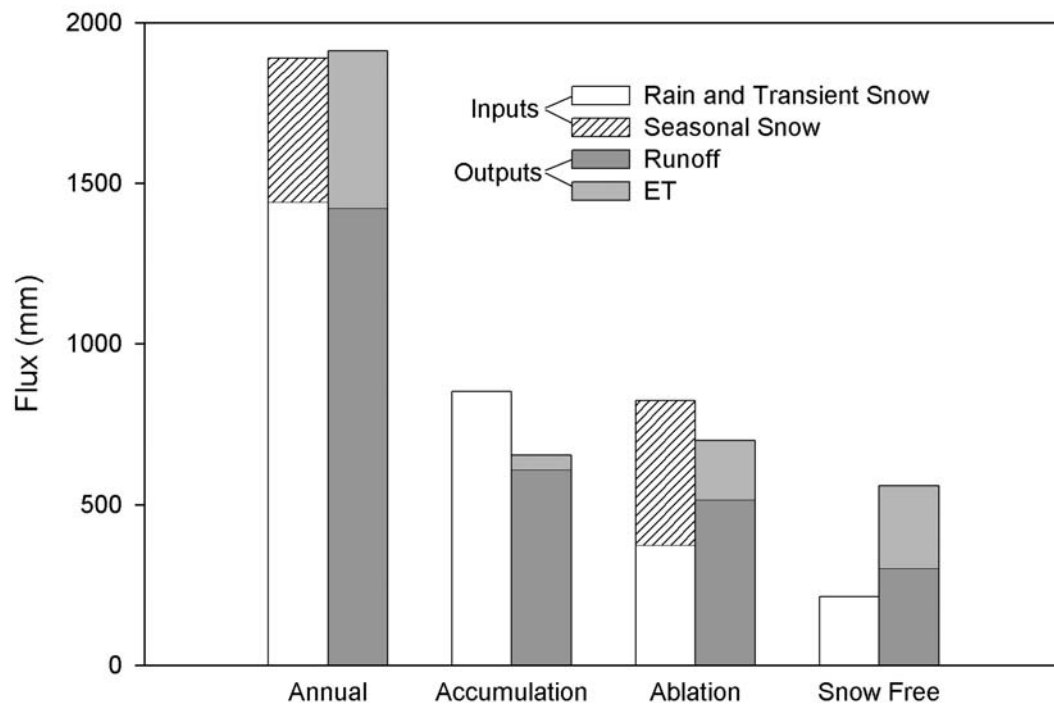
Figure 3.4: Water budget for the Clear Lake watershed for water years 2001-2004. The accumulation season is defined as November-March, while the ablation season is April-June. The snow-free season occurs between July and October. The rain plus transient snow category includes all liquid precipitation and snow that falls and ablates within the same season. Seasonal snow falls during the accumulation seasons and ablates during the ablation season.
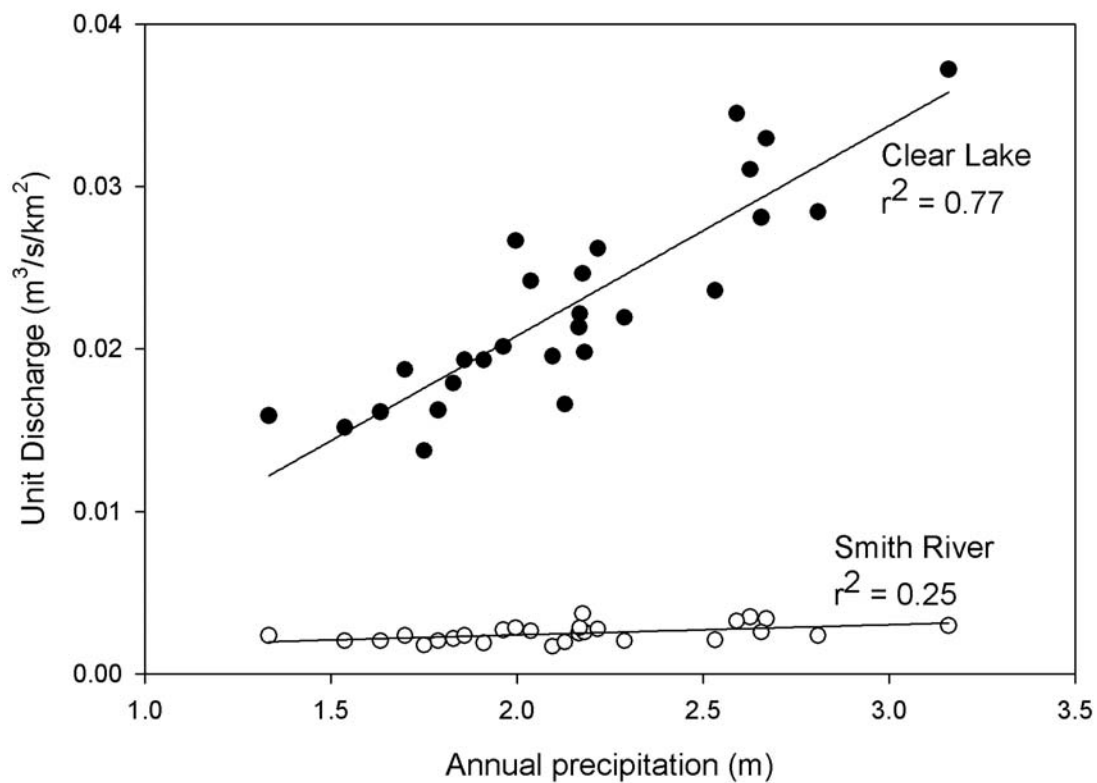
Figure 3.5: Relationship between annual precipitation at Santiam Junction and autumn minimum unit discharge for the Clear Lake and Smith River watersheds.
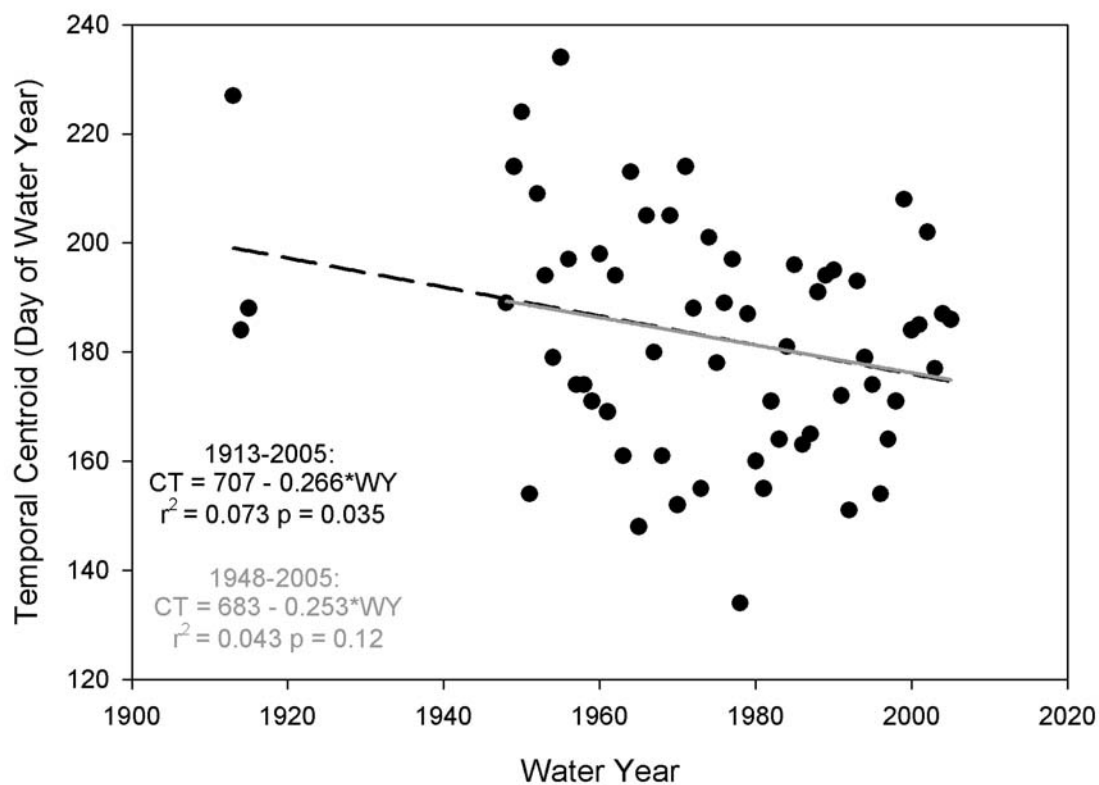
Figure 3.6: Relationship between water year and the temporal centroid of the Clear Lake hydrograph. The temporal centroid is defined as the day when half of the annual discharge has occurred.
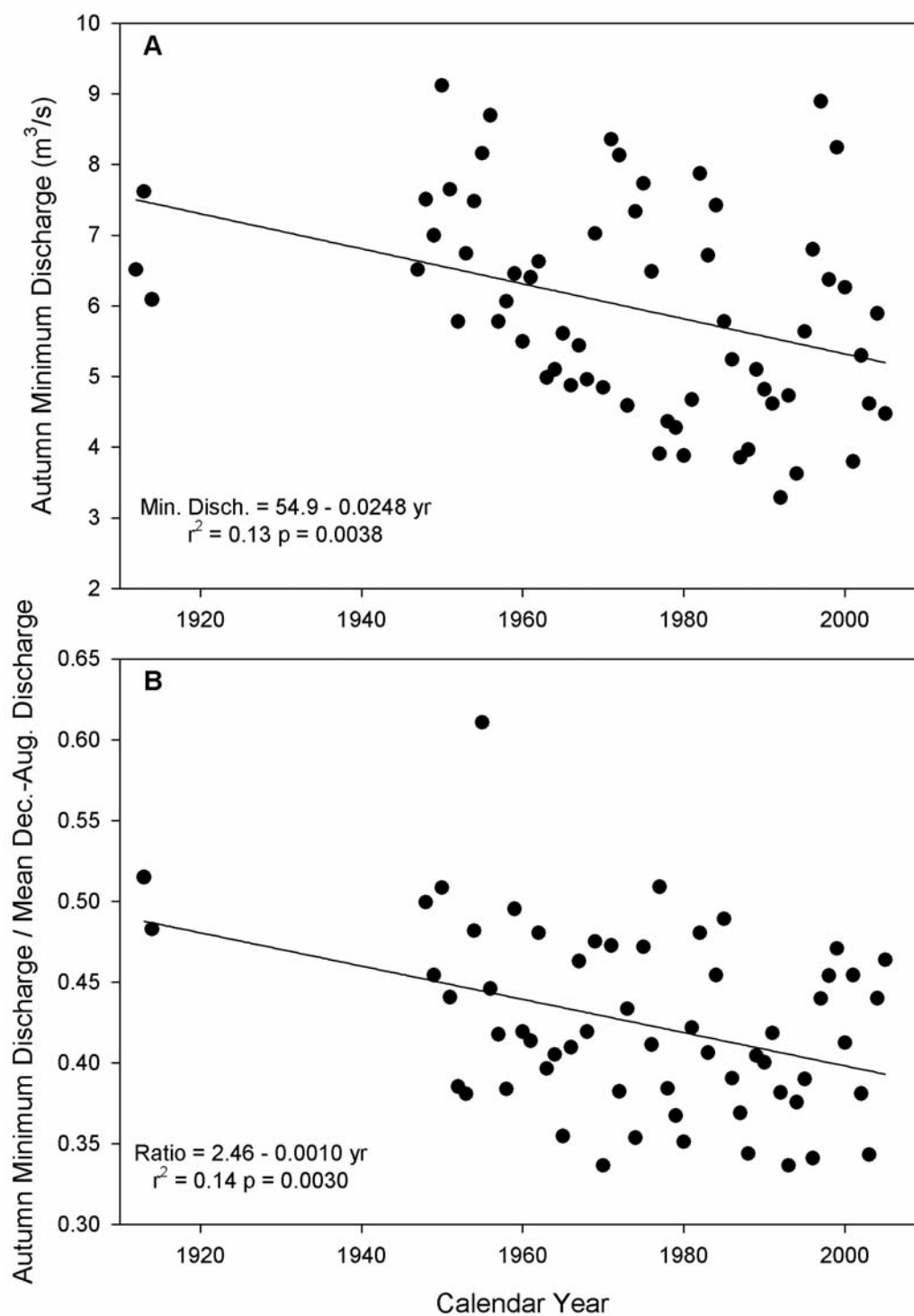
Figure 3.7: Relationship between calendar year and: (a) autumn minimum discharge for the Clear Lake watershed; (b) the ratio of autumn minimum discharge to the average discharge of the preceding nine months for the Clear Lake watershed.
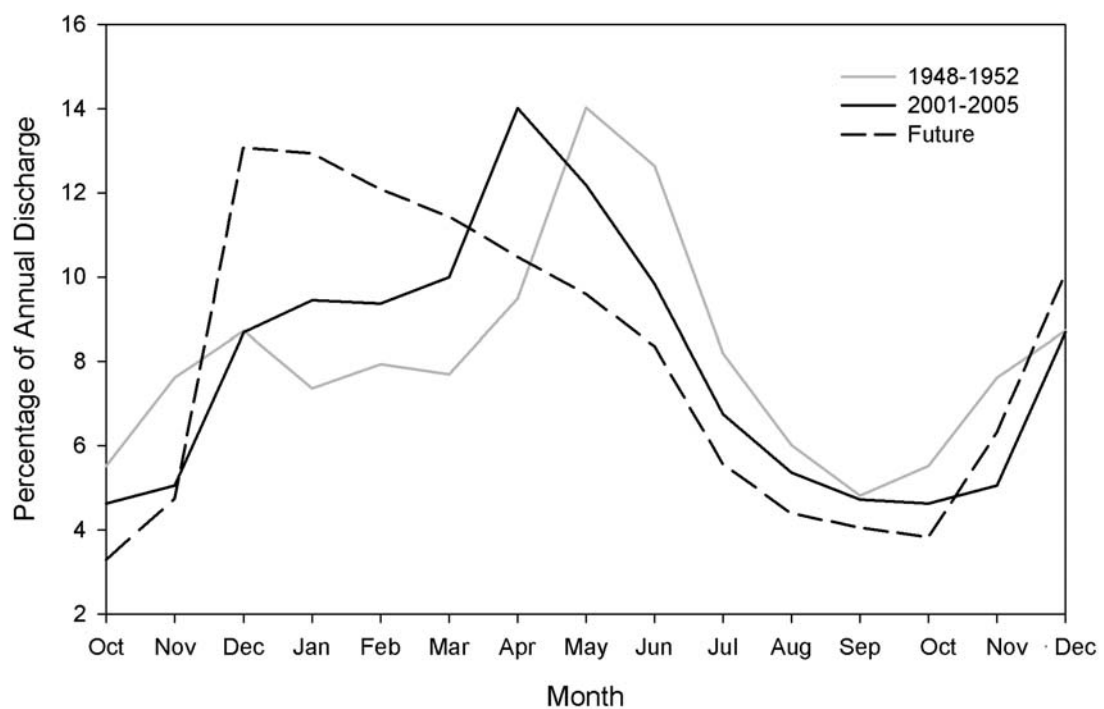
Figure 3.8. Monthly percent values of annual discharge for the Clear Lake watershed in two historical periods (1948-1952, 2001-2005) and a predicted future graph based on continuation of current trends and increasingly warm winters. October to December are repeated to illustrate the low flow period.

4 Drainage development on permeable basaltic landscapes

4.1 Abstract

Drainage density increases with time on basaltic landscapes on the western slope of the Oregon Cascades, as a result of permeability declining from its initial high values. In young landscapes, groundwater systems transmit most of the recharge to large springs, but there is no evidence for groundwater seepage erosion. Large springs disappear within one million years, after the establishment of runoff-dominated channels. The relationships between local slopes and contributing areas indicate that watersheds with Quaternary basalts have experienced little fluvial erosion, whereas Pliocene watersheds show classic slope-area trends and the influence of debris flows. Thus, despite the abundance of water on the west slope of the Oregon Cascades, the High Cascades landscape is dominantly shaped by volcanic activity and glaciation. A number of mechanisms have been proposed to account for the reduction of permeability necessary for drainage development and valley incision. In the Oregon Cascades, glaciation and chemical weathering appear to be the primary drivers of post-constructional landscape evolution.

4.2 Introduction

The process of landscape evolution is one of the fundamental topics of geomorphological research, and the mechanisms and rates of landscape evolution drive modern land-surface characteristics. Landscape evolution is also important because the degree of drainage development may control other hydrologic and geomorphic processes, including groundwater residence times and sediment delivery processes. In turn, these processes affect the sensitivity of the landscape to climate change. Landscape evolution models have recently emerged as a primary tool for exploring the rates of fluvial incision and landscape development. Most of these models presume that erosion is primarily driven by water flowing over the land

surface, driven by an energy gradient that is both inherited from and resulting in topography. These models drive drainage development using the stream power law, wherein the ability of a stream to incise a channel is related to its contributing area and slope.

However, the stream power law cannot be used to address lithologies or evolutionary periods where the permeable nature of the subsurface precludes surface runoff. In these areas, landscape evolution is largely driven by other processes until surface permeability has been reduced sufficiently for overland flow to occur. These processes may include tectonics, volcanism, glaciation, landsliding, dissolution, and groundwater seepage erosion. Such permeable landscapes are found in regions with unconsolidated sediments, limestone, fractured rock, and young basaltic lava flows.

Some modeling studies have explored the geomorphological implications of saturation overland flow as opposed to Hortonian overland flow [*Ijjasz-Vasquez et al.*, 1992; *Tucker and Bras*, 1998]. While these models likely envisioned shallow subsurface flow, some aspects of their results may apply to permeable landscapes with deeper bedrock aquifers and springs. One noteworthy difference between the model simulations and permeable landscapes is that modeled subsurface flow is only driven by surface topography whereas groundwater flowpaths can also cross topographical divides [e.g., *Genereux et al.*, 2002; *Jefferson et al.*, 2006]. Also, landscape evolution models with saturation overland flow assume constant transmissivity, whereas permeability likely evolves over time.

Of all permeable landscapes, those constructed from basaltic lava flows have the advantage of being independently datable, using radiocarbon, $^{40}Ar/^{39}Ar$, K/Ar and other methods, and thus provide the opportunity to rigorously constrain timescales of drainage network development. However, the key processes and timescales that reduce the permeability of lava flows to the point where the stream power law can be applied are poorly documented. An improved understanding of the mechanisms and

rates of drainage development on basalt may also provide insight to the processes responsible for valley formation on Mars [*Hynek and Phillips*, 2003], where much of the planet is covered with basalt [*Bandfield et al.*, 2000]. Basaltic lavas have very high initial porosity and permeability associated with vesicles, cooling fractures, and rubble zones at flow tops and bottoms. Individual basaltic lava flows are only 3-20 m thick, so a vertical section of 100 m or more encompasses many near-horizontal high permeability zones at each of the flow boundaries [*Davis*, 1969; *Kilburn*, 2000], resulting in a high overall permeability for young basaltic landscapes.

In this paper, we examine timescales and processes underlying drainage network development in the Oregon Cascades, where basalts have been produced for over 30 million years [*Sherrod and Smith*, 2000]. Undissected Quaternary basalts with major groundwater systems and spring-dominated flow are juxtaposed against adjacent deeply-dissected Tertiary basalts with runoff-dominated channels along the western slopes of the Cascades. We conduct an in-depth examination of drainage structure and landscape evolution in the Oregon Cascades, with the goal of understanding the controls on drainage development in permeable basaltic landscapes.

Baker [1988] proposed that drainage evolution on volcanoes proceeds as a function of climate, relief, rock type, and time. This model is similar to the concept of soil development factors [*Jenny*, 1941]. Thus, if three factors are held constant, the effect of one variable, such as time, can be studied by assembling a sequence of landscapes spanning a range of ages. Chronosequences of drainage development on basalts have been observed in varying climates throughout the world, and a variety of conceptual models have been formulated (Figure 4.1). These conceptual models attempt to explain part or all of a basalt drainage chronosequence from recently emplaced lava with no surface drainage to deeply dissected landscapes with well developed runoff-dominated stream networks.

In Iceland, *Gislason et al.* [1996] noted that young Quaternary lavas have no surface drainage, whereas Tertiary lava landscapes are runoff-dominated. On Quaternary

basaltic lava fields in California and Nevada, drainage density increases logarithmically with time. Channel incision through the 1-3 m thick fine-grained eolian mantle rarely exposes the underlying basalt, but the network structure is controlled by the lava flow topography [*Dohrenwend et al.*, 1987]. On the Badia plateau in Jordan basaltic landscapes show increasing levels of drainage development with age. Poorly-connected drainages into small depressions occur on 0.1-1.45 million year old (Ma) basalts, whereas well-connected, incised wadi networks are found on 8.45-8.9 Ma basalts [*Allison et al.*, 2000]. A number of researchers have tackled aspects of drainage development in the basalts of the Hawaiian Islands. Along the Kohala Coast of Hawaii, deep U-shaped amphitheater-headed canyons have attracted considerable interest as possible analogs to Martian topography [*Baker*, 1988]. Groundwater seepage erosion has been proposed as the mode of formation for these features [*Kochel and Piper*, 1986], although alternative models exist [*Dunne*, 1990; *Lamb et al.*, 2006].

Kochel and Piper [1986] proposed a five stage sequence for Hawaiian drainage development, presuming a pre-existing high drainage density, with runoff-dominated streams in parallel arrangement. Such drainage patterns are found on Mauna Loa, Mauna Kea and the leeward side of Kohala. In their model, as streams cut downward, some intersect high elevation, dike-confined aquifers, leading to accelerated erosion by groundwater seepage. The valleys then widen and lengthen headward by mass-wasting of the valley walls, resulting in a characteristic U-shaped cross-section. This stage is seen on the windward side of Kohala. Eventually headward retreat reaches the watershed divides, and the valleys widen into light-bulb shapes by piracy of adjacent channels, such as the form exhibited on parts of Molokai. When the valleys can no longer grow by seepage erosion, they are subjected to dissection by surface processes. This late stage of evolution was proposed to explain the complex topographies of Oahu and Kauai. In the *Kochel and Piper* [1986] model of landscape evolution, drainage density decreases and local relief increases as seepage erosion forms deep valleys and abstracts lower tributaries. In later stages, drainage density increases and

relief decreases as the seepage valleys are degraded. *Seidl et al.* [1994] showed that the stream power law applies to runoff-dominated channels on 5.1 Ma basalts on Kauai, suggesting that after an elapsed time of several million years a classical runoff-dominated drainage network is in place.

Baker and Gulick [1987] proposed a three-stage model for drainage evolution on Hawaiian and Martian volcanoes. In the first stage, many runoff-dominated ravines form, which the authors attribute to low permeability cap rocks, wet climates, or high relief. Some of these ravines then deeply incise into highly permeable groundwater-bearing strata. These valleys grow headward by seepage erosion, leaving the remaining shallow runoff-dominated ravines as a relict landscape. In this model of drainage evolution, drainage density decreases as seepage valleys replace runoff-dominated channels.

Baker and Gulick [1987] report ranges of drainage densities for humid and dry areas for the major Hawaiian Islands, which range in age from active to 5 Ma. For a given age, median drainage density is higher in humid areas than arid areas. Additionally, drainage density generally increases with time for both climate zones, although median drainage density is actually highest for humid areas of Molokai (1.76 to 1.9 Ma). The observed pattern of drainage density changes through time is not consistent with either the *Baker and Gulick* [1987] or the *Kochel and Piper* [1986] models of landscape evolution, nor do their models adequately address the initial establishment of channels on the land surface. These results suggest that an alternate model of drainage evolution is required for the Hawaiian Islands. Recent research suggests that major landslides combined with waterfall erosion may instead drive the formation of amphitheater-headed valleys in Hawaii [*Lamb et al.*, 2005]. The Hawaiian studies largely leave open the question of how land surface permeability affects rates and processes of drainage development.

A detailed study of hydrological properties of soils developed on 300 year old and 4.1 Ma Hawaiian basalts showed contrasting saturated hydraulic conductivity profiles resulting from subsurface clay accumulation over time [*Lohse and Dietrich*, 2005]. The young soil had a consistently high hydraulic conductivity, while the old soil had clay horizons with hydraulic conductivities two to three orders of magnitude lower than upper coarser horizons. These clay horizons increased the importance of lateral shallow subsurface flow and surface runoff from saturation overland flow. This study does not investigate linkages between plot scale hydrologic changes and the larger question of landscape evolution on the Hawaiian islands, but the authors suggest increased overland flow as a result of clay horizons would increase erosion and might lead to channel development [*Lohse and Dietrich*, 2005].

In the Oregon Cascades, young Quaternary landscapes have lower drainage densities and slower, deeper water routing than nearby Tertiary landscapes [*Grant*, 1997; *Tague and Grant*, 2004]. The Quaternary basalts are characterized by high hydraulic conductivity for the upper several hundred meters [*Manga*, 1997; *Jefferson et al.*, 2006]. On Tertiary basaltic landscapes, similar hydraulic conductivities are found only for the 1-3 m deep soil mantle [*Dyrness*, 1969; *Harr*, 1977].

We propose a conceptual model of drainage development for the basalts that emphasizes the role of permeability reduction in allowing drainage network establishment (Figure 4.1). Effectively all net precipitation infiltrates into young lava, forming groundwater systems. In order for surface drainage to develop, infiltration capacity must be reduced, as drainage density has been shown to vary as a function of transmissivity [*Carlston*, 1963]. We propose that weathering and deposition of a lower permeability mantle may both play roles in reducing permeability, but that the rates and relative importance of each in contributing to surface drainage network formation are poorly understood. Once the land surface permeability is sufficiently low, recharge to the groundwater systems is shut off and shallow subsurface flow becomes the major

drainage mechanism, resulting in the establishment of a channel network and the eventual dissection of the landscape.

We test our proposed conceptual model on the basaltic landscapes on the west slope of the Oregon Cascades. Permeability can vary by several orders of magnitude, even at scales of a few square meters, so we focus on soil development, flowpaths, and geomorphic evolution as indicators of permeability and drainage network development. Using dated rock units as a constraint on the space for time substitution, we establish a chronosequence, with homogeneous climate, elevation, and rock type to investigate drainage evolution on these basalts. We combine field observations, slope-area relationships, and estimates of process efficacy to constrain rates and processes of drainage development on basalts less than 7 Ma. We explore how insights developed from the Oregon Cascades may be applicable to understanding landscape evolution in basaltic landscapes of other regions.

4.3 Field area

The Oregon Cascades are a volcanic arc formed by the subduction of the Juan de Fuca slab under the North American Plate, and they are commonly divided into two provinces: the High Cascades and the Western Cascades. The High Cascades, the active portion of the arc, mostly lies within a graben where extensive Quaternary and Pliocene volcanism has been associated with nearly 3 km of rift-related subsidence in the past 5 million years [*Conrey et al.*, 2002]. The region has produced dominantly basaltic and basaltic andesite lavas from shield volcanoes and cinder cones, but it is also interspersed with composite volcanoes of more diverse composition, such as the Three Sisters [*Sherrod and Smith*, 2000]. The permeability of young basalts is $\sim 10^{-5}$ to 10^{-7} cm^2 [*Jefferson et al.*, 2006]. The crest of the range lies 1500-2000 m above sea level, with the high peaks exceeding 3000 m. The Western Cascades represents the Miocene-Eocene arc, with dacitic tuffs, andesite lava flows, and lesser basaltic and

rhyolitic volcanic rocks. Western Cascades rocks are extensively faulted and strongly folded [*Conrey et al.*, 2002], and peak elevations reach 1800 m.

The Cascades region has been subject to three Pleistocene glaciations, each of which formed an ice cap over the Cascade crest with outlet glaciers carving U-shaped valleys [*Scott*, 1977]. Glaciation also occurred in the higher elevations of the Western Cascades, as evidenced by cirques and U-shaped valleys [*Swanson and Jones*, 2002]. At the last glacial maximum, equilibrium line altitudes in the Mt. Jefferson to Three Sisters area were between 1650 and 2000 m on the east side of the crest [*Scott et al.*, 1989]. Two minor glacial advances occurred in the past 8000 years, with equilibrium line altitudes in the range of 2300 to 2500 m. Present equilibrium altitudes are between 2500 and 2600 m in the Three Sisters area [*O'Connor et al.*, 2001], and glaciers are restricted to the flanks of the composite volcanoes. There is evidence for subglacial volcanic activity in palagonites exposed at North Sister [*Schmidt et al.*, 2002] and in isolated tuya forms [*Conrey et al.*, 2002]. Most pre-Holocene High Cascades volcanoes show extensive glacial erosion.

The study area is located in the watershed of the upper McKenzie River at McKenzie Bridge (44.1-44.5°N, 121.7-122.2°W) on the west slope of the central Oregon Cascades (Figure 4.2). It covers an area of 901 km^2, 68% of which is basalt or basaltic andesite, and has an elevation range of 435 to 3075 m. The upper McKenzie River has a north-south trajectory because its position is aligned along the graben boundary. In the Cascades, >75% of annual precipitation falls during the winter, with seasonal snowpacks above 1200 m and transient snowpacks and rain below 1200 m. There is a strong orographic effect, with ~2 m of precipitation at lower elevations and up to 3.8 m on peaks along the Cascade crest [*Taylor and Hannan*, 1999]. The High Cascades are the major source of summer streamflow to Western Oregon [*Jefferson et al.*, 2004; *Tague and Grant*, 2004], owing to the steady discharge of groundwater emanating from the young basalts [*Jefferson et al.*, 2006; Chapter 3].

4.4 Methods

To test the proposed conceptual model and to constrain timescales of drainage network development, a chronosequence of dated rock units was established. Mapped and previously dated rock units were supplemented with ^{40}Ar/^{39}Ar ages of spring-producing basalts, in order to constrain the longevity of groundwater flowpaths. Field observations were made to identify and characterize the stages of geomorphic evolution, and drainage density was used as a measure of the trajectory of drainage development. Relationships between local slope and contributing area (slope-area relationships) were used to infer the influence of different processes on watershed morphology and the extent of the fluvial and debris flow channel networks, following the precedents of *Montgomery and Dietrich* [1989], *Tarboton et al.* [1992], and *Stock and Dietrich* [2003] among others.

Samples were collected in the vicinity of three springs for ^{40}Ar/^{39}Ar dating of rock age, in order to constrain the duration of major groundwater systems. At Roaring Spring, a basaltic andesite sample (AJ-04-5) was collected from the spring orifice, and at Olallie North Spring, a basalt sample (AJ-04-3) was obtained from an outcrop 10 m from the spring. Olallie South spring emerges from beneath a talus slope, so a basalt sample (AJ-05-5) was collected from an outcrop on the ridge above the talus slope. Major and trace element chemistry data for the samples are published in *Jefferson et al.* [2006]. Whole rock samples were analyzed using a MAP 215-50 rare gas mass spectrometer at the Noble Gas Laboratory, College of Oceanographic and Atmospheric Sciences, Oregon State University. The methods of *Duncan and Hogan* [1994] were followed for the analysis and ages were calculated using ArArCalc V2.2 [*Koppers*, 2002].

Extensive reconnaissance of the field area was accompanied by descriptions of incipient channels and springs on basalts of varying age, and measurements were made along transects of Holocene and late Pleistocene lava flows. Five transects were

selected to span a range of independently established ages. These transects range in elevation from 700-1100 m, lack glacial cover, and are located near the distal end of the lava flow. The 75-130 m transects were established perpendicular to the major lava flow direction, and exhibited a range of forest and soil development conditions. At 2 m or 4 m intervals along each transect, soil depth and clast size were measured and vegetative cover was estimated in a 1 m^2 plot.

Within the McKenzie Bridge watershed, stream networks were digitized from "blue lines" on 1:24,000 USGS topographic maps, and twelve channel head locations were verified in the field using handheld GPS and compared to mapped blue line termini. Drainage densities were calculated for each mapped rock unit, using the classification of *Sherrod and Smith* [2000], which differentiates units based on rock type and age.

Using a 10-m DEM derived from 1:24,000 USGS topographic maps, we delineated the watershed for the McKenzie River at McKenzie Bridge (901 km^2). In order to infer process domains acting in watersheds of different ages, slope-area relationships of four watersheds were computed from D-infinite algorithm-derived contributing areas and slopes for each DEM pixel [*Tarboton*, 1997]. Results were binned into 100-pixel groups sorted by contributing area, and regression lines were fitted to data with contributing areas ≥1000 m^2. The four watersheds for which this analysis was completed are Belknap, Boulder Creek, Browder Creek, and Olallie Creek (Figure 4.2).

4.5 Chronology

Our ^{40}Ar/^{39}Ar dates add to the array of dated basaltic lava flows in the study area (Figure 4.3). The sample from Roaring Spring, in the southern McKenzie River watershed, yielded an age of 684,000 ± 40,000 years, and the sample from the cliff above Olallie South Spring yielded an age of 535,000 ± 63,000 years. Olallie North Spring emerges from a Scott Mountain basaltic lava [*Jefferson et al.*, 2006], and we

found an ^{40}Ar/^{39}Ar date of 35,000 ± 25,000 years. The sample is at the lower end of the range of applicability for the method, because of the long half-life of ^{40}K, leading to high uncertainty in the age estimate. Lavas in the field area are age-constrained by the presence or absence of till and Mazama ash (7700 years before present (ybp), [*Bacon*, 1983]), and several lava flows in the field area had previously been dated by radiocarbon. Collier Cone basaltic andesite is dated at 1511 cal. ^{14}C ybp, the west flow from Belknap Crater is 1296-1505 ^{14}C ybp, and Nash Crater basalt is 2748-3186 ^{14}C ybp [*Sherrod et al.*, 2004].

Two recent geologic maps depict substantial portions of the field area. *Sherrod and Smith* [2000] map volcanic rocks of the Oregon Cascades. They break the Quaternary and Tertiary into ten age classes, seven of which are present as basalts and basaltic andesites in the watershed (Figure 4.3): Qb1 (0-12 thousand years [ka]), Qb3 (25-120 ka), Qb4 (120-780 ka), Qb5 (780 ka-2 Ma), Tb1 (2-7 Ma), and Tb2 (7-17 Ma). The other map [*Sherrod et al.*, 2004] provides more detail, particularly of late Quaternary lava flows, but covers only the eastern portion of the field area to W 122° longitude. Thus, we used a combination of both maps to understand geologic ages and features of the study area.

Weighted ages for study watersheds were calculated by assigning each mapped rock unit to the lower limit of its age range, because this limit best corresponded to ^{40}Ar/^{39}Ar and radiocarbon dates within the study watersheds. We designated an age of 11 ka for till and outwash, coinciding with the end of the Canyon Creek advance [*Scott et al.*, 1989]. Using the map units of *Sherrod and Smith* [2000], Belknap watershed has a weighted age of 9 ka, Boulder Creek watershed has an age of 109 ka, Olallie Creek watershed has an age of 275 ka, and Browder Creek watershed has an age of 2 Ma (Figure 4.3). The more detailed *Sherrod et al.* [2004] map spans the entire Belknap watershed, 85% of the Olallie Creek watershed, 80% of the Boulder Creek watershed, and none of the Browder Creek watershed. Weighted ages using this map are ~17 ka for Belknap, 52 ka for Olallie Creek, and 232 ka for Boulder Creek. The

weighted ages produced using the *Sherrod et al.* [2004] map are our favored interpretation, because of the higher resolution of geologic data.

4.6 Geomorphology of basaltic landscapes

4.6.1 Holocene lavas

Holocene lavas primarily exhibit constructional topography, with gentle slopes characteristic of shield volcanoes, clearly defined cinder cones, and elongate lava flows following pre-existing valleys. At the scale of individual lava flows, the surfaces are rough, with pressure ridges, flow levees, swales and closed depressions (Figure 4.4). Swales are ≤3 m deep on basalts and up to 7 m deep on the thicker basaltic andesite flows. Swales generally do not extend more than ~150 m longitudinally.

Most of the areas covered by Holocene lavas show no evidence of channel development. Springs are common at flow toes, and channels that intersect Holocene lavas rapidly become dewatered as the water infiltrates permeable units. Holocene lava flows often dam pre-existing drainages, and lava forms partial lake shores and bottoms for at least seven lakes in the McKenzie Bridge watershed. These lakes have sinkholes, springs, or both. Along the three transects on Holocene flows, there is only one instance of incipient surface drainage. On the Belknap lava flow, a 0.6 m deep, <50 m long, sloping swale has continuous moss and sedum cover, suggesting that the feature collects or retains more moisture than the surrounding landscape. On the Collier lava flow 1 km upslope of the transect, rounded gravel and flow aligned wood provide evidence for ephemeral flow in a shallow 2 m-wide channel.

Vegetative cover is less than 50% on all three transects and consists primarily of lichens and mosses with scattered forbs, shrubs, and trees. Tree species include vine maple (*Acer circinatum* Pursh), Douglas fir (*Pseudotsuga menziesii* (Mirbel) Franco), incense cedar (*Calocedrus decurrens* (Torr.) Florin), western redcedar (*Thuja plicata*

Donn ex. D. Don) and western white pine (*Pinus monticola* Dougl. ex. D. Don). Soils are thin (<5 mm) with high organic content, and the greatest soil accumulations are under tree canopies. Lava clasts average 26-56 cm in diameter and are angular. Decaying branches and logs are scattered across the flows, but the density of both living and dead vegetation increases towards the flow margins. This suggests that vegetation colonizes young lava flows from the flow margins, where adjacent older landscapes harbor dense forests.

Two major springs emerge from Holocene lavas in the McKenzie Bridge watershed. Great Spring (Figure 4.5a) emerges near the lateral contact between two Sand Mountain lava flows, and forms a ~12 m wide, 7 m deep pool leading to a 100 m, channel between the flows, that enters Clear Lake. Water seeps out through multiple small orifices in the younger lava close to the pool surface. Local relief above the pool is ~10 m. The pool level fluctuates by <0.5 m seasonally. Tamolitch Spring (Figure 4.5b) emerges in the bed of McKenzie River at the base of an 18 m waterfall. This waterfall is dry under most flow conditions because the entire discharge of the McKenzie River below Carmen Reservoir sinks into Belknap lava and emerges 1.5 km downstream at the spring [*Stearns*, 1929]. Under natural flow conditions, groundwater emerges from fissures ~3 m above the spring pool and falls into the ~10 m deep pool. Currently, a hydroelectric project diverts the McKenzie River around the losing reach and spring, and water emerging from the spring seeps out below the pool level. Both Great and Tamolitch springs have morphologies that are largely controlled by the constructional morphology of the groundwater-bearing lava flow. At Tamolitch Spring there is some evidence for plunge pool erosion from the ephemeral waterfall. Neither spring shows evidence for groundwater seepage erosion, such as overhanging alcoves or large rock debris in the pool.

4.6.2 Pleistocene lavas

Throughout the Quaternary, glaciation has been more important than fluvial erosion as a geomorphic agent, as evidenced by the abundance of cirques and glacial troughs and by the paucity of V-shaped valleys. Pleistocene lavas have been extensively glaciated and are mantled by till in many places. In unglaciated areas of Scott Mountain age, the undulating constructional volcanic topography is still detectable, although subdued by soil accumulation in the swales.

Two transects are located on unglaciated late Pleistocene lava flows (Figure 4.2b). Western hemlock, Douglas fir, and vine maple form the canopy over the Sims Butte lava transect, with low ground cover dominated by dwarf Oregon-grape (*Mahonia nervosa* Pursh (Nutt.)). The Scott Mountain lava transect has an open Douglas fir canopy, with moss, ferns, and forbs closer to the ground. For both transects, average soil depth is 16-17 cm, clasts average 4-5 cm in diameter, have visible weathering rinds, and are subangular to subrounded.

On Pleistocene basalts, both springs and runoff-dominated channels occur. Some streams are exclusively spring-fed (e.g., Olallie Creek), while some are runoff-dominated (e.g., Boulder Creek), and others contain a mixture of both spring water and runoff (e.g., Roaring River). Some channels begin where glacial scour has removed surficial rubble from the lava flow. In the upper reaches of many channels, incision is discontinuous, with 20-70 cm deep scour holes alternating with 1-3 m wide areas showing diffuse flow and little incision. Small, closed-basin lakes are common in glaciated areas. Springs rarely occur on till, but watersheds that are largely till-covered may still have springs in other areas.

There are four major springs on Pleistocene lavas in the McKenzie Bridge watershed, and none of them show any evidence for groundwater seepage erosion. Lost Spring (Figure 4.5c) emerges in a series of quiet shallow pools over an area of several acres.

Water appears to surface and resink several times before eventually forming a single-thread channel named Lost Creek. Most pools are <1 m deep with <2 m local relief above the pool level. Water levels in the pools vary <1 m per year. The spring emerges from Sims Butte basalt, 2.5 km upstream of the flow toe. A similar morphology is observed at Sweetwater Spring, which emerges from Scott Mountain lava. The main Olallie North Spring (Figure 4.5d) cascades out of Scott Mountain lava and down a steep slope for 5 m, before joining a channel with water from secondary springs. The channel lies in a narrow v-shaped valley, possibly resulting from the boundaries of two lava flows. The morphology of Olallie South Spring is obscured by large (≥1.5 m) talus blocks fallen from a cliff face to the south. Downstream from the spring, the channel is <3 m wide, conveys bankfull discharge for most of the year, and lacks evidence for overbank flow or incision of a valley larger than the modern channel. Spring-fed streams do not seem to be effective geomorphic agents of valley incision, possibly because they lack large floods or sufficient time for bedrock incision.

The ^{40}Ar/^{39}Ar ages of lava flows from which springs emerge provide evidence that permeability is sufficient for 650-700 ka for groundwater flow to be a major drainage mechanism. There are no dated spring-producing lava flows older than ~700 ka, suggesting that beyond this time permeability has been reduced enough to prevent high rates of groundwater recharge, and most water is instead routed into surface channels. However, small seeps and springs are found in older basalts, and the lack of large springs does not conclusively prove that permeability is too low to support their existence.

4.6.3 Pliocene lavas

Landscape forms in Pliocene High Cascade watersheds are similar to older Western Cascade watersheds. Tertiary lava landscapes are characterized by well-integrated networks of runoff-dominated channels. The overall landscape form is dominated by hillslope and fluvial processes, but glacial cirques are present at high elevations.

Hillslopes are relatively short (250 m - 1 km) and steep, averaging ~35° (Figure 4.6). Soils are generally loamy with poorly developed profiles, and have extremely high infiltration capacities [*Dyrness*, 1969]. Soil depths in the vicinity of three channel heads ranged from 30-130 cm. Overland flows have not been observed, large springs (≥ 1 m^3/s) are absent, and small springs are uncommon. Streams may have exposed bedrock in upper reaches, but are often alluvial step-pool streams for most of their length. Channel morphology is strongly influenced by low frequency, high-magnitude floods and debris flows [*Grant et al.*, 1990]. Debris flows following heavy precipitation events are a major mode of sediment transport [*Swanson and Fredriksen*, 1982]. Forests are dominated by Douglas fir, western hemlock (*Tsuga heterophylla* (Raf.) Sarg.), and western redcedar at lower elevations, and have noble fir (*Abies procera* Rehd.), Pacific silver fir (*Abies amabilis* (Dougl. ex Loud.) Dougl. ex Forbes), Douglas fir, and western hemlock at higher elevations.

4.7 Drainage development on basaltic landscapes

Drainage density increases with time (Figure 4.7) for the basalts in the McKenzie Bridge watershed. Upstream termini of the "blue line" network on 1:24,000 USGS topographic maps generally correspond with field-observed channel heads for Pleistocene and Tertiary basalts. The average distance between the blue line termini and field-observed channel heads is 210 m, with seven out of twelve field locations <80 m from mapped channel heads. However, we are unable to find any evidence for two first order streams on Holocene lavas. This suggests that the blue line network may substantially overestimate the extent of stream channels developed on the youngest basalts (Qb1), and that true drainage density might be lower than that calculated. Additionally, the drainage density of the oldest Quaternary basalts (Qb5) might be lower than otherwise expected, because it is primarily exposed along ridges having low contributing areas. Because the majority of the field area was covered with basaltic lava, we are unable to compare drainage densities on basalts to those on rock units of similar age but differing lithologies. The density of springs identified on

1:24,000 topographic maps drops from 0.07 per km^2 on Quaternary basalts to zero on Tertiary basalts. Within the Quaternary there is no relationship between basalt age and spring density. Thus, drainage density and the density of springs show an inverse relationship with time.

By calculating slope-area relationships we gain more insight into landscape evolution processes and timescales than by examining drainage density alone. Comparisons of field observations and DEM-derived slope-area domains suggest that process transitions are represented by scaling breaks in the slope-area relationship [e.g., *Montgomery and Foufoula-Georgiou*, 1993; *Ijjasz-Vasquez and Bras*, 1995; *Stock and Dietrich*, 2003]. Fluvial networks occupy the portions of watersheds with the greatest contributing areas and channel slopes show a power law decline with increasing contributing area. This power law exponent generally falls in the range of -0.4 to -0.7 for the fluvial domain [*Tucker and Whipple*, 2002]. Many steep watersheds also exhibit a debris flow channel network, with the transition between the fluvial and debris flow channel networks occurring at a slope of ~0.10 [*Stock and Dietrich*, 2003]. Slope-area relationships in the debris flow domain may be curved [*Stock and Dietrich*, 2003] or have a power law exponent of -0.25 [*Lague and Davy*, 2003]. Individual hillslopes account for the smallest contributing areas and have slopes that increase with contributing area. The inflection in the slope-area relationship at the point where slopes begin to decrease with contributing area is the inferred transition to convergent topography of hollows and channels [e.g., *Montgomery and Foufoula-Georgiou*, 1993; *Roering et al.*, 1999].

We selected four representative watersheds to form a chronosequence of landscape evolution in the study area and calculated slope-area relationships and longitudinal stream profiles for each of them. Each of the watersheds has a similar drainage area (20-33 km^2) and is tributary to the upper McKenzie River (Figure 4.2). The watersheds lack obvious morphologic features of glacial erosion, but two of the watersheds have glacial till.

4.7.1 Belknap (17 ka) and Browder Creek (2 Ma) watersheds

Belknap watershed (27.1 km^2) has no surface drainage and consists predominantly of <5000 year old lavas from Belknap Crater and the Inaccessible Cones (88% of area). Glacial till comprises 11% of the watershed area, with Qb5 covering <1%. The slope-area relationship (Figure 4.8a) shows some scatter for small contributing areas, but the dataset can be fit with a single power law equation, with a slope of -0.087. This trend is interpreted to represent the constructional morphology of the shield volcano.

Browder Creek watershed (20.0 km^2) consists primarily of Tb1 (98%) with a small area of Tertiary dacite (2%). Drainage density in this watershed is 1.05 km/km^2, and the longitudinal profile for Browder Creek has a generally concave shape with an average gradient of 4% (Figure 4.9). The slope-area relationship (Figure 4.8a) has some scatter at small contributing areas, but reveals breaks in slope at 700 m^2 and ~5x10^5 m^2. Contributing areas less than 700 m^2 are inferred to represent hillslopes, while those between 700 and ~5x10^5 m^2 represent the debris flow channel network. Above ~5x10^5 m^2 is the fluvial network. Slope-area relationships with similar inflections are seen in watersheds with debris flow channels in Marin County, California and the Oregon Coast Range [*Montgomery and Foufoula-Georgiou*, 1993] and in modeled landscapes subject to pore pressure-sensitive land-sliding [*Tucker and Bras*, 1998]. Furthermore, the transition between debris flow and fluvial domains in the Browder Creek watershed at ~0.2 is similar to field observed debris flow-fluvial transitions in the Oregon Coast Range and Marin County, California [*Montgomery and Foufoula-Georgiou*, 1993] although it is higher than the ~0.03 to 0.1 reported by *Stock and Dietrich* [2003]. Channel heads in the watershed indicated by blue line termini on 1:24,000 topographic maps have an average contributing area of 3x10^4 m^2. However, the slope-area relationship indicates that the fluvial network begins at ~5x10^5 m^2, suggesting that some debris flow channels may have been mapped as fluvial features by the map makers. The slope-area relationship emphasizes the

importance of debris flows as a geomorphic process in mature watersheds of the Oregon Cascades.

The older landscape has steeper hillslopes and as contributing areas increase, slopes decline more rapidly than in the young landscape. The divergence between the Belknap and Browder Creek slope-area relationships indicates that the constructional morphology has been completely obliterated by hillslope, mass movement, and fluvial processes during the Quaternary.

4.7.2 Olallie Creek (52 ka) and Boulder Creek (232 ka) watersheds

The Olallie Creek and Boulder Creek watersheds have a mixture of rock types, and differ in terms of their drainage development. Olallie Creek watershed (29.6 km^2) has a drainage density of 0.55 km/km^2, with channels beginning at two large springs, and a concave stream profile with an average gradient of 4.7% (Figure 4.9). The watershed's geology is 34% Qb5, 31% Qb3, 33% till, and 2% outwash.

Boulder Creek watershed (32.7 km^2) has a drainage density of 0.94 km/km^2, and the streams are runoff-dominated. The geology is 63% till, 30% Qb3, and the remainder is comprised of small areas of Tb2, Tb1, Qb5, Qb4, and outwash. The longitudinal profile of Boulder Creek (Figure 4.9) has distinct slope changes that may be the result of differential rock hardness or may reflect knickpoint propagation. Unlike a classic graded concave form, the stream is steeper in its lower reaches where it is flowing over the older Tb1 and Qb5 than in its upper reaches on younger till and Qb3. Knickpoint retroregression may also have been set off the lower elevation local base level of the McKenzie River, as a result of its location along the graben boundary and higher incision rates along the trunk stream.

Slope-area relationships for the two watersheds plot in the space between the trends of the Belknap and Browder Creek watersheds (Figure 4.8). Even though there are fluvial

channels in both watersheds, there are no pronounced inflections in the slope-area trend. Data from both watersheds are best fit with single power law slopes of -0.13 for Olallie Creek watershed and -0.14 for Boulder Creek watershed. In the Olallie Creek data, there is a suggestion of a slope break at $\sim6 \times 10^6$ m^2, but there is considerable scatter in the data and field-observed channel heads at the springs have a contributing area of $\sim1.2 \times 10^6$ m^2. For Boulder Creek, slopes are generally constant at areas $>2 \times 10^5$ m^2, the average fluvial channel head contributing area as determined from the digitized stream network. The lack of concave longitudinal profiles and scaling breaks at the channel heads might reflect insufficient time for equilibrium profiles to develop.

Multiple factors may influence the extent of drainage network development in the Olallie Creek and Boulder Creek watersheds, particularly groundwater flowpaths, till cover, and watershed age. The absence of large springs in the Boulder watershed may be related to the vagaries of groundwater flowpaths, which are not necessarily concordant with surface topography and watershed boundaries in the study area. In fact, Olallie South Spring may be deriving some of its discharge from the Boulder Creek watershed [*Jefferson et al.*, 2006]. However, a paucity of groundwater cannot solely explain the presence of surface drainage development, which requires a sufficiently impermeable land surface to promote runoff at the expense of infiltration.

Till has lower permeability than young basalts [*Freeze and Cherry*, 1979], so abundant till in a watershed may promote channel development and inhibit the expression of springs. However, in the southern McKenzie River watershed, the watershed of Roaring Spring is >99% covered by glacial till, but sustains a 1.9 m^3/s spring emerging from a basaltic andesite outcrop. Upslope of the spring there is a network of ephemeral runoff-dominated channels. Discharge measurements in the summer of 2002 show that <1% of the flow below Roaring Spring originated in the ephemeral channels. The groundwater feeding the spring largely recharges outside of the topographic watershed [*Jefferson et al.*, 2006]. These data suggest that deposition

of glacial till in the topographic watershed is not sufficient to cause a transition from groundwater-dominance to surface runoff-dominance.

Thus, the difference in drainage development between the two transitional stage watersheds is not exclusively a result of groundwater flowpaths or till deposition. More extensive drainage development in the Boulder Creek watershed may reflect its older weighted age, meaning that more time has elapsed for permeability reduction and drainage network evolution. However, the similarities between the slope-area relationships of the two transitional watersheds suggest that the Boulder Creek watershed is one in which fluvial erosion has not had sufficient time or power to leave a significant landscape signature.

Well developed, runoff-dominated stream networks with smooth, concave longitudinal stream profiles are not found on Quaternary basaltic landscapes in the field area. Rather, slope-area relationships and stream profiles are controlled by some combination of constructional form, glacial processes, and knickpoint propagation. The relative importance of each of these factors probably varies across the landscape. However, it is very clear that, despite the abundance of water, the Quaternary High Cascades landscape is not dominated by fluvial processes. The changeover to a landscape sculpted by fluvial and mass-wasting processes seems to require the passage of considerable geologic time and the accompanying reduction in land surface permeability.

4.8 Mechanisms for permeability reduction

There is no evidence for seepage erosion in the field area, and recent work has questioned its general efficacy in bedrock landscapes [*Lamb et al.*, 2006]. Therefore drainage development must occur through some form of permeability reduction resulting in a transition from groundwater to runoff-dominance. Permeability reduction likely occurs by decreasing pore and void volume, through in-filling by

allochthonous material, stripping of rubble, and in-filling by autochthonous weathering and alteration processes. Each permeability-reducing mechanism would have its own rate of efficacy, but multiple processes likely operate simultaneously, resulting in a faster rate of permeability reduction than that of any one process alone (Figure 4.10). Some mechanisms, like ash or loess deposition, would cause punctuated changes in permeability, while processes like chemical weathering would proceed continuously. Here we discuss each process in relation to the Oregon Cascades field area. Figure 4.10 conceptually illustrates possible mechanisms for reducing permeability in the field area, with a qualitative assessment of the relative efficacies of each process.

4.8.1 Allochthonous processes

Permeability reduction processes that are driven by the introduction of solid materials external to the lava flow, i.e., allochthonous material, includes ash mantling, deposition of eolian sediment, glaciation, and senescence of biological material. These processes are controlled by the availability of material, and may operate in a punctuated fashion.

Volcanic ash initially has high porosity and permeability, but weathers quickly to form soils with very high water retention capacities and permeability lower than that of young basaltic lavas [*Shoji et al.*, 1993; *Ping*, 2000]. Ash from explosive volcanic eruptions could fill pore spaces in lava flow rubble zones, clog fractures in flow interiors, and potentially penetrate to clog pores in underlying flows. Ash could also mantle the land surface, allowing drainage to develop above underlying basalts. Ash mantling may be significant in promoting drainage development in some environments. On Hawaii there is a correspondence between surface and near-surface ash deposits and valley incision [*Gulick*, 2005].

However, there are substantial obstacles to ash infilling as a major mechanism for permeability reduction in the Oregon Cascades and elsewhere. Basaltic eruptions generally do not produce voluminous ash, so silicic volcanic vents are necessary to increase the probability of substantial ash fall on basaltic lavas. Ash producing eruptions would have to occur upwind of basaltic lava fields, and be close, frequent, and voluminous enough to deposit substantial amounts of material. In the Cascade Range prevailing winds blow to the east. Volcanic centers are located along the Cascade crest or to its east, suggesting that ash infilling should be less important on the west side of the range than on the east side. In the field area, ash deposits from the cataclysmic Mt. Mazama eruption are 15-50 cm thick [*Skinner and Radosevich*, 1991]. Assuming an initial 15% porosity and 5 m thickness for an individual flow, 75 cm of ash would be required to fill the void spaces. Isopleth maps of ash thickness show that for major Cascade eruptions, uncompacted ash depths exceeded 75 cm only within 100 km of the volcanic vent, and for the 1980 Mount St. Helens eruption this depth was not exceeded even within a few kilometers of the vent [*Hoblitt et al.*, 1987]. Thus, geographically concentrated eruptions larger than that of Mount St. Helens would have to occur with a smaller recurrence interval than that of lava flow burial by subsequent flows. In the central portion of the Cascades arc, mafic volcanism has far exceeded more silicic volcanism during the Quaternary [*Sherrod and Smith*, 1990], making such void infilling by ash a secondary mechanism for permeability reduction in the field area.

Mantling of flows or infilling of voids by glacially-derived loess or other eolian sediment would work in the same manner as with volcanic ash to permit drainage development. The importance of these processes in a particular area is constrained by the availability of eolian sediment, but lava flows may be effective traps of eolian material because of their high surface roughness and lack of runoff to remove material [*Wells et al.*, 1985]. Loess likely promotes surface drainage, because it has a permeability range (10^{-8} to 10^{-12} cm^2) that is several orders of magnitude lower than those of young basalts [*Freeze and Cherry*, 1979]. In eastern Washington, Pleistocene

Palouse loess thickly covers Miocene Columbia River basalts, in some places to a depth of 75 m. Groundwater recharge is most limited where intense soil development occurred during lulls between loess deposition episodes [*O'Green et al.*, 2005]. At the Cima and Lunar Crater volcanic fields of California and Nevada, 1-3 m of eolian sediments mantle 15 ka to 1.95 Ma basaltic lavas. Shallow channel networks are cut into the eolian mantle, and only locally into the underlying basalt [*Dohrenwend et al.*, 1987]. On the west slope of the Oregon Cascades, the climate is sufficiently humid to make eolian processes unimportant during the Holocene. Some loess deposition may have occurred following Pleistocene deglaciations of the Cascades.

Glaciation potentially has several impacts on land-surface permeability in basaltic terrains, including deposition of till, scour of surface material, compaction of voids, or bedrock fracturing. Glacial till has fairly low permeability (10^{-9} to 10^{-15} cm^2) [*Freeze and Cherry*, 1979], reducing groundwater recharge. Till may not only overlie basaltic lavas, but some particles may also penetrate the fractures and voids in the lava and reduce its permeability. Glacial scour may also reduce the surface permeability by removing rubble at the flow top and exposing the massive interior. However, flow interiors also have permeability associated with cooling fractures. The overburden pressure from glacial ice may compact sediments or soils overlying lava flows [*Clarke*, 2005], and may also compact rubble zones on flow tops and bottoms. Overburden from glacial ice may also increase permeability by inducing fracturing. However, the uniaxial compressive strength of basalt is 80-120 MPa [*Middleton and Wilcock*, 1994], which translates to an ice thickness greater than that for continental glaciers, so fracturing from glacial overburden pressure is unlikely. Simulation of a continental glaciation using a transient, coupled hydro-mechanical model showed that in a fractured crystalline rock, glacial loading resulted in some compression of pore space, but did not induce failure [*Chan et al.*, 2005]. Permeable glacierized watersheds can also have major groundwater flow systems. Modeling suggests that up to ~30% of subglacial water from the Icelandic icecap Vatnajökull may be carried by buried lava aquifers [*Flowers et al.*, 2003]. These findings suggest that till deposition, erosion of

rubble, and compaction of overlying sediment have more important effects on permeability than bedrock compaction or fracturing.

In the Oregon Cascades there have been at least three major Quaternary glaciations [*Scott*, 1977]. There are no comprehensive maps of glacial extent for the west side of the Cascades, because of dense vegetation and subsequent emplacement of Holocene lava fields. In the McKenzie Bridge watershed, areas mapped as glacial till have a greater drainage density than basalts younger than 780 ka (Figure 4.7). Glacial scour has also been associated with channel development in the study area, as evidenced by channel heads on glacially striated massive basalt. However, springs emerge from glaciated watersheds and runoff-dominated streams flow from low-elevation, non-glaciated watersheds. These results suggest that glaciation accelerates drainage development in the Oregon Cascades, although glaciation is neither sufficient nor necessary to render surface runoff more important than groundwater.

As noted, vegetation first colonizes the edges of young lava flows, possibly from pre-existing habitats not overrun by lava flows [*Inbar*, 1994; *Inbar et al.*, 1995]. Trees that overhang the margins of a flow drop leaves, needles, and branches onto the flow. This litter fall may serve a minor void-filling role, but, more importantly, it facilitates soil development and accelerates weathering rates, allowing more vegetation to colonize the lava. In the McKenzie Bridge watershed, on lava less than 5000 years old, vegetation density increases toward the flow edges, and mature forests are found on most lava older than 5000 years. Thus, vegetative colonization greatly precedes the transition from groundwater-dominance to runoff-dominance.

4.8.2 Autochthonous processes

The processes of mechanical and chemical weathering and hydrothermal alteration do not require the episodic input of outside solid materials, so weathering and hydrothermal alteration may represent more continuous mechanisms for reducing

permeability than the allochthonous mechanisms described above. Mechanical weathering may reduce permeability by creating fine rock fragments that fill spaces between clasts in rubble zones, but the weathering process can also increase permeability by creating new fractures. Filling of topographic lows by basaltic colluvium on Quaternary lava flows in California was attributed to mechanical weathering and mass failure [*Wells et al.*, 1985]. Mechanical weathering processes acting in the Oregon Cascades include frost and root wedging.

Chemical weathering of basalts has been extensively studied [e.g., *Colman*, 1982; *Gislason et al.*, 1996; *Dessert et al.*, 2003]. Chemical weathering occurs when water dissolves primary minerals, causing the formation of secondary clay minerals, and resulting in dissolved loads in groundwater and rivers and soil formation. Basalts weather to spheroidal forms with unaltered cores surrounded by rinds of increasingly weathered materials [*Colman*, 1982]. Weathering of basalts in southeastern Oregon generates smectites from volcanic glass, olivine, pyroxene, and plagioclase [*Banfield et al.*, 1991]. In unaltered Western Cascade volcanic and volcaniclastic rocks, smectite is the most abundant clay mineral, and smectite-rich soils hold water and are prone to mass wasting [*Ambers*, 2001]. For basalts and andesites in the western United States, the ultimate weathering product takes ~100,000 years to develop and contains a sizable fraction of clay-sized particles [*Colman*, 1982]. In basaltic landscapes permeability decreases as the amount of clays in the rock and soil profile increases [*Lohse and Dietrich*, 2005], and volume collapse may occur as leaching removes material [*Vitousek et al.*, 1997].

Runoff and temperature are the main controls on chemical weathering of basalts. Rock mineralogy, vegetation, glacial cover, and rock age have also been cited as influencing weathering rate [*Gislason et al.*, 1996; *Benedeti et al.*, 2003; *Pokrovsky et al.*, 2005]. A limited dataset suggests that glacier cover slows the chemical weathering rate of basaltic watersheds [*Gislason et al.*, 1996]. However, high rates of mechanical weathering associated with glaciation may also increase the rate of chemical

weathering by increasing the surface area of the rocks. Glassy basalt, such as hyaloclastite, dissolves ~10 times more quickly than crystalline basalt [*Gislason et al.*, 1996]. In southwest Iceland the chemical weathering rate decreases with increasing age of basalts (0.2 to 7.7 Ma), which may be due the greater abundance of hyaloclastite in basalts <1 Ma. Hyaloclastite is produced during subglacial volcanic eruptions, the frequency of which increased with increasing glacierization in the past 1 Ma. Data from weathering rinds on basalts and andesites from the western United States suggest that the rate of weathering rind growth and element loss declines with time [*Colman and Pierce*, 1981; *Colman*, 1982]. Due to temperature and glaciation effects, chemical weathering rates may have been slower during the Pleistocene than in modern and Pliocene times. Weathering may be occurring faster on younger Quaternary basalts than their older counterparts.

Basalt weathering rates are higher than for most other rocks, but they vary widely around the world. The average chemical weathering rate is 55 t/km^2/yr for 0.2-7.7 Ma basalts in southwest Iceland, where mean annual temperatures are 2-5 °C lower than in the Oregon Cascades [*Gislason et al.*, 1996]. Chemical weathering rates of 0-11 Ma basalts on Mount Cameroon in equatorial west Africa range from 3-56 t/km^2/yr for high elevations with low temperatures and precipitation to 3-288 t/km^2/yr for low elevations with high temperatures and precipitation [*Benedeti et al.*, 2003]. On Sao Miguel, a Pleistocene basaltic island in the Azores Islands, chemical weathering rates are 26-50 t/km^2/yr [*Louvat and Allegre*, 1998]. In all of the above environments, mechanical weathering rates are calculated to exceed chemical weathering rates.

Chemical weathering rates have not been constrained in the Cascades, although work is currently underway to do so using solute fluxes from springs in the field area. In the Oregon Coast Range, chemical weathering rates from a small greywacke catchment are 32±10 t/km^2/yr [*Anderson et al.*, 2002]. The Coast Range estimate combined with studies on other basaltic landscapes suggests that basalt weathering rates in the field area may be on the order of 50-75 t/km^2/yr. The global runoff and temperature-based

weathering correlations of *Dessert et al.* [2003] yield a weathering rate of ~36 t/km^2/yr for the study area. Given the density of basalt, these estimates translate as 0.013 to 0.029 mm/yr, which is an order of magnitude lower than estimated trunk stream incision rates of 0.14 to 0.33 mm/yr in the central Oregon Cascades [*Sherrod*, 1986]. Chemical weathering may play an important role in reducing the permeability of basaltic lavas in the Oregon Cascades, but erosion rates clearly demonstrate that mechanical processes dominantly produce material for erosion.

Hydrothermal alteration occurs when hot fluids interact with rock resulting in changes to the mineralogy and texture, and it is associated with geothermal systems in volcanic regions. The rates and mineralogies of alteration are controlled by temperature, pressure, fluid composition, rock composition, and permeability [*Wohletz and Heiken*, 1992]. Highly permeable rocks and high permeability zones within rocks show more extensive alteration than lower permeability zones [*Larsson et al.*, 2002]. Like chemical weathering, hydrothermal alteration lowers the permeability of the bedrock by converting basalts to clay minerals. In the Western Cascades, some areas have experienced significant hydrothermal alteration in the past. In these areas illite, chlorite, smectite, and vermiculite are the dominant clay minerals [*Ambers*, 2001]. In the upper 300 m of the High Cascades, however, hydrothermal systems appear to be very spatially limited, and are associated only with fault zones [*Ingebritsen et al.*, 1994; *Saar and Manga*, 2004; *Jefferson et al.*, 2006]. Low-temperature, near-surface hydrothermal alteration to zeolite is found outside of fault zones in the High Cascades [*Schmidt et al.*, 2002], and vesicle-filling zeolites may be the most important source of permeability reduction associated with hydrothermal alteration in Cascades Quaternary lavas.

4.9 General discussion

Field and geomorphic observations constrain the timescales of drainage development. Holocene lava flows are exclusively drained by groundwater, as a result of their high

initial permeability. Pleistocene lava flows are drained by both groundwater and surface water, with groundwater remaining dominant for at least 700 ka in some watersheds, while runoff-dominated stream networks become established in less than 200 ka in other watersheds. Large springs seem to disappear after the establishment of runoff-dominated channels upslope, so that there is a period with co-dominance of the two drainage mechanisms. By 2 Ma all watersheds have established runoff-dominated drainage networks and lack major springs. The observed timescales for drainage development in the Oregon Cascades are not perfectly defined, nor are they translatable to regions with a different climate or volcanic history.

In terms of geomorphic evolution, groundwater seepage erosion and incision by spring-fed streams are geomorphically ineffective agents of landscape change. In runoff-dominated watersheds on Quaternary basalt, slope-area relationships are still controlled by constructional form, glacial processes, and knickpoint propagation, but in older watersheds topographic form is set by fluvial and hillslope processes. We suggest that the combination of glaciation and chemical weathering are the most significant processes driving drainage development in the study area. The timescales on which these processes operate are in line with the rates of landscape evolution observed on the west slope of the Oregon Cascades.

The above results combined with the discussion of permeability reducing mechanisms suggest a revised conceptual model for drainage development on permeable basaltic landscapes. At an early stage, groundwater is the sole drainage mechanism, but as an overlying mantle of material develops, initiation of surface drainage occurs when a land surface permeability on the order of 10^{-8} cm^2 is attained. Loss of substantial groundwater flow occurs at a somewhat lower permeability, as the mantle material reduces recharge and chemical weathering reduces bedrock permeability. The timescale of surface drainage initiation is largely constrained by the time required to accrete a sufficiently thick or impermeable mantle layer. Initially, the channel network incises through the mantle material, and the landscape form has little fluvial signature.

By the time streams begin to incise bedrock, chemical weathering has reduced lava permeability to such an extent that flow does not disappear into the subsurface, and fluvial and mass-wasting processes take over as dominant agents of geomorphic change, resulting in a classical runoff-dominated dissected landscape. This conceptual model should be applicable to other climatic regions, although the processes and rates of permeability reduction may vary.

This study supports the findings of *Lohse and Dietrich* [2005], who show that clay development by chemical weathering is an important process driving the hydrological evolution of basaltic landscapes. The geomorphology of the Cascades argues against conceptual models that assign groundwater seepage erosion or incision by groundwater-fed streams significant roles in the evolution of permeable landscapes. Instead, the results suggest that punctuated processes like glaciation, knickpoint generating events, ash fall, and loess deposition can be important drivers of drainage network evolution. Chemical weathering and punctuated processes are generally neglected in landscape evolution models, but those processes would be important to include in models of landscapes where initial permeability is too high for surface drainage and stream power-driven erosion.

We have shown that permeability reduction is an important component of drainage development on basaltic landscapes. In the Oregon Cascades permeability reduction is largely accomplished through glaciation and chemical weathering, but in other volcanic settings, processes such as eolian deposition or hydrothermal alteration may play a more important role. Regardless of the setting, drainage evolution on basaltic landscapes likely follows the sequence of early groundwater dominance being replaced by a runoff-dominated channel network as permeability decreases over geologic time.

4.10 Acknowledgements

4.11 References Cited

Allison, R. J., J. R. Grove, D. L. Higgitt, A. J. Kirk, N. J. Rosser, and J. Warburton (2000), Geomorphology of the eastern Badia basalt plateau, Jordan, *The Geographical Journal*, *166*, 352-370.

Ambers, R. K. R. (2001), Relationships between clay mineraology, hydrothermal metamorphism, and topography in a Western Cascades watershed, Oregon, USA, *Geomorphology*, *38*, 47-61.

Anderson, S. P., W. E. Dietrich, and G. H. J. Brimhall (2002), Weathering profiles, mass-balance analysis, and rates of solute loss: linkages between weathering and erosion in a small, steep catchment, *GSA Bulletin*, *114*, 1143-1158.

Bacon, C. R. (1983), Eruptive history of Mount Mazama and Crater Lake Caldera, Cascade Range, USA, *Journal of Volcanology and Geothermal Research*, *19*, 57-115.

Baker, V. R. (1988), Evolution of valleys dissecting volcanoes on Mars and Earth, in *Sapping Features of the Colorado Plateau: A Comparative Planetary Geology Field Guide*, edited by A. D. Howard, et al., pp. 96-97, National Aeronautics and Space Administration, Washington, DC.

Baker, V. R., and V. C. Gulick (1987), Valley development on Hawaiian volcanoes, 297-299 pp, National Aeronautics and Space Administration, Washington.

Bandfield, J. L., V. E. Hamilton, and P. R. Christensen (2000), A global view of Martian surface compositions from MGS-TES, *Science*, *287*, 1626-1630.

Banfield, J. F., B. F. Jones, and D. R. Veblen (1991), An AEM-TEM study of weathering and diagenesis, Abert Lake, Oregon: Weathering reactions in the volcanics, *Geochimica et Cosmochimica Acta*, *55*, 2781-2793.

Benedeti, M. F., A. Dia, J. Riotte, F. Chabaux, M. Gerard, J. Boulegue, B. Fritz, C. Chauvel, M. Bulourde, B. Deruelle, and P. Ildefonse (2003), Chemical weathering of basaltic lava flows undergoing extreme climatic conditions: the water geochemistry record, *Chemical Geology*, *201*, 1-17.

Carlston, C. W. (1963), Drainage density and streamflow, *Prof. Pap. 422-C*, U.S. Geol. Surv., Washington, D.C.

Chan, T., R. Christiansson, G. S. Boulton, L. O. Ericsson, J. Hartikainen, M. R. Jensen, D. M. Ivars, F. W. Stanchell, P. Vistrand, and T. Wallroth (2005), DECOVALEX III BMT3/BENCHPAR WP4: The thermo-hydromechanical

responses to a glacial cycle and their potential implications for deep geological disposal of nuclear fuel waste in a fractured crystalline rock mass, *International Journal of Rock Mechanics & Mining Sciences, 42*, 805-827.

Clarke, G. K. C. (2005), Subglacial processes, *Annual Review of Earth and Planetary Science, 33*, 247-276.

Colman, S. M. (1982), Chemical Weathering of Basalts and Andesites: Evidence from Weathering Rinds, *Prof. Pap. 1246*, 51 pp, U.S. Geol. Surv., Washington.

Colman, S. M., and K. L. Pierce (1981), Weathering Rinds on Andesitic and Basaltic Stones as a Quaternary Age Indicator, Western United States, *Prof. Pap. 1210*, 41 pp, U.S. Geol. Surv., Washington, D.C.

Conrey, R. M., E. M. Taylor, J. M. Donnely-Nolan, and D. R. Sherrod (2002), North-central Oregon Cascades: exploring petrologic and tectonic intimacy in a propagating intra-arc rift, in *Field Guide to Geologic Processes in Cascadia*, edited by G. W. Moore, Special Paper 36, pp. 47-90, Oregon Department of Geology and Mineral Industries, Salem.

Davis, S. N. (1969), Porosity and permeability of natural materials, in *Flow Through Porous Media*, edited by R. J. M. De Wiest, pp. 53-89, Academic Press, New York.

Dessert, C., B. Dupre, J. Gaillardet, L. M. Francois, and C. J. Allegre (2003), Basalt weathering laws and the impact of basalt weathering on the global carbon cycle, *Chemical Geology, 202*, 257-273.

Dohrenwend, J. C., A. D. Abrahams, and B. D. Turrin (1987), Drainage development on basaltic lava flows, Cima volcanic field, southeast California and Lunar Crater volcanic field, south-central Nevada, *Geological Society of America Bulletin, 99*, 405-413.

Duncan, R. A., and L. G. Hogan (1994), Radiometric dating of young MORB using the ^{40}Ar-^{39}Ar incremental heating method, *Geophysical Research Letters, 21*, 1927-1930.

Dunne, T. (1990), Hydrology, mechanics, and geomorphic implications of erosion by subsurface flow, in *Groundwater Geomorphology: The Role of Subsurface Water in Earth-Surface Processes and Landforms*, edited by C. G. Higgins and D. R. Coates, pp. 1-28, Geological Society of America, Boulder, Colo.

Dyrness, C. T. (1969), Hydrologic properties of soils on three small watersheds in the Western Cascades of Oregon, *Res. Note PNW-111*, Pac. Northwest For. and Range Exp. Stn., For. Serv., U.S. Dep. of Agric., Portland, Ore.

Flowers, G. E., H. Bjornsson, and F. Palsson (2003), New insights into the subglacial and periglacial hydrology of Vatnajokull, Iceland, from a distributed physical model., *Journal of Glaciology, 49*, 257-270.

Freeze, R. A., and J. A. Cherry (1979), *Groundwater*, 604 pp., Prentice Hall, Englewood Cliffs, NJ.

Genereux, D. P., S. J. Wood, and C. M. Pringle (2002), Chemical tracing of interbasin groundwater transfer in the lowland rainforest of Costa Rica, *Journal of Hydrology, 258*, 163-178.

Gislason, S. R., S. Arnorsson, and H. Armannsson (1996), Chemical weathering of basalt in southwest Iceland: effects of runoff, age of rocks, and vegetative/glacial cover, *American Journal of Science*, *296*, 837-907.

Grant, G. E. (1997), A geomorphic basis for the hydrologic behavior of large river systems., in *River Quality: Dynamics and Restoration*, edited by A. Laenen and D. A. Dunnette, pp. 105-116, Lewis Publishers, Boca Raton.

Grant, G. E., F. J. Swanson, and M. G. Wolman (1990), Pattern and origin of stepped-bed morphology in high-gradient streams, Western Cascades, Oregon, *Geological Society of America Bulletin*, *102*, 340-352.

Gulick, V. C. (2005), Revisiting valley development on Martian volcanoes using MGS and Odyssey data, paper presented at Lunar and Planetary Science Conference, League City, Tex.

Harr, R. D. (1977), Water flux in soil and subsoil on a steep forested slope, *Journal of Hydrology*, *33*, 37-58.

Hoblitt, R. P., C. D. Miller, and W. E. Scott (1987), Volcanic Hazards with Regard to Siting Nuclear-Power Plants in the Pacific Northwest, *Open File Report 87-297*, USGS, Vancouver, Wash.

Hynek, B. M., and R. J. Phillips (2003), New data reveal mature, integrated drainage systems on Mars indicative of past precipitation, *Geology*, *31*, 757-760.

Ijjasz-Vasquez, E. J., and R. L. Bras (1995), Scaling regimes of local slope versus contributing area in digital elevation models, *Geomorphology*, *12*, 299-311.

Ijjasz-Vasquez, E. J., R. L. Bras, and G. E. Moglen (1992), Sensitivity of a basin evolution model to the nature of runoff production and to initial conditions, *Water Resources Research*, *28*, 2733-2741.

Inbar, M. (1994), The geomorphological evolution of the Paricutin cone and lava flows, Mexico, 1943-1990, *Geomorphology*, *9*, 57-76.

Inbar, M., C. Risso, and C. Parica (1995), The morphological development of a young lava flow in the South Western Andes -- Neuquen, Argentina, *Zeitschrift fur Geomorphologie*, *39*, 479-484.

Ingebritsen, S. E., R. H. Mariner, and D. R. Sherrod (1994), Hydrothermal systems of the Cascade Range, north-central Oregon, *Prof. Pap. 1044-L.*, 86 pp. pp, U.S. Geol. Surv., Washington, D.C.

Jefferson, A., G. E. Grant, S. L. Lewis, and C. Tague (2004), Geology broadly predicts summer streamflow in volcanic terrains: lessons from the Oregon Cascades, *Eos Transactions American Geophysical Union*, *85*, Fall Meet. Suppl. Abstract H33C-0475.

Jefferson, A., G. E. Grant, and T. P. Rose (2006), The influence of volcanic history on groundwater patterns on the west slope of the Oregon High Cascades, *Water Resources Research*, *in press*, 2005WR004812.

Jenny, H. (1941), *Factors of Soil Formation: A System of Quantitative Pedology*, 281 pp., McGraw-Hill, New York. Reprinted 1994, Dover, Mineola, N.Y.

Kilburn, C. R. J. (2000), Lava flows and flow fields, in *Encyclopedia of Volcanoes*, edited by H. Sigurdsson, pp. 291-305, Academic Press, San Diego, Calif.

Kochel, R. C., and J. F. Piper (1986), Morphology of large valleys on Hawaii: evidence for groundwater sapping and comparisons with Martian valleys, *Journal of Geophysical Research*, *91*, E175-E192.

Koppers, A. A. P. (2002), ArArCALC--software for $^{40}Ar/^{39}Ar$ age calculations, *Computers & Geosciences 28*, 605-619.

Lague, D., and P. Davy (2003), Constraints on the long-term colluvial erosion law by analyzing slope-area relationships at various tectonic uplift rates in the Siwaliks Hills (Nepal), *Journal of Geophysical Research*, *108*, 2129, doi:2110.1029/2002JB001893.

Lamb, M. P., A. D. Howard, W. E. Dietrich, and J. T. Perron (2005), Hawaiian analog for Martian amphitheatre-headed valleys, *American Geophysical Union*, *Fall Meeting 2005*, H33C-1404.

Lamb, M. P., A. D. Howard, J. Johnson, K. X. Whipple, W. E. Dietrich, and J. T. Perron (2006), Can springs cut canyons into rock?, *Journal of Geophysical Research*, *111*, E07002, doi:07010.01029/02005JE002663.

Larsson, D., K. Gronvold, N. Oskarsson, and E. Gunnlaugsson (2002), Hydrothermal alteration of plagioclase and growth of secondary feldspare in the Hengill Volcanic Centre, SW Iceland, *Journal of Volcanology and Geothermal Research*, *114*, 275-290.

Lohse, K. A., and W. E. Dietrich (2005), Contrasting effects of soil development on hydrological properties and flow paths, *Water Resources Research*, *41*, W12419, doi:12410.11029/12004WR003403.

Louvat, P., and C. J. Allegre (1998), Riverine erosion rates on Sao Miguel volcanic island, Azores archipelago, *Chemical Geology*, *148*, 177-200.

Manga, M. (1997), A model for discharge in spring-dominated streams and implications for the transmissivity and recharge of quaternary volcanics in the Oregon Cascades, *Water Resources Research*, *33*, 1813-1822.

Middleton, G. V., and P. R. Wilcock (1994), *Mechanics in the Earth and Environmental Sciences*, 459 pp., Cambridge UP, Cambridge.

Montgomery, D. R., and W. E. Dietrich (1989), Source areas, drainage density, and channel initiation, *Water Resources Research*, *25*, 1907-1918.

Montgomery, D. R., and E. Foufoula-Georgiou (1993), Channel network source representation using digital elevation models, *Water Resources Research*, *29*, 3925-3934.

O'Connor, J. E., J. H. I. Hardisson, and J. E. Costa (2001), Debris Flows from Failures of Neoglacial-Age Moraine Dams in the Three Sisters and Mount Jefferson Wilderness Areas, Oregon, *Prof. Pap. 1606*, 93 pp, U.S. Geol. Surv., Washington, D.C.

O'Green, A. T., P. A. McDaniel, J. Boll, and C. K. Keller (2005), Paleosols as deep regolith: implications for ground-water recharge across a loessial climosequence, *Geoderma*, *126*, 85-99.

Ping, C.-L. (2000), Volcanic soils, in *Encyclopedia of Volcanoes*, edited by H. Sigurdsson, pp. 1259-1270, Academic Press, San Diego, Calif.

Pokrovsky, O. S., J. Schott, D. I. Kudryavtzev, and B. Dupre (2005), Basalt weathering in Central Siberia under permafrost conditions, *Geochimica et Cosmochimica Acta*, *69*, 5659-5680.

Roering, J. J., J. W. Kirchner, and W. E. Dietrich (1999), Evidence for nonlinear, diffusive sediment transport on hillslopes and implications for landscape morphology, *Water Resources Research*, *35*, 853-870.

Saar, M. O., and M. Manga (2004), Depth dependence of permeability in the Oregon Cascades inferred from hydrogeologic, thermal, seismic, and magmatic modeling constraints, *Journal of Geophysical Research*, *109*, B04204, 04210.01029/02003JB002855.

Schmidt, M. E., A. L. Grunder, and R. M. Conrey (2002), Basaltic andesite and palagonitic tuff at North Sister Volcano, Oregon High Cascades, paper presented at Geological Society of America, Cordilleran Section, 98th annual meeting, Geological Society of America, Corvallis, Ore.

Scott, W. E. (1977), Quaternary glaciation and volcanism, Metolius River area, Oregon, *Geological Society of America Bulletin*, *88*, 113-124.

Scott, W. E., C. A. Gardner, and A. M. e. Sarna-Wojcicki (1989), Guidebook for Field Trip to the Mount Bachelor-South Sister-Bend Area, Central Oregon High Cascades, *Open-File Report 89-645*, U.S. Geol. Surv., Vancouver, Wash.

Seidl, M. A., W. E. Dietrich, and J. W. Kirchner (1994), Longitudinal profile development into bedrock: an analysis of Hawaiian channels, *Journal of Geology*, *102*, 457-474.

Sherrod, D. R. (1986), Geology, petrology, and volcanic history of a portion of the Cascade Range between latitudes 43-44 degrees N, central Oregon, U.S.A., Ph.D. thesis, 320 pp pp, University of California, Santa Barbara, Santa Barbara.

Sherrod, D. R., and J. G. Smith (1990), Quaternary extrusion rates of the Cascade Range, northwestern United States and southern British Columbia, *Journal of Geophysical Research*, *95*, 19465-19474.

Sherrod, D. R., and J. G. Smith (2000), Geologic Map of Upper Eocene to Holocene Volcanic and Related Rocks of the Cascade Range, Oregon, *Geol. Invest. Ser. I-2569*, U.S. Geol. Surv., Washington, D.C.

Sherrod, D. R., E. M. Taylor, M. L. Ferns, W. E. Scott, R. M. Conrey, and G. A. Smith (2004), Geologic Map of the Bend 30- x 60-Minute Quadrangle, Central Oregon, *Geol. Invest. Ser. I-2683*, U.S. Geol.l Surv., Washington, D.C.

Shoji, S., M. Nanzyo, and R. Dahlgren (1993), *Volcanic Ash Soils*, 288 pp., Elsevier, Amsterdam.

Skinner, C. E., and S. F. Radosevich (1991), Holocene volcanic tephra in the Willamette National Forest, Linn and Lane Counties, Oregon: distribution, geochemical characterization, and geoarchaeological evaluation, Report prepared for the Willamette National Forest, Eugene, Ore. by Northwest Research and Trans-World Geology, Corvallis, Ore.

Stearns, H. T. (1929), Geology and Water Resources of the Upper McKenzie Valley, Oregon, *Water Supply Paper 597-D*, U.S. Geol. Surv., Washington, D.C.

Stock, J., and W. E. Dietrich (2003), Valley incision by debris flows: Evidence of a topographic signature, *Water Resources Research*, *39*, 1089, doi:1010.1029/2001WR001057.

Swanson, F. J., and R. L. Fredriksen (1982), Sediment routing and budgets: implications for juding impacts of forestry practices, *General Technical Report*, 129-137 pp, Pacific Northwest Forest and Range Experiment Station, Portland, Ore.

Swanson, F. J., and J. A. Jones (2002), Geomorphology and hydrology of the H.J. Andrews Experimental Forest, Blue River, Oregon, in *Field Guide to Geologic Processes in Cascadia*, edited, pp. 289-314, Oregon Department of Geology and Mineral Industries Special Paper 36, Salem.

Tague, C., and G. E. Grant (2004), A geological framework for interpreting the low flow regimes of Cascade streams, Willamette River Basin, Oregon, *Water Resources Research*, *40*, W04303 04310.01029/02003WR002629.

Tarboton, D. G. (1997), A new method for the determination of flow directions and upslope areas in grid digital elevation models, *Water Resources Research*, *33*, 309-319.

Tarboton, D. G., R. L. Bras, and I. Rodriguez-Iturbe (1992), A physical basis for drainage density, *Geomorphology*, *5*, 59-76.

Taylor, G. H., and C. Hannan (1999), *The Climate of Oregon: From Rain Forest to Desert*, 211 pp., Oregon State University Press, Corvallis.

Tucker, G. E., and R. L. Bras (1998), Hillslope processes, drainage density, and landscape morphology, *Water Resources Research*, *34*, 2751-2764.

Tucker, G. E., and K. X. Whipple (2002), Topographic outcomes predicted by stream erosion models: sensitivity analysis and intermodel comparison, *Journal of Geophysical Research*, *107*, 2179, doi:2110.1029/2001JB000162.

Vitousek, P. M., O. A. Chadwick, T. E. Crews, J. H. Fownes, D. M. Hendricks, and D. Herbert (1997), Soil and ecosystem development across the Hawaiian Islands, *GSA Today*, *7*, 1-8.

Wells, S. G., J. C. Dohrenwend, L. D. McFadden, B. D. Turrin, and K. D. Mahrer (1985), Late Cenozoic landscape evolution on lava flow surfaces of the Cima volcanic field, Mojave Desert, California, *GSA Bulletin*, *96*, 1518-1529.

Wohletz, K., and G. Heiken (1992), *Volcanology and Geothermal Energy*, 432 pp., University of California Press, Berkeley, Calif.

Figure 4.1. Conceptual models of drainage evolution on basaltic landscapes, synthesized from the literature. Numbers adjacent to the arrows indicate those papers who reference the sequence: (1) Kochel and Piper [1986]; (2) Baker and Gulick [1987]; (3) Dohrenwend *et al*. [1987]; (4) Allison *et al.* [2000]; (5) Lohse and Dietrich [2005]; and (6) Lamb *et al.* [2006]. Rounded boxes represent starting points proposed in the above papers, rectangular boxes are intermediate steps, and hexagons indicate model endpoints from the above papers. Gray arrows and boxes represent our proposed model.
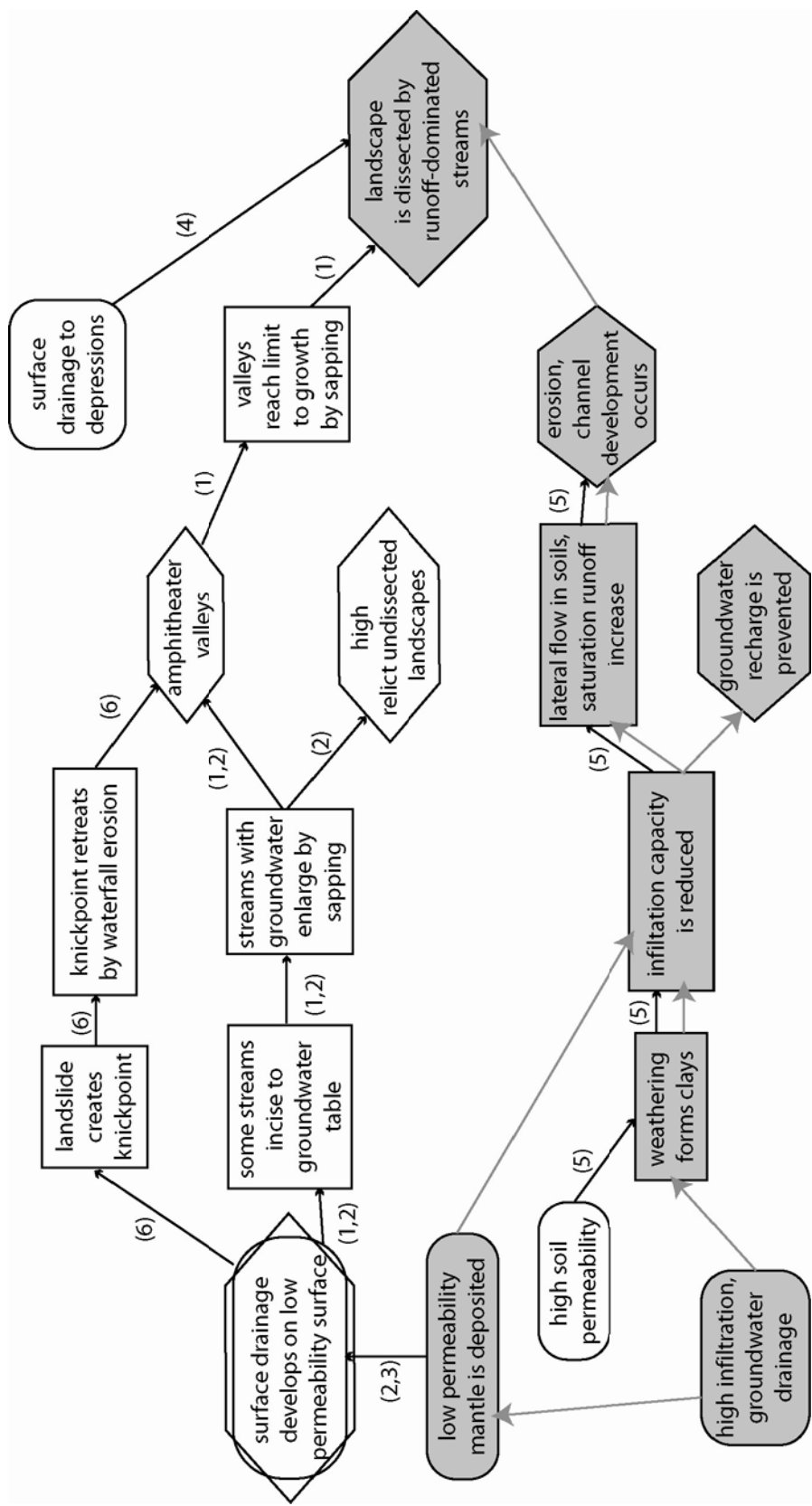
Figure 4.1.

Figure 4.2. Maps of the field area. (a) Map of Oregon showing the study area (outlined), Tertiary (dark gray) and Quaternary (light gray) basalts of the Cascades, major volcanic centers (triangles), and Roaring Spring (circled), referred to in the text. (b) Map of McKenzie Bridge watershed study area, showing topography. Study sub-watersheds are shaded and labeled. Volcanic peaks referred to in the text are labeled (in black). Lava transects are labeled from north to south: [a] Nash Crater basalt; [b] Belknap Crater basalt; [c] Scott Mountain basalt; [d] Sims Butte basalt; and [e] Collier Cone basalt. (c) Map of McKenzie Bridge watershed study area, showing geology. Basalt and basaltic andesite units shown as mapped by Sherrod and Smith [2000]. Springs referred to in text are labeled from north to south: [1] Great Spring; [2] Tamolitch Spring; [3] Sweetwater Spring; [4] Olallie North Spring; [5] Olallie South Spring; and [6] Lost Spring.
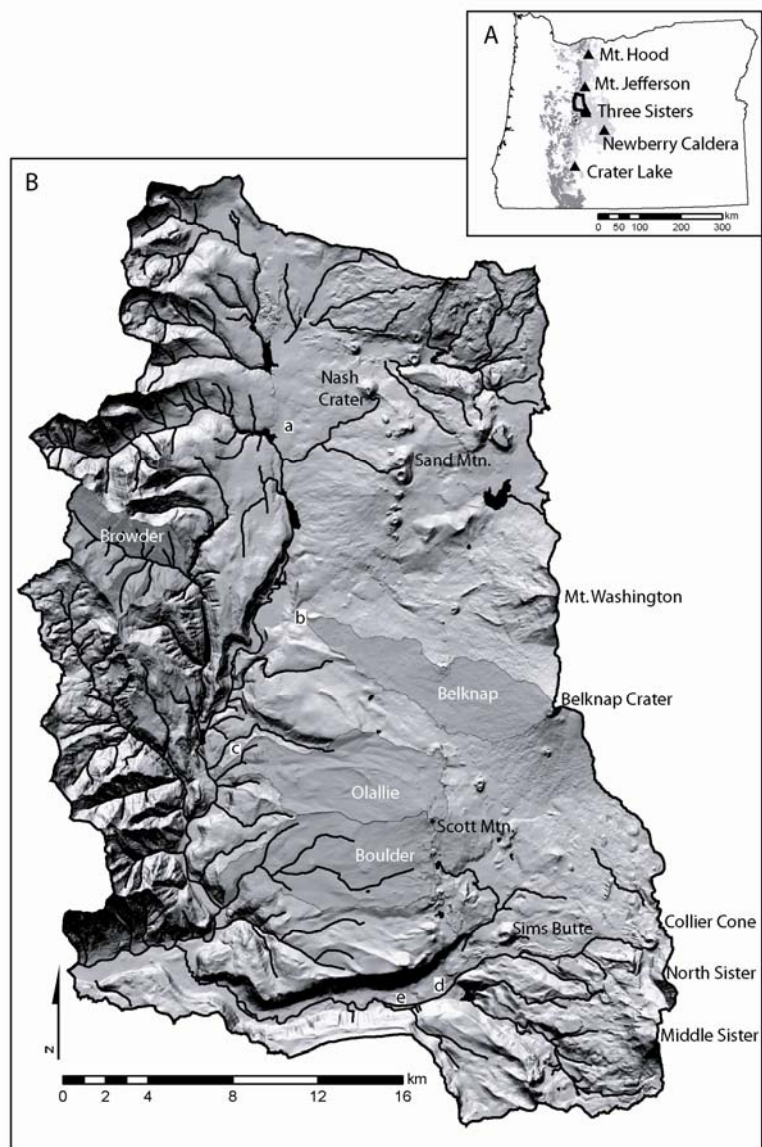
Figure 4.2.
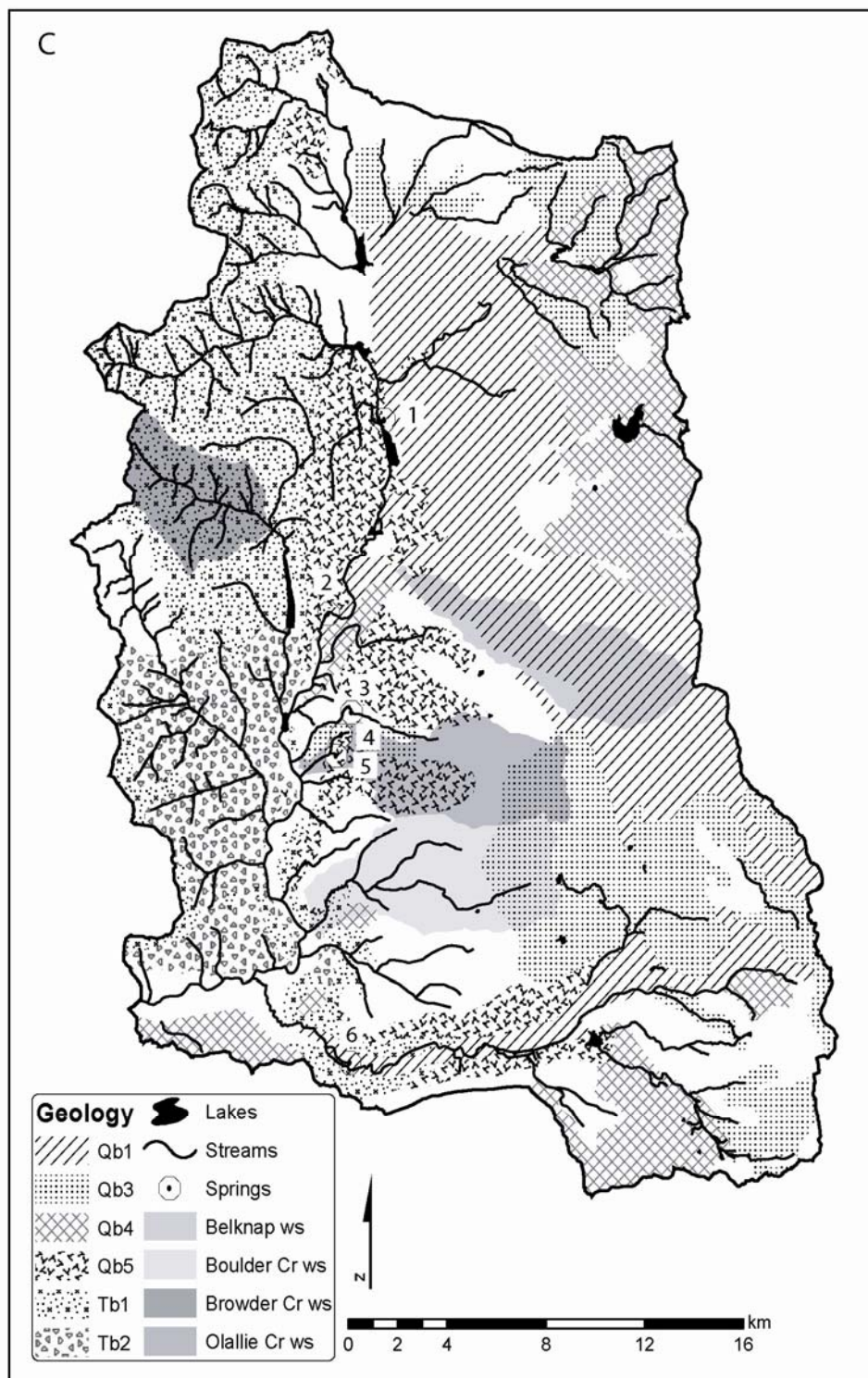
Figure 4.2 (continued).
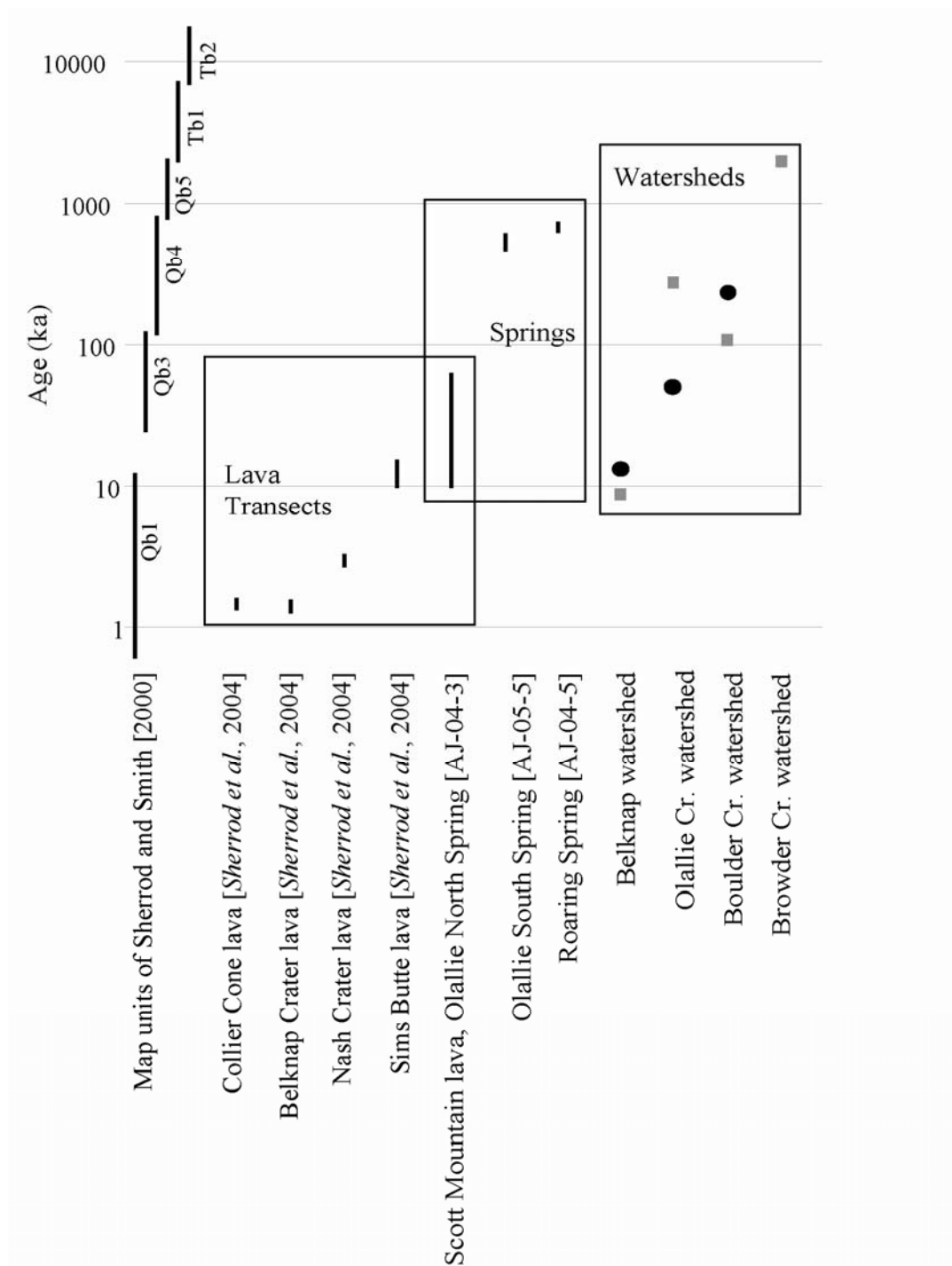
Figure 4.3. Chronology of map units, lava transects, spring-bearing rocks, watersheds, and drainage development stages for the McKenzie Bridge watershed, Oregon. Lava transect ages are based on calibrated ^{14}C years, and spring ages are from ^{40}Ar/^{39}Ar dates. Watershed ages represent weighted ages based on map units of Sherrod *et al.* [2004] (black circles) and Sherrod and Smith [2000] (gray squares).

Figure 4.4. Photograph of transect across lava from Belknap Crater (1296-1505 cal. ^{14}C years before present). Note the rough surface texture, abundant voids, sparse vegetation, and lack of soil cover.

Figure 4.5. Photographs of springs. (a) Great Spring, August 2006. (b) Tamolitch Spring, October 2003. At the time of this photograph all streamflow in the upper McKenzie River was disappearing into the subsurface ~1 km upstream of the spring. The spring was discharging water originating from the McKenzie River and groundwater recharging on the slopes of Belknap Crater. This photograph represents the natural condition of the spring. (c) Lost Spring, July 2002 (photograph by S. Lewis). (d) Olallie North Spring, August 2006.

Figure 4.6. Photograph of landscape in Browder Creek watershed. Hillslope is composed of 2-7 Ma basalt. Note the landslide scar on the center of the hillside. There are no major springs in this watershed.
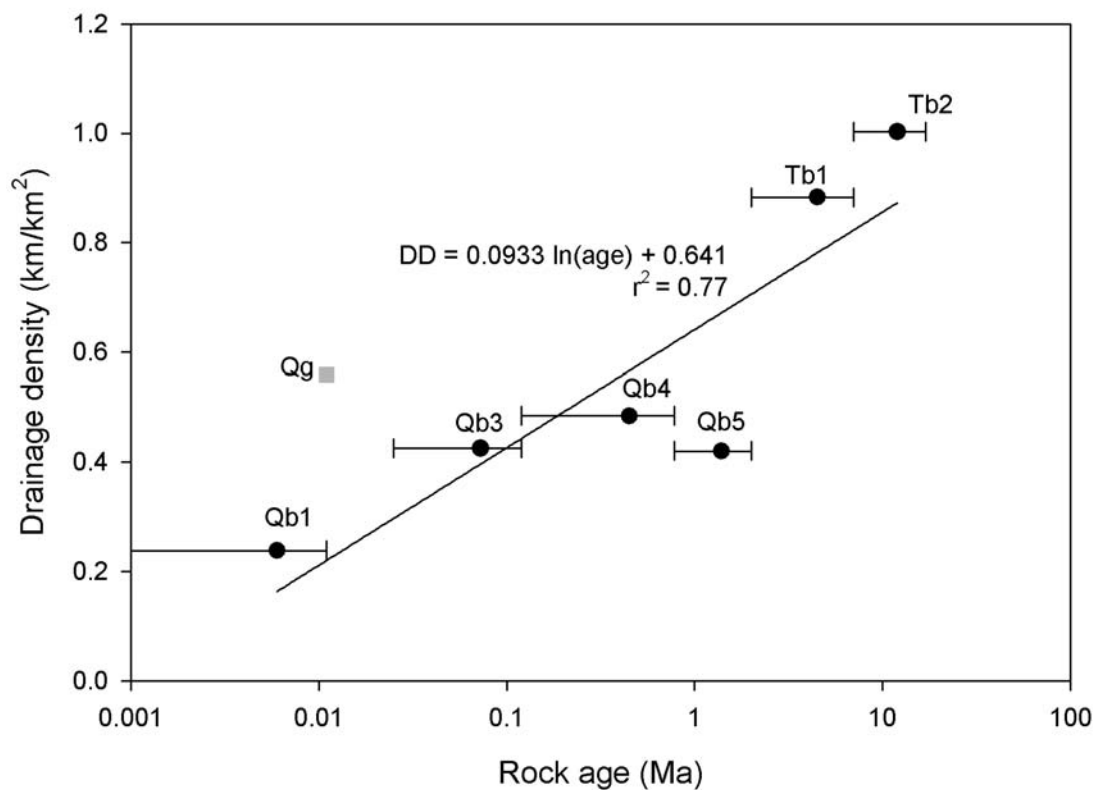
Figure 4.7. Drainage density versus rock unit age for the McKenzie Bridge watershed. Stream lengths were measured from digitized 1:24,000 USGS topographic maps, and rock unit areas were calculated from a digital version of Sherrod and Smith [2000]. Circles represent the median age of each basalt unit through which the regression line was computed, with the bars representing the range of ages for each rock unit. The gray square represents glacial deposits, using an age of 11 ka, which corresponds to the end of the Canyon Creek advance [*Scott et al.*, 1989].

Figure 4.8. Slope-area relationships for study watersheds. (a) Belknap and Browder Creek watersheds. (b) Olallie Creek watershed. (c) Boulder Creek watershed. Regression lines are fitted to points with contributing areas ≥ 1000 m^2. In (b) and (c) the regression line for Belknap is depicted as a dashed and dotted line, while the regression lines for Browder Creek are depicted as dashed lines.
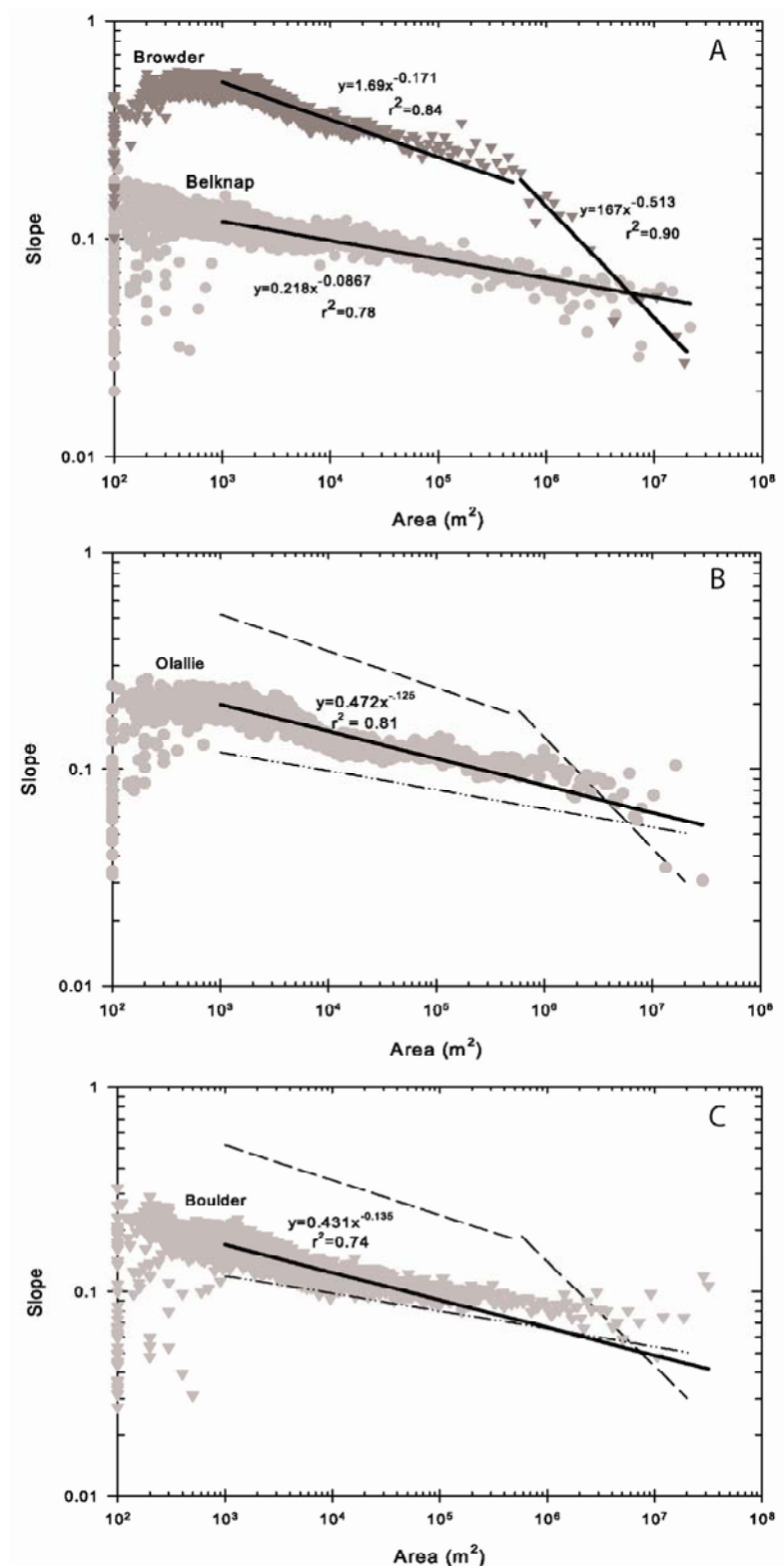
Figure 4.8.
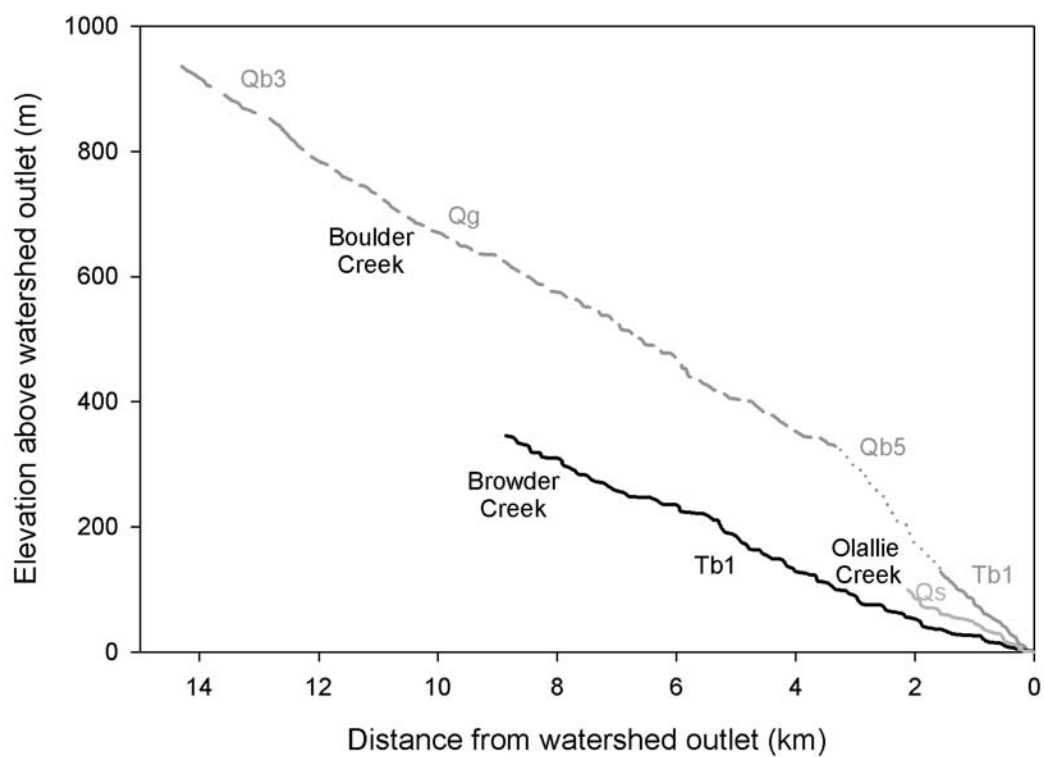
Figure 4.9. Stream profiles for Boulder, Browder and Olallie Creeks, showing influences of rock units. Qg represents glacial deposits, and the other units are defined in Figure 4.3.
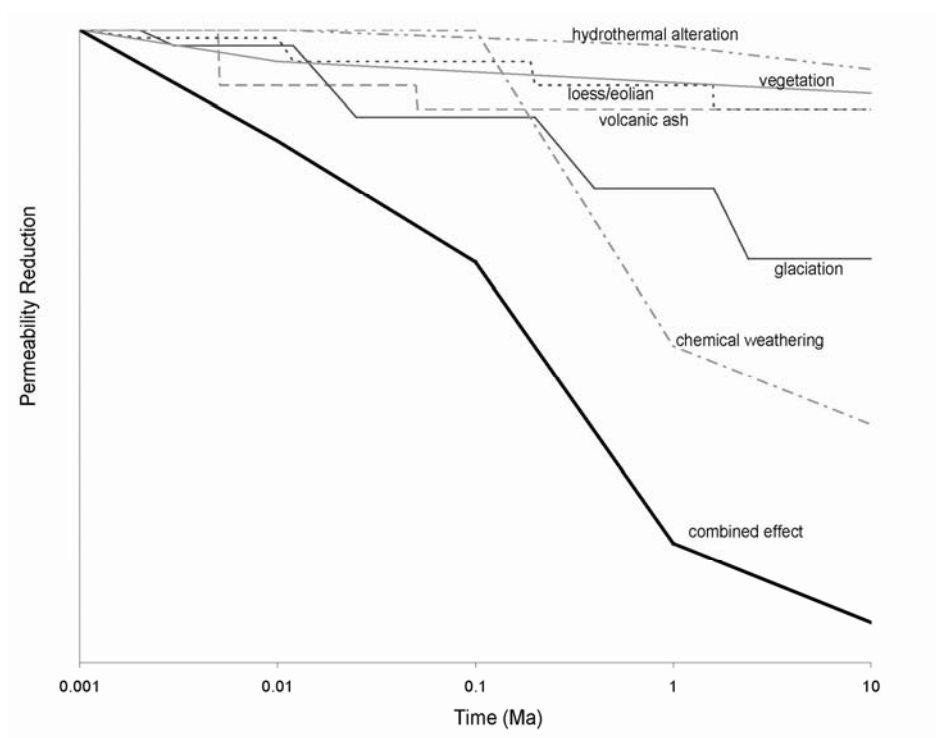
Figure 4.10. Conceptual illustration of permeability reduction of basaltic landscapes over geologic time. Lines illustrate expected trends and relative magnitudes for the Oregon Cascades.

5 Future research directions, management implications, and conclusions

5.1 Conclusions

The Oregon Cascades form a natural laboratory for investigating the effects of geology on hydrologic processes. The McKenzie River watershed has been used to examine how geologic history influences groundwater flowpaths, streamflow sensitivity to climate, and landscape evolution. Although specific details of recharge areas, hydrograph shapes, and rates of change are particular to the region studied, the processes underlying those details apply throughout the young basaltic terrains of the world.

High Cascades aquifers are the dominant natural source of summer streamflow in the Willamette River watershed, despite supplementation of summer flow by releases from flood-control reservoirs. In watersheds with large areas of High Cascades geology, like that of the McKenzie River, spring-fed streams can provide over 80% of August discharge. The reason for the dominant source of summer streamflow lies in the high near-surface permeability of the basaltic lava that mantles the High Cascades landscape.

When coupled with high annual precipitation, such as in the Oregon Cascades, basaltic landscapes form extensive groundwater systems. These groundwater systems are expressed at the surface by large volume, cold springs, often at lava flow toes or contacts. The individual aquifers are locally constrained by modern and paleo-topography and outcrops of older, less permeable rocks, resulting in recharge areas and flow paths that may lie outside the spring's topographic watershed. Flowpaths to the springs are generally shallow and have limited contact with deeper, geothermal systems, except where fault zones provide opportunities for mixing. Thus, the volcanic history of the region sets the spatial template for the recharge, flowpath, and discharge of groundwater.

The slow recession associated with groundwater storage is critically important for sustaining summer streamflow in Oregon's Mediterranean climate, because groundwater release provides discharge even when the seasonal or annual water balance is negative. Although groundwater significantly influences the shape of the annual hydrograph, climatic factors dominate the inter-annual streamflow signal. The one-year memory associated with groundwater systems in the Oregon Cascades is not enough to dampen year-to-year flow fluctuations. Over the past ~60 years, increasingly warm winters and earlier snowmelt have lengthened the summer recessions and lowered autumn minimum discharges in a groundwater-dominated watershed in the study area. Projections of future climate suggest that this trend will continue. Groundwater-dominated streams are more susceptible to changes in summer discharge resulting from shifts in snowmelt amount and timing than are runoff-dominated streams, and those watersheds perched at the transition between transient and seasonal snow cover regimes may be particularly susceptible to changes in summer streamflow. Therefore, the distribution of permeable rocks and resultant groundwater systems strongly influence streamflow response to climate forcing on the event, seasonal, and multi-year time scales.

Over geologic time, permeability declines and drainage networks develop on the basaltic landscapes of the Oregon Cascades. In young landscapes, the dominant drainage mechanism is groundwater flow to large springs, and these bedrock flowpaths remain important for up to one million years. As chemical weathering and glaciation work to reduce landscape permeability, groundwater recharge declines and channel networks grow up-slope of the springs. Within three million years, water is dominantly transported via shallow subsurface flow and the runoff-dominated stream network. Watersheds with Quaternary basalts have experienced little fluvial erosion, with gentle topography dominated by volcanic constructional forms and glacial activity. In contrast, Pliocene basaltic watersheds have been extensively fluvially dissected and have steep slopes where debris flows are common. In basaltic

landscapes in other settings, processes such as ash and eolian deposition or hydrothermal alteration may play a more important role in permeability reduction, but the general sequence of early groundwater dominance slowly replaced by shallow subsurface flow is probably still applicable. Thus, the age and geologic history of a watershed controls the stage of drainage development and dictates the dominant hydrologic pathways, and, in turn, the dominant pathways are indicators of the watershed's geologic history.

5.2 Areas for future research

This work suggests several potential areas for future research on hydrology in young volcanic terrains. Although the scope of this study was limited to a dominantly basalt and basaltic andesite landscape, an exploration of lithologic influences would yield interesting insights into similarities and differences in hydrology of silicic effusive or tephra-rich volcanic landscapes. Such a study might be undertaken in the Washington Cascades where basaltic volcanism has been less significant in the Quaternary. Satellite-based measurements of gravimetric changes (e.g., GRACE [*Adam*, 2002]) of seasonal aquifer water storage could help constrain water fluxes and groundwater extent in volcanic regions, once technology for improved resolution develops.

At a smaller scale, lava-dammed lakes appear to be important point sources of recharge, and potential avenues for aquifer contamination. Water budgets of such lakes would identify the relative importance of evaporation versus recharge, which might be dependent on bathymetry, sediment cover, or magnitude of inflow. Finally, plot-scale processes of recharge through soil-covered lava flows have not been examined in detail.

There are several outstanding questions relating to the landscape evolution of basaltic terrains. A survey of global basaltic landscapes is needed to identify and rank permeability-reducing processes in other climate zones. Once the important processes

are identified, mechanistic studies would be useful to understand exactly how these processes affect permeability and drainage development. Once this mechanistic understanding is developed, landscape evolution models could incorporate processes such as chemical weathering and till deposition into their simulations, allowing a more complete and accurate depiction of the evolution of permeable terrains. How the structure and porosity of lava affects erosion mechanisms and rates as compared to other rock types would also be interesting to examine. Finally, spring-fed streams do not appear to be effective agents of erosion. Is their geomorphic effectiveness determined by the relatively short periods of geologic time over which they operate, or is it determined by the limited discharge variability, lack of sediment-mobilizing large floods or lack of available sediment?

This research has shown that there is variability in discharge dynamics between spring-fed streams, even those in close proximity to each other. These differences may be the result of aquifer characteristics or amount and timing of precipitation inputs at different recharge elevations. Differences between spring dynamics need to be quantified and responsible processes identified and quantified. Cascades springs exist in close proximity to active volcanic centers, and may provide an opportunity to examine the effects of regional volcanic or earthquake activity on the dynamics of groundwater systems and spring-fed streams. Volcanic and earthquake activity would both be expected to change the permeability structure of the subsurface, resulting in either short-term or long-term changes to flowpaths, hydraulic conductivity, and discharge dynamics.

Another avenue for research focuses on climate change impacts on groundwater and spring-fed streams. Cascades springs provide an ideal window for monitoring long-term changes in temperature, because of their lack of daily and seasonal variability and connection to recharge temperatures. Conjunctive decreases in late summer streamflow and increases in groundwater temperature may cause significant rises in summer stream temperatures in the Cascades. Modeling studies linking climate

forcing, groundwater discharge, and stream temperature are needed to understand the potential magnitude of the effect and plan management strategies for temperature-sensitive aquatic species.

There are open questions regarding the impact of natural and anthropogenic disturbance on High Cascades landscapes. Timber harvest is a major industry in the Oregon Cascades, and the effects of timber harvest and road building on groundwater recharge, spring discharge, and spring water quality have not been studied. One complicating factor is the possible discordance between topographically-defined watersheds and recharge areas, which means that the recharge area of a particular spring-fed stream must first be identified before land-use effects can be quantified. Forest fires are a natural disturbance recurring at intervals of several decades to several centuries, however, the impacts of fire-generated pulses of organic material and sediment on spring-fed streams are not known. How fine fire-generated materials might act to clog pores or speed soil development on basaltic terrains is also not understood. The potential effects of fire retardants on groundwater quality are also poorly constrained.

5.3 Management implications

Given the importance of spring-fed streams for summer streamflow, water quality, and habitat in the Oregon Cascades, water resources planning and management should differentiate between spring-fed and runoff-dominated streams in the decision-making process. Managers should consider not just the stream, but also the spring and groundwater recharge area. Maintaining the good water quality and outstanding environmental attributes of High Cascades water resources will involve cooperation between local and federal organizations, management of springs, source areas, and streams, and continued assessment of long-term behavior of spring-fed streams in light of climate variability and change.

Most of the High Cascades springs and recharge areas are on National Forest lands, and springs are included in the riparian reserve management classification under the Northwest Forest Plan [*Interagency SEIS Team*, 1994]. Riparian reserve areas are relatively well protected from forest harvest and road building, but groundwater recharge areas may not lie within special protection categories. Understanding the effects of human activities on groundwater recharge, discharge, and quality could be a priority for future research investment.

Mean groundwater transit times on the order of 3 to 14 years for the High Cascades imply that spring water is susceptible to chemical spills or deposition of atmospheric contaminants in recharge areas. Contamination of spring water may appear several years after a spill, and the effects may persist for decades. Delineation of recharge areas may help resource managers understand the risks associated with particular spill scenarios and plan effective mitigation strategies.

Water quality downstream of the springs may be affected by various activities on private land, including timber harvest, application of forestry or agricultural chemicals, and spills from roadways. Spring water mingles with runoff as it flows downstream, meaning that management of distal parts of the watershed can negatively impact water quality. Human activities downstream from springs likely have the greatest impact on water quality for human uses. The McKenzie River is the drinking water source for 200,000 people in the Eugene metropolitan area, and the Eugene Water and Electric Board has an active source water protection program aimed at reducing and responding to water quality threats [*Karl Morgenstern*, personal comm.]. Additionally, stream temperature, an important habitat criteria for bull trout and other aquatic species, is generally lower and more stable in spring-fed than runoff-dominated streams, suggesting that conservation efforts for some species might be concentrated in spring-fed streams.

Despite their importance to water supply during low flow seasons, none of the springs and few of the spring-fed streams in the High Cascades have established long-term monitoring facilities, such as U. S. Geological Survey gages. Although spring-fed streams provide more consistent flow than do runoff-dominated streams, they do experience high flows in response to rain and rain-on-snow events. Differences in flow dynamics between spring-fed streams, even those in close proximity to each other, preclude generalizing data from one spring system to others. These dynamics will be complicated by increasingly warm winters. With each spring having a unique distribution of recharge elevations, some spring-fed streams will experience the effects of climate change more profoundly than will others. Thus, adequate gauging of these systems is important for reservoir management and water resources planning.

At a broader scale, young basaltic landscapes should be managed with consideration to their close linkage to groundwater systems that may be regional in extent. Human activities on the surface of permeable landscapes have a greater impact on groundwater quantity and quality than in areas with lower near-surface hydraulic conductivity. Regulations and outreach programs similar to those used in karst landscapes might be adapted for basaltic areas. One example is Minnesota's "Karst Campaign for Clean Water, Productive Soils and Profitable Farms" [http://wrc.coafes.umn.edu/outreach/karst/]. Perhaps more fancifully, imagine visitor overlooks of young lava fields with a placard informing visitors that the area drains to a stream, in a similar fashion to the stenciled signs on storm sewer drains.

5.4 Denouement

Groundwater patterns on the western slope of the Oregon High are strongly influenced by volcanic history, and that groundwater flow, while sustaining summer streamflow in western Oregon, is susceptible to the effects of climate variability and change. Over geologic time, groundwater-dominated landscapes of the High Cascades will transition into runoff-dominated systems. This work suggests areas for further investigation, and it has implications for management of water resources in groundwater-dominated

regions. This topic is particularly relevant to human use of recharge areas and climate variability and change.

Geologic setting and history control landscape permeability, and that permeability, in turn, exerts a strong influence on groundwater flowpaths, climate sensitivity, and geomorphic evolution of basaltic landscapes. Hydrological features, such as springs and steady discharge, are also indicators of the geologic history of a watershed. These results emphasize the importance of understanding a landscape's geology and geologic history for a thorough comprehension of hydrological processes, and the results also highlight how hydrology provides clues to geologic processes.

5.5 References cited

Adam, D. (2002), Amazing grace, *Nature*, *416*, 10-11.

Interagency SEIS Team (1994), Record of decision for amendments to Forest Service and Bureau of Land Management planning documents within the range of the northern spotted owl; standards and guidelines for management of habitat for late-successional and old-growth forest related species within the range of the northern spotted owl, Interagency SEIS Team, Portland, Ore.

6 Bibliography

Adam, D. (2002), Amazing grace, *Nature, 416*, 10-11.

Aeschbach-Hertig, W., P. Schlosser, M. Stute, H. J. Simpson, A. Ludin, and J. F. Clark (1998), A ^{3}H/^{3}He study of ground water flow in a fractured bedrock aquifer, *Ground Water, 36*, 661-670.

Aharonson, O., M. T. Zuber, D. H. Rothman, N. Schorghofer, and K. X. Whipple (2002), Drainage basins and channel incision on Mars, *PNAS, 99*, 1780-1783.

Allison, R. J., J. R. Grove, D. L. Higgitt, A. J. Kirk, N. J. Rosser, and J. Warburton (2000), Geomorphology of the eastern Badia basalt plateau, Jordan, *The Geographical Journal, 166*, 352-370.

Ambers, R. K. R. (2001), Relationships between clay mineraology, hydrothermal metamorphism, and topography in a Western Cascades watershed, Oregon, USA, *Geomorphology, 38*, 47-61.

Anderson, S. P., W. E. Dietrich, and G. H. J. Brimhall (2002), Weathering profiles, mass-balance analysis, and rates of solute loss: linkages between weathering and erosion in a small, steep catchment, *GSA Bulletin, 114*, 1143-1158.

Baker, V. R. (1988), Evolution of valleys dissecting volcanoes on Mars and Earth, in *Sapping Features of the Colorado Plateau: A Comparative Planetary Geology Field Guide*, edited by A. D. Howard, et al., pp. 96-97, National Aeronautics and Space Administration, Washington, DC.

Bandfield, J. L., V. E. Hamilton, and P. R. Christensen (2000), A global view of Martian surface compositions from MGS-TES, *Science, 287*, 1626-1630.

Banfield, J. F., B. F. Jones, and D. R. Veblen (1991), An AEM-TEM study of weathering and diagenesis, Abert Lake, Oregon: Weathering reactions in the volcanics, *Geochimica et Cosmochimica Acta, 55*, 2781-2793.

Barnett, T. P., J. C. Adam, and D. P. Lettenmaier (2005), Potential impacts of warming climate on water availability in snow-dominated regions, *Nature, 438*, 303-308.

Beebee, R., and M. Manga (2004), Variation in the relationship between snowmelt runoff in Oregon and ENSO and PDO, *Journal of the American Water Resources Association, 40*, 1011-1024.

Benedeti, M. F., A. Dia, J. Riotte, F. Chabaux, M. Gerard, J. Boulegue, B. Fritz, C. Chauvel, M. Bulourde, B. Deruelle, and P. Ildefonse (2003), Chemical weathering of basaltic lava flows undergoing extreme climatic conditions: the water geochemistry record, *Chemical Geology, 201*, 1-17.

Blackwell, D. D., J. L. Steele, M. K. Frohme, C. F. Murphey, G. R. Priest, and G. L. Black (1990), Heat flow in the Oregon Cascade Range and its correlation with regional gravity, Curie point depths, and geology, *Journal of Geophysical Research, 95*, 19475-19493.

Bowen, G. J., and B. Wilkinson (2002), Spatial distribution of δ^{18}O in meteoric precipitation, *Geology, 30*, 315-318.

Box, G. E. P., and G. Jenkins (1976), *Time Series Analysis: Forecasting and Control*, 575 pp., Holden-Day, Boca Raton, Fla.

Carlston, C. W. (1963), Drainage density and streamflow, *Prof. Pap. 422-C*, U.S. Geol. Surv., Washington, D.C.

Carter, R. W., and J. Davidian (1968), General procedure for gaging streams, in *Techniques of Water-Resources Investigations of the United States Geological Survey*, Book 3 Chap. A6, U.S. Geol. Surv., Washington, D.C.

Cayan, D. R., S. A. Kammerdiener, M. D. Dettinger, J. M. Caprio, and D. H. Peterson (2001), Changes in the onset of spring in the western United States, *Bulletin of the American Meteorological Society*, *82*, 399-415.

Chan, T., R. Christiansson, G. S. Boulton, L. O. Ericsson, J. Hartikainen, M. R. Jensen, D. M. Ivars, F. W. Stanchell, P. Vistrand, and T. Wallroth (2005), DECOVALEX III BMT3/BENCHPAR WP4: The thermo-hydromechanical responses to a glacial cycle and their potential implications for deep geological disposal of nuclear fuel waste in a fractured crystalline rock mass, *International Journal of Rock Mechanics & Mining Sciences*, *42*, 805-827.

Christiansen, L. B., S. Hurwitz, M. O. Saar, S. E. Ingebritsen, and P. A. Hsieh (2005), Seasonal seismicity at western United States volcanic centers, *Earth and Planetary Science Letters*, *240*, 307-321.

Clarke, G. K. C. (2005), Subglacial processes, *Annual Review of Earth and Planetary Science*, *33*, 247-276.

Clarke, W. B., W. J. Jenkins, and Z. Top (1976), Determination of tritium by mass-spectrometric measurement of ^{3}He, *International Journal of Applied Radiation and Isotopes*, *27*, 515-522.

Coleman, M. L., T. J. Sheperd, J. J. Durham, J. E. Rouse, and G. R. Moore (1982), Reduction of water with zinc for hydrogen isotope analysis, *Analytical Chemistry*, *54*, 993-995.

Colman, S. M. (1982), Chemical Weathering of Basalts and Andesites: Evidence from Weathering Rinds, *Prof. Pap. 1246*, 51 pp, U.S. Geol. Surv., Washington.

Colman, S. M., and K. L. Pierce (1981), Weathering Rinds on Andesitic and Basaltic Stones as a Quaternary Age Indicator, Western United States, *Prof. Pap. 1210*, 41 pp, U.S. Geol. Surv., Washington, D.C.

Conrey, R. M., D. R. Sherrod, P. R. Hooper, and D. Swanson (1997), Diverse primitive magmas in the Cascade arc, northern Oregon and southern Washington, *The Canadian Mineralogist*, *35*, 367-296.

Conrey, R. M., E. M. Taylor, J. M. Donnely-Nolan, and D. R. Sherrod (2002), North-central Oregon Cascades: exploring petrologic and tectonic intimacy in a propagating intra-arc rift, in *Field Guide to Geologic Processes in Cascadia*, edited by G. W. Moore, Special Paper 36, pp. 47-90, Oregon Department of Geology and Mineral Industries, Salem.

Cook, P. G., A. J. Love, N. I. Robinson, and C. T. Simmons (2005), Groundwater ages in fractured rock aquifers, *Journal of Hydrology*, *308*, 284-301.

Craig, H. (1961), Isotopic variations in meteoric waters, *Science*, *133*, 1702-1170.

Daly, C., W. P. Gibson, G. H. Taylor, G. L. Johnson, and P. Pasteris (2002), A knowledge-based approach to the statistical mapping of climate, *Climate Research*, *22*, 99-113.

Daly, C., R. P. Nielson, and D. L. Phillips (1994), A statistical-topographic model for mapping climatological precipitation over mountanious terrain, *Journal of Applied Meteorology*, *33*, 140-158.

Daly, C., G. Taylor, and W. Gibson (1997), The PRISM approach to mapping precipitation and temperature, paper presented at 10th Conf. on Applied Climatology, American Meteorological Society, Reno, NV.

Dansgaard, W. (1964), Stable isotopes in precipitation, *Tellus*, *16*, 436-468.

Davis, S. N. (1969), Porosity and permeability of natural materials, in *Flow Through Porous Media*, edited by R. J. M. De Wiest, pp. 53-89, Academic Press, New York.

Davis, W. M. (1902), *Geographical Essays*, 777 pp., Ginn Publishing, Boston. Reprinted 1954, Dover, New York.

Descloitres, M., M. Ritz, B. Robineau, and M. Courteaud (1997), Electrical structure beneath the eastern collapsed flank of Piton de la Fournaise volcano, Reunion Island: Implications for the quest for groundwater, *Water Resources Research*, *33*, 13-19.

Dessert, C., B. Dupre, J. Gaillardet, L. M. Francois, and C. J. Allegre (2003), Basalt weathering laws and the impact of basalt weathering on the global carbon cycle, *Chemical Geology*, *202*, 257-273.

Devito, K. J., A. R. Hill, and N. Roulet (1996), Groundwater-surface water interactions in headwater forested wetlands of the Canadian shield, *Journal of Hydrology*, *181*, 127-147.

Duncan, R. A., and L. G. Hogan (1994), Radiometric dating of young MORB using the ^{40}Ar-^{39}Ar incremental heating method, *Geophysical Research Letters*, *21*, 1927-1930.

Dunne, T. (1990), Hydrology, mechanics, and geomorphic implications of erosion by subsurface flow, in *Groundwater Geomorphology: The Role of Subsurface Water in Earth-Surface Processes and Landforms*, edited by C. G. Higgins and D. R. Coates, pp. 1-28, Geological Society of America, Boulder, Colo.

Dyrness, C. T. (1969), Hydrologic properties of soils on three small watersheds in the Western Cascades of Oregon, *Res. Note PNW-111*, Pac. Northwest For. and Range Exp. Stn., For. Serv., U.S. Dep. of Agric., Portland, Ore.

Epstein, S., and T. Mayeda (1953), Variation of ^{18}O content of water from natural sources, *Geochimica Cosmochimica Acta*, *4*, 213-224.

Etcheverry, D., and P. Perrochet (2000), Direct simulation of groundwater transit-time distributions using reservoir theory, *Hydrogeology Journal*, *8*, 200-208.

Evans, W. C., M. C. van Soest, R. H. Mariner, S. Hurwitz, S. E. Ingebritsen, C. W. J. Wicks, and M. E. Schmidt (2004), Magmatic intrusion west of Three Sisters, central Oregon, USA: the perspective from spring geochemistry, *Geology*, *32*, 69-72.

EWEB (2003), Initial consultation document for the Carmen-Smith Hydroelectric Project (FERC No. 2242), Final Report, Prepared by Stillwater Sciences, Arcata, Calif. for Eugene Water and Electric Board, Eugene, Ore.

Faybishenko, B., C. Doughty, M. Steiger, J. C. S. Long, T. R. Wood, J. S. Jacobsen, J. Lore, and P. T. Zawislanski (2000), Conceptual model of the geometry and

physics of water flow in a fractured basalt vadose zone, *Water Resources Research*, *36*, 3499-3520.

Flowers, G. E., H. Bjornsson, and F. Palsson (2003), New insights into the subglacial and periglacial hydrology of Vatnajokull, Iceland, from a distributed physical model., *Journal of Glaciology*, *49*, 257-270.

Folland, C. K., T. R. Karl, and coauthors (2001), Observed climate variability and change, in *Climate Change 2001: The Scientific Basis. Contribution of Working Group I to the Third Assessment Report of the Intergovernmental Panel on Climate Change*, edited by J. T. Houghton, et al., pp. 99-181, Cambridge Univ. Press, Cambridge.

Freer, J., J. J. McDonnell, K. J. Beven, N. E. Peters, D. A. Burns, R. P. Hooper, B. Aulenbach, and C. Kendall (2002), The role of bedrock topography on subsurface storm flow, *Water Resources Research*, *38*, 1269.

Freeze, R. A., and J. A. Cherry (1979), *Groundwater*, 604 pp., Prentice Hall, Englewood Cliffs, NJ.

Gannett, M. W., and K. E. J. Lite (2004), Simulation of regional groundwater flow in the upper Deschutes Basin, Oregon, *Water-Resour. Invest. Report 03-4195*, 84 pp, U.S. Geol. Surv., Washington.

Gannett, M. W., M. Manga, and K. E. J. Lite (2003), Groundwater hydrology of the Upper Deschutes Basin and its influence on streamflow, in *A Peculiar River: Geology, Geomorphology, and Hydrology of the Deschutes river*, edited by J. E. O'Connor and G. E. Grant, 7, pp. 31-49, American Geophysical Union, Washington.

Gislason, S. R., S. Arnorsson, and H. Armannsson (1996), Chemical weathering of basalt in southwest Iceland: effects of runoff, age of rocks, and vegetative/glacial cover, *American Journal of Science*, *296*, 837-907.

Grant, G. E. (1997), A geomorphic basis for the hydrologic behavior of large river systems., in *River Quality: Dynamics and Restoration*, edited by A. Laenen and D. A. Dunnette, pp. 105-116, Lewis Publishers, Boca Raton.

Grant, G. E., F. J. Swanson, and M. G. Wolman (1990), Pattern and origin of stepped-bed morphology in high-gradient streams, Western Cascades, Oregon, *Geological Society of America Bulletin*, *102*, 340-352.

Gulick, V. C. (2005), Revisiting valley development on Martian volcanoes using MGS and Odyssey data, paper presented at Lunar and Planetary Science Conference, League City, Tex.

Harmon, R. S., and C. M. Wicks (Eds.) (2006), *Perspectives on Karst Geomorphology, Hydrology, and Geochemistry: A Tribute Volume to Derek C. Ford and William B. White*, 366 pp., Geological Society of America, Boulder, Colo.

Harr, R. D. (1977), Water flux in soil and subsoil on a steep forested slope, *Journal of Hydrology*, *33*, 37-58.

Harr, R. D. (1981), Some characteristics and consequences of snowmelt during rainfall in western Oregon, *Journal of Hydrology*, *53*, 277-304.

Hayhoe, K., D. R. Cayan, C. B. Field, P. C. Frumhoff, E. P. Maurer, N. L. Miller, S. C. Moser, S. H. Schneider, K. N. Cahill, E. E. Cleland, L. Dale, R. Draek, R.

M. Hanemann, L. S. Kalkstein, J. Lenihan, C. K. Lunch, R. P. Neilson, S. C. Sheridan, and J. H. Verville (2004), Emissions pathways, climate change, and impacts on California, *PNAS, 101*, 12422-12427.

Head, J. W., L. Wilson, and K. L. Mitchell (2003), Generation of recent massive water floods at Cerberus Fossae, Mars by dike emplacement, cryospheric cracking, and confined aquifer groundwater release, *Geophysical Research Letters, 30*, 1577, doi:1510.1029/2003GL017135.

Herrett, T. A., G. W. Hess, J. G. House, G. P. Ruppert, and M.-L. Courts (2004), Water Resources Data for Oregon, Water Year 2004., *Water Data Report OR-04-1*, 968 pp, U.S. Geol. Surv., Washington, D.C.

Herrett, T. A., G. W. Hess, M. A. Stewart, G. P. Ruppert, and M.-L. Courts (2005), Water Resources Data for Oregon, Water Year 2005, *Water Data Report OR-05-1*, 942 pp, U.S. Geol. Surv., Washington, D.C.

Hilton, D. R. (1996), The helium and carbon isotope systematics of a continental geothermal system: results from monitoring studies at Long Valley caldera (California, U.S.A.), *Chemical Geology, 127*, 269-295.

Hoblitt, R. P., C. D. Miller, and W. E. Scott (1987), Volcanic Hazards with Regard to Siting Nuclear-Power Plants in the Pacific Northwest, *Open File Report 87-297*, USGS, Vancouver, Wash.

Hopson, R. E. (1946), The Study of a Valley -- The McKenzie River Region of Oregon, with Special Reference to the Educational Significance of its Natural History, PhD thesis, Cornell U., Ithaca, NY.

Hurwitz, S., F. Goff, C. J. Janik, W. C. Evans, D. A. Counce, M. L. Sorey, and S. E. Ingebritsen (2003a), Mixing of magmatic volatiles with groundwater and interaction with basalt on the summit of Kilauea Volcano, Hawaii, *Journal of Geophysical Research, 108*, 2028, doi:2010.1029/2001JB001594.

Hurwitz, S., K. L. Kipp, S. E. Ingebritsen, and M. E. Reid (2003b), Groundwater flow, heat transport, and water table position within volcanic edifices: Implications for volcanic processes in the Cascade Range, *Journal of Geophysical Research-Solid Earth, 108*.

Hynek, B. M., and R. J. Phillips (2003), New data reveal mature, integrated drainage systems on Mars indicative of past precipitation, *Geology, 31*, 757-760.

IAEA/WMO (2005), The GNIP Database, http://isohis.iaea.org, Global Network of Isotopes in Precipitation, Vienna, Austria.

Inbar, M. (1994), The geomorphological evolution of the Paricutin cone and lava flows, Mexico, 1943-1990, *Geomorphology, 9*, 57-76.

Inbar, M., C. Risso, and C. Parica (1995), The morphological development of a young lava flow in the South Western Andes -- Neuquen, Argentina, *Zeitschrift fur Geomorphologie, 39*, 479-484.

Ingebritsen, S. E., D. L. Galloway, E. M. Colvard, M. L. Sorey, and R. H. Mariner (2001), Time-variation of hydrothermal discharge at selected sites in the western United States: implications for monitoring, *Journal of Volcanology and Geothermal Research, 111*, 1-23.

Ingebritsen, S. E., R. H. Mariner, and D. R. Sherrod (1994), Hydrothermal systems of the Cascade Range, north-central Oregon, *Prof. Pap. 1044-L.*, 86 pp. pp, U.S. Geol. Surv., Washington, D.C.

Ingebritsen, S. E., and M. A. Scholl (1993), The hydrogeology of Kilauea volcano, *Geothermics*, *22*, 255-270.

Ingebritsen, S. E., D. R. Sherrod, and R. H. Mariner (1989), Heat flow and hydrothermal circulation in the Cascade Range, north-central Oregon, *Science*, *243*, 1458-1462.

Interagency SEIS Team (1994), Record of decision for amendments to Forest Service and Bureau of Land Management planning documents within the range of the northern spotted owl; standards and guidelines for management of habitat for late-successional and old-growth forest related species within the range of the northern spotted owl, Interagency SEIS Team, Portland, Ore.

IPCC (2001), Climate Change 2001: The Scientific Basis. Contribution of Working Group I to the Third Assessment Report of the Intergovernmental Panel on Climate Change, edited by J. T. Houghton, et al., Cambridge University Press., Cambridge.

Izuka, S. K., and S. B. Gingerich (2003), A thick lens of fresh groundwater in the southern Lihue Basin, Kauai, Hawaii, USA, *Hydrogeology Journal*, *11*, 240-248.

James, E. R., M. Manga, and T. P. Rose (1999), CO2 degassing in the Oregon Cascades, *Geology*, *27*, 823-826.

James, E. R., M. Manga, T. P. Rose, and G. B. Hudson (2000), The use of temperature and isotopes of O,H,C and noble gases to determine the pattern and spatial extent of groundwater flow, *Journal of Hydrology*, *237*, 100-112.

Jefferson, A., and G. E. Grant (2003), Recharge areas and discharge of groundwater in a young volcanic landscape, McKenzie River, Oregon, *Geological Society of America Annual Meeting Abstracts with Programs*, *35*, 151-151.

Jefferson, A., G. E. Grant, S. L. Lewis, and C. Tague (2004), Geology broadly predicts summer streamflow in volcanic terrains: lessons from the Oregon Cascades, *Eos Transactions American Geophysical Union*, *85*, Fall Meet. Suppl. Abstract H33C-0475.

Jefferson, A., G. E. Grant, and T. P. Rose (2006), The influence of volcanic history on groundwater patterns on the west slope of the Oregon High Cascades, *Water Resources Research*, *in press*, 2005WR004812.

Jenny, H. (1941), *Factors of Soil Formation: A System of Quantitative Pedology*, 281 pp., McGraw-Hill, New York. Reprinted 1994, Dover, Mineola, N.Y.

Join, J.-L., J.-L. Folio, and B. Robineau (2005), Aquifers and groundwater within active shield volcanoes. Evolution of conceptual models in the Piton de la Fournaise volcano, *Journal of Volcanology and Geothermal Research*, *147*, 187-201.

Jones, B. E., and H. T. Stearns (1931), Water-Power Resources of the McKenzie River and its Tributaries, Oregon, *Water-Supply Pap. 637-C*, U.S. Geol. Surv., Washington, D.C.

Jones, J. A., and D. A. Post (2004), Seasonal and successional streamflow response to forest cutting and regrowth in the northwest and eastern United States, *Water Resources Research*, *40*, W05203, doi:05210.01029/02003WR002952.

Kiernan, K., C. Wood, and G. Middleton (2003), Aquifer structure and contamination risk in lava flows: insights from Iceland and Australia, *Environmental Geology*, *43*, 852-865.

Kilburn, C. R. J. (2000), Lava flows and flow fields, in *Encyclopedia of Volcanoes*, edited by H. Sigurdsson, pp. 291-305, Academic Press, San Diego, Calif.

Kirchner, J. W., X. Feng, and C. Neal (2000), Fractal stream chemistry and its implications for contaminant transport in catchments, *Nature, 403*, 524-527.

Kochel, R. C., and J. F. Piper (1986), Morphology of large valleys on Hawaii: evidence for groundwater sapping and comparisons with Martian valleys, *Journal of Geophysical Research, 91*, E175-E192.

Koltermann, C. E., and S. M. Gorelick (1996), Heterogeneity in sedimentary deposits: A review of structure-imitating, process-imitating, and descriptive approaches, *Water Resources Research, 32*, 2617-2658.

Koppers, A. A. P. (2002), ArArCALC--software for ^{40}Ar/^{39}Ar age calculations, *Computers & Geosciences 28*, 605-619.

Kulkarni, H., S. B. Deolankar, A. Lalwani, B. Joseph, and S. Pawar (2000), Hydrogeologic framework of the Deccan basalt groundwater systems, west-central India, *Hydrogeology Journal, 8*, 368-378.

Lamb, M. P., A. D. Howard, W. E. Dietrich, and J. T. Perron (2005), Hawaiian analog for Martian amphitheatre-headed valleys, *American Geophysical Union, Fall Meeting 2005*, H33C-1404.

Lamb, M. P., A. D. Howard, J. Johnson, K. X. Whipple, W. E. Dietrich, and J. T. Perron (2006), Can springs cut canyons into rock?, *Journal of Geophysical Research, 111*, E07002, doi:07010.01029/02005JE002663.

Larsson, D., K. Gronvold, N. Oskarsson, and E. Gunnlaugsson (2002), Hydrothermal alteration of plagioclase and growth of secondary feldspare in the Hengill Volcanic Centre, SW Iceland, *Journal of Volcanology and Geothermal Research, 114*, 275-290.

Leonardi, V., F. Arthaud, J. C. Grillot, V. Avetissian, and P. Bochnaghian (1996), Modelling of a fractured basaltic aquifer with respect to geologic setting, and climatic and hydraulic conditions: the case of perched basalts at Garni (Armenia), *Journal of Hydrology, 179*, 87-109.

Leung, L. R., Y. Qian, X. Bian, W. Washington, J. Han, and J. O. Roads (2004), Mid-century ensemble regional climate change scenarios for the western United States, *Climatic Change, 62*, 75-113.

Lindholm, G. F., and J. J. Vaccaro (1988), Region 2, Columbia Lava Plateau, in *Hydrogeology*, edited by W. Back, et al., pp. 37-50, Geological Society of America, Boulder, Colo.

Lohse, K. A., and W. E. Dietrich (2005), Contrasting effects of soil development on hydrological properties and flow paths, *Water Resources Research, 41*, W12419, doi:12410.11029/12004WR003403.

Louvat, P., and C. J. Allegre (1998), Riverine erosion rates on Sao Miguel volcanic island, Azores archipelago, *Chemical Geology*, *148*, 177-200.

Lund, E. H. (1977), Geology and hydrology of the Lost Creek glacial trough, *The Ore Bin*, *39*, 141-156.

Maloszewski, P., W. Stichler, and A. Zuber (2004), Interpretation of environmental tracers in groundwater systems with stagnant water zones, *Isotopes in Environmental and Health Studies*, *40*, 21-33.

Maloszewski, P., and A. Zuber (1985), On the theory of tracer experiments in fissured rocks with a porous matrix, *Journal of Hydrology*, *79*, 333-358.

Manga, M. (1996), Hydrology of spring-dominated streams in the Oregon Cascades., *Water Resources Research*, *32*, 2435-2440.

Manga, M. (1997), A model for discharge in spring-dominated streams and implications for the transmissivity and recharge of quaternary volcanics in the Oregon Cascades, *Water Resources Research*, *33*, 1813-1822.

Manga, M. (1998), Advective heat transport by low-temperature discharge in the Oregon Cascades, *Geology*, *26*, 799-802.

Manga, M. (1999), On the timescales characterizing groundwater discharge at springs, *Journal of Hydrology*, *219*, 56-69.

Manga, M., and J. W. Kirchner (2004), Interpreting the temperature of water at cold springs and the importance of gravitational potential energy, *Water Resources Research*, *40*, W05110, doi:05110.01029/02003WR002905.

Mantua, N. J., S. R. Hare, Y. Zhang, J. M. Wallace, and R. C. Francis (1997), A Pacific interdecadal climate oscillation with impacts on salmon production, *Bulletin of the American Meteorological Society*, *78*, 1069-1079.

Mariner, R. H., W. C. Evans, T. S. Presser, and L. D. White (2003), Excess nitrogen in selected thermal and mineral springs of the Cascade Range in northern California, Oregon, and Washington: sedimentary or volcanic in origin?, *Journal of Volcanology and Geothermal Research*, *121*, 99-114.

Mazor, E., and R. Nativ (1992), Hydraulic calculation of groundwater flow velocity and age: examination of the basic premises, *Journal of Hydrology*, *138*, 211-222.

McDonnell, J. J., J. Freer, R. Hooper, C. Kendall, D. Burns, and J. Peters (1996), New method developed for studying flow on hillslopes, *Eos*, *77*, 465-472.

McGuire, K. J., J. J. McDonnell, M. Weiler, C. Kendall, B. L. McGlynn, J. M. Welker, and J. Seibert (2005), The role of topography on catchment-scale water residence time, *Water Resources Research*, *41*, W05002, doi:05010.01029/02004WR003657.

Michel, R. L. (1989), Tritium deposition in the continental United States: 1953-1983, *Water-Res. Invest. Report 89-4072*, 46 pp, U.S. Geol. Surv., Reston, Va.

Middleton, G. V., and P. R. Wilcock (1994), *Mechanics in the Earth and Environmental Sciences*, 459 pp., Cambridge UP, Cambridge.

Montgomery, D. R., and W. E. Dietrich (2002), Runoff generation in a steep, soil-mantled landscape, *Water Resources Research*, *38*, 1168, doi:1110.1029/2001WR000822.

Montgomery, D. R., and E. Foufoula-Georgiou (1993), Channel network source representation using digital elevation models, *Water Resources Research, 29,* 3925-3934.

Mote, P. W. (2003), Trends in snow water equivalent in the Pacific Northwest and their climatic causes, *Geophysical Research Letters*, *30*, 1601, doi:1610.1029/2003GL017258.

Mote, P. W., A. F. Hamlet, M. Clark, and D. P. Lettenmaier (2005), Declining mountain snowpack in western North America, *Bulletin of the American Meteorological Society*, *86*, 39-49.

Mote, P. W., E. Parson, A. F. Hamlet, W. S. Keeton, D. P. Lettenmaier, N. J. Mantua, E. L. Miles, D. Peterson, D. L. Peterson, R. Slaughter, and A. K. Snover (2003), Preparing for climatic change: the water, salmon, and forests of the Pacific Northwest, *Climatic Change*, *61*, 45-88.

Naiman, R. J., K. L. Fetherston, S. J. McKay, and J. Chen (1998), Riparian forests, in *River Ecology and Management: Lessons from the Pacific Northwest*, edited by R. J. Naiman and R. E. Bilby, pp. 289-323, Springer, New York City.

Nathenson, M., and J. M. Thompson (2003), Slightly thermal springs and non-thermal springs at Mount Shasta, California: Chemistry and recharge elevations, *Journal of Volcanology and Geothermal Research*, *121*, 137-153.

Nolin, A. W., and C. Daly (2006), Mapping "at-risk" snow in the Pacific Northwest, U.S.A., *Journal of Hydrometeorology*, *in press*.

O'Connor, J. E., and G. E. Grant (Eds.) (2003), *A Peculiar River: Geology, Geomorphology, and Hydrology of the Deschutes River, Oregon*, 219 pp., American Geophysical Union, Washington, D.C.

O'Connor, J. E., J. H. I. Hardisson, and J. E. Costa (2001), Debris Flows from Failures of Neoglacial-Age Moraine Dams in the Three Sisters and Mount Jefferson Wilderness Areas, Oregon, *Prof. Pap. 1606*, 93 pp, U.S. Geol. Surv., Washington, D.C.

O'Green, A. T., P. A. McDaniel, J. Boll, and C. K. Keller (2005), Paleosols as deep regolith: implications for ground-water recharge across a loessial climosequence, *Geoderma*, *126*, 85-99.

Onda, Y. (1993), Underlying rock type controls of hydrological processes and shallow landslide occurrence, in *Sediment Problems: Strategies for Monitoring, Prediction and Control*, edited by R. F. Hadley and T. Mizuyama, pp. 47-55, International Association of Hydrological Sciences, Wallingford, Oxfordshire.

Onda, Y. (1994), Contrasting hydrological characteristics, slope proceses and topography underlain by paleozoic sedimentary rocks and granite, *Transactions, Japanese Geomorphological Union*, *15A*, 49-65.

OWRD (2005), Well Log Database, http://apps2.wrd.state.or.us/apps/gw/well_log/Default.aspx/, Oregon Water Resources Department, Salem, Ore.

Ping, C.-L. (2000), Volcanic soils, in *Encyclopedia of Volcanoes*, edited by H. Sigurdsson, pp. 1259-1270, Academic Press, San Diego, Calif.

PNWERC (2002), *Willamette River Basin Planning Atlas: Trajectories of environmental and ecological change*, 178 pp., Oregon State University Press, Corvallis, OR.

Pokrovsky, O. S., J. Schott, D. I. Kudryavtzev, and B. Dupre (2005), Basalt weathering in Central Siberia under permafrost conditions, *Geochimica et Cosmochimica Acta*, *69*, 5659-5680.

Priest, G. R., N. M. Woller, G. L. Black, and S. H. Evans (1983), Overview of the geology of the central Oregon Cascade Range, in *Geology and Geothermal Resources of the Central Oregon Cascade Range*, edited by G. R. Priest and B. F. Vogt, 15, pp. 3-28, Oregon Department of Geology and Mineral Industries, Salem, Ore.

Rademacher, L. K., J. F. Clark, D. W. Clow, and G. B. Hudson (2005), Old groundwater influence on stream hydrochemistry and catchment response times in a small Sierra Nevada catchment: Saheghen Creek, California, *Water Resources Research*, *41*, W02004, doi:02010.01029/02003WR002805.

Regonda, S. K., B. Rajagopalan, M. Clark, and J. Pitlick (2005), Seasonal cycle shifts in hydroclimatology over the western United States, *Journal of Climate*, *18*, 372-384.

Revil, A., A. Finizola, F. Sortina, and M. Ripepe (2004), Geophysical investigations at Stromboli volcano, Italy: implications for ground water flow and paroxysal activity, *Geophysical Journal International*, *157*, 426-440.

Ropelewski, C. F., and P. D. Jones (1987), An extension of the Tahiti-Darwin Southern Oscillation Index, *Monthly Weather Review*, *115*, 2161-2165.

Rose, T. P., M. L. Davisson, and R. E. Criss (1996), Isotope hydrology of voluminous cold springs in fractured rock from an active volcanic region, northeastern California, *Journal of Hydrology*, *179*, 207-236.

Saar, M. O., M. C. Castro, C. M. Hall, M. Manga, and T. P. Rose (2005), Quantifying magmatic, crustal, and atmospheric helium contributions to volcanic aquifers using all stable noble gases: Implications for magmatism and groundwater flow, *Geochemistry Geophysics Geosystems*, *6*, Q03008, doi:03010.01029/02004GC000828.

Saar, M. O., and M. Manga (1999), Permeability-porosity relationship in vesicular basalts, *Geophysical Research Letters*, *26*, 111-114.

Saar, M. O., and M. Manga (2003), Seismicity induced by seasonal groundwater recharge at Mt. Hood, Oregon, *Earth and Planetary Science Letters*, *214*, 605-618.

Saar, M. O., and M. Manga (2004), Depth dependence of permeability in the Oregon Cascades inferred from hydrogeologic, thermal, seismic, and magmatic modeling constraints, *Journal of Geophysical Research, 109*, B04204, 04210.01029/02003JB002855.

Sanderson, R. B. (1963), Ground-water inflow into the Carmen-Smith diversion tunnel McKenzie River Basin, Oregon, 4 pp, U.S. Geological Survey, Washington.

Schlosser, P., M. Stute, C. Sonntag, and K. O. Munnich (1989), Tritogenic 3He in shallow groundwater, *Earth and Planetary Science Letters*, *94*, 245-256.

Schmidt, M. E., A. L. Grunder, and R. M. Conrey (2002), Basaltic andesite and palagonitic tuff at North Sister Volcano, Oregon High Cascades, paper presented at Geological Society of America, Cordilleran Section, 98th annual meeting, Geological Society of America, Corvallis, Ore.

Scholl, M. A., S. E. Ingebritsen, C. J. Janik, and J. P. Kauahikaua (1996), Use of precipitation and groundwater isotopes to interpret regional hydrology on a tropical volcanic island: Kilauea volcano area, Hawaii, *Water Resources Research*, *32*, 3525-3537.

Scott, W. E. (1977), Quaternary glaciation and volcanism, Metolius River area, Oregon, *Geological Society of America Bulletin*, *88*, 113-124.

Scott, W. E., C. A. Gardner, and A. M. e. Sarna-Wojcicki (1989), Guidebook for Field Trip to the Mount Bachelor-South Sister-Bend Area, Central Oregon High Cascades, *Open-File Report 89-645*, U.S. Geol. Surv., Vancouver, Wash.

Seidl, M. A., W. E. Dietrich, and J. W. Kirchner (1994), Longitudinal profile development into bedrock: an analysis of Hawaiian channels, *Journal of Geology*, *102*, 457-474.

Selong, J. H., T. E. McMahon, A. V. Zale, and F. T. Barrows (2001), Effects of temperature on growth and survival of bull trout, with application of an improved method for determining thermal tolerance in fishes, *Transactions of the American Fisheries Society*, *130*, 1026-1037.

Sherrod, D. R. (1986), Geology, petrology, and volcanic history of a portion of the Cascade Range between latitudes 43-44 degrees N, central Oregon, U.S.A., Ph.D. thesis, 320 pp pp, University of California, Santa Barbara, Santa Barbara.

Sherrod, D. R. (1991), Geologic map of a part of the Cascade Range between latitudes 43°-44°, Central Oregon, *Misc. Invest. Ser. I-1891*, US Geol. Surv., Reston, Va.

Sherrod, D. R., and J. G. Smith (1990), Quaternary extrusion rates of the Cascade Range, northwestern United States and southern British Columbia, *Journal of Geophysical Research*, *95*, 19465-19474.

Sherrod, D. R., and J. G. Smith (2000), Geologic Map of Upper Eocene to Holocene Volcanic and Related Rocks of the Cascade Range, Oregon, *Geol. Invest. Ser. I-2569*, U.S. Geol. Surv., Washington, D.C.

Sherrod, D. R., E. M. Taylor, M. L. Ferns, W. E. Scott, R. M. Conrey, and G. A. Smith (2004), Geologic Map of the Bend 30- x 60-Minute Quadrangle, Central Oregon, *Geol. Invest. Ser. I-2683*, U.S. Geol.l Surv., Washington, D.C.

Shoji, S., M. Nanzyo, and R. Dahlgren (1993), *Volcanic Ash Soils*, 288 pp., Elsevier, Amsterdam.

Sivapalan, M., K. Takeuchi, S. W. Franks, V. K. Gupta, H. Karambiri, V. Lakshmi, X. Liang, J. J. McDonnell, E. M. Mendiondo, P. E. O'Connell, T. Oki, J. W. Pomeroy, D. Schertzer, S. Uhlenbrook, and E. Zehe (2003), IAHS decade on predictions in ungauged basis (PUB), 2003-2012: shaping an exciting future for the hydrological sciences, *Hydrological Sciences Journal*, *48*, 857-880.

Skinner, C. E., and S. F. Radosevich (1991), Holocene volcanic tephra in the Willamette National Forest, Linn and Lane Counties, Oregon: distribution,

geochemical characterization, and geoarchaeological evaluation, Report prepared for the Willamette National Forest, Eugene, Ore. by Northwest Research and Trans-World Geology, Corvallis, Ore.

Squyres, S. W., A. H. Knoll, R. E. Arvidson, B. C. Clark, J. P. Grotzinger, B. L. Joliff, S. M. McLennan, N. Tosca, J. F. Bell, III, W. M. Calvin, W. H. Farrand, T. D. Glotch, M. P. Golombek, K. E. Herkenhoff, J. R. Johnson, G. Klingelhofer, H. Y. McSween, and A. S. Yen (2006), Two years at Meridian Planum: results from the Opportunity rover, *Science*, *313*, 1403-1407.

Stearns, H. T. (1929), Geology and Water Resources of the Upper McKenzie Valley, Oregon, *Water Supply Paper 597-D*, U.S. Geol. Surv., Washington, D.C.

Stearns, H. T. (1942), Hydrology of volcanic terranes, in *Hydrology*, edited by O. E. Meinzer, pp. 678-703, McGraw-Hill, New York.

Stearns, H. T. (1985), *Geology of the State of Hawaii*, 2nd ed., 335 pp., Pacific Books, Palo Alto, Calif.

Stewart, I. T., D. R. Cayan, and M. D. Dettinger (2005), Changes toward earlier streamflow timing across western North America, *Journal of Climate*, *18*, 1136-1155.

Storck, P., D. P. Lettenmaier, and S. M. Bolton (2002), Measurement of snow interception and canopy effects on snow accumulation and melt in a mountainous maritime climate, Oregon, United States, *Water Resources Research*, *38*, 1223, doi:1210.1029/2002WR001281.

Swanson, F. J., and R. L. Fredriksen (1982), Sediment routing and budgets: implications for juding impacts of forestry practices, *General Technical Report*, 129-137 pp, Pacific Northwest Forest and Range Experiment Station, Portland, Ore.

Swanson, F. J., and J. A. Jones (2002), Geomorphology and hydrology of the H.J. Andrews Experimental Forest, Blue River, Oregon, in *Field Guide to Geologic Processes in Cascadia*, pp. 289-314, Oregon Department of Geology and Mineral Industries Special Paper 36, Salem.

Tague, C., M. Farrell, G. E. Grant, S. L. Lewis, and S. Rey (2006), Hydrogeologic controls on summer stream temperatures in the McKenzie River basin, Oregon, *Hydrological Processes*, *in press*.

Tague, C., and G. E. Grant (2004), A geological framework for interpreting the low flow regimes of Cascade streams, Willamette River Basin, Oregon, *Water Resources Research*, *40*, W04303 04310.01029/02003WR002629.

Tague, C., G. E. Grant, M. Farrell, J. Choate, and A. Jefferson (in review), Deep groundwater mediates streamflow response to climate warming in the Oregon Cascades, *Climatic Change*.

Tague, C. L., and L. E. Band (2004), RHESSys: regional hydro-ecologic simulation system--an object-oriented approach to spatially distributed modeling of carbon, water, and nutrient cycling, *Earth Interactions*, *8*, Paper No. 19, p. 11-42.

Tarboton, D. G. (1997), A new method for the determination of flow directions and upslope areas in grid digital elevation models, *Water Resources Research*, *33*, 309-319.

Taylor, G. H., and C. Hannan (1999), *The Climate of Oregon: From Rain Forest to Desert*, 211 pp., Oregon State University Press, Corvallis.

Thornbury, W. D. (1954), *Principles of Geomorphology*, 618 pp., John Wiley, New York.

Torres, R., W. E. Dietrich, D. R. Montgomery, S. P. Anderson, and K. Loague (1998), Unsaturated zone processes and the hydrologic response of a steep, unchanneled catchment, *Water Resources Research*, *34*, 1865-1879.

Townley, L. R. (1995), The response of aquifers to periodic forcing, *Advances in Water Resources*, *18*, 125-146.

Trenberth, K. E., and D. P. Stepaniak (2001), Indices of El Niño evolution, *Journal of Climate*, *14*, 1697-1701.

Tromp-van Meerveld, I., N. E. Peters, and J. J. McDonnell (2006), Effect of bedrock permeability on subsurface stormflow and the water balance of a trenched hillslope at the Panola Mountain Research Watershed, Georgia, *Hydrological Processes*, *in press*.

Tucker, G. E., and R. L. Bras (1998), Hillslope processes, drainage density, and landscape morphology, *Water Resources Research*, *34*, 2751-2764.

Vitousek, P. M., O. A. Chadwick, T. E. Crews, J. H. Fownes, D. M. Hendricks, and D. Herbert (1997), Soil and ecosystem development across the Hawaiian Islands, *GSA Today*, *7*, 1-8.

Washington, W. M., J. W. Weatherly, G. A. Meehl, A. J. Semtener, T. W. Bettge, A. P. Craig, W. G. Strant, J. Arblaster, V. B. Wayland, R. James, and Y. Zhang (2000), Parallel Climate Model (PCM) control and transient simulations, *Climate Dynamics*, *16*, 755-774.

Webb, B. W., P. D. Clack, and D. E. Walling (2003), Water-air temperature relationships in a Devon river system and the role of flow, *Hydrological Processes*, *17*, 3069-3084.

Wells, S. G., J. C. Dohrenwend, L. D. McFadden, B. D. Turrin, and K. D. Mahrer (1985), Late Cenozoic landscape evolution on lava flow surfaces of the Cima volcanic field, Mojave Desert, California, *GSA Bulletin*, *96*, 1518-1529.

Whipple, K. X., and G. E. Tucker (1999), Dynamics of the stream-power river incision model: Implications for height limits of mountain ranges, landscape response timescales, and research needs, *Journal of Geophysical Research*, *104*, 17661-17674.

White, W. B. (2002), Karst hydrology: recent developments and open questions, *Engineering Geology*, *65*, 85-105.

Whiting, P. J., and D. B. Moog (2001), The geometric, sedimentologic, and hydrologic attributes of spring-dominated channels in volcanic areas, *Geomorphology*, *39*, 131-149.

Whiting, P. J., and J. Stamm (1995), The hydrology and form of spring-dominated channels, *Geomorphology*, *12*, 223-240.

Willett, S. D. (1999), Orogeny and orography: The effects of erosion on the structure of mountain belts, *Journal of Geophysical Research*, *104*, 28957-28981.

Wohletz, K., and G. Heiken (1992), *Volcanology and Geothermal Energy*, 432 pp., University of California Press, Berkeley, Calif.

Wolock, D. M., T. C. Winter, and G. McMahon (2004), Delineation and evaluation of hydrologic-landscape regions in the United States using geographic information system tools and multivariate statistical analyses, *Environmental Management*, *34*, S71-S88.

APPENDIX

Table 1. Water samples analyzed for hydrogen and oxygen isotopes.

Site	Latitude (N)	Longitude (W)	Date	δD	δ^{18}O
Alder Sp.	44.179	121.913	8/25/03	-81	-11.6
Anderson Cr.	44.264	122.040	8/18/03	-87	-12.6
Anderson Cr.	44.264	122.040	10/14/03	-93	-12.7
Anderson Cr.	44.264	122.040	11/17/03	-82	-12.6
Anderson Sp.	44.264	122.040	8/8/03	-91	-12.6
Beeler Sp.	43.981	122.082	7/30/03	-84	-12.2
Bobby Cr.	44.292	122.026	3/23/03	-84	-12.0
Bobby Cr.	44.292	122.026	6/13/03	-85	-12.4
Bobby Cr.	44.292	122.026	8/15/03	-89	-12.6
Boulder Cr.	44.205	122.037	3/23/03	-80	-11.7
Boulder Cr.	44.205	122.037	8/18/03	-80	-11.4
Carmen Res. Sp.	44.342	122.023	8/26/03	-87	-12.6
Cascade Cr.	43.961	122.114	3/23/03	-75	-11.8
Cascade Cr.	43.961	122.114	8/14/03	-84	-12.2
Coldwater Sp.	44.345	121.867	7/17/2004	-57	-9.9
D7 Rd830 Sp.	44.280	122.010	8/26/2004	-77	-12.6
East Fork	44.118	122.202	8/31/2002		-11.1
French Pete Cr.	44.042	122.205	3/23/03	-81	-11.9
French Pete Cr.	44.042	122.205	8/14/03	-82	-11.9
Great Sp.	44.377	121.996	7/16/02	-89	-12.8
Great Sp.	44.377	121.996	9/2/02	-92	-12.9
Great Sp.	44.377	121.996	3/23/03	-89	-12.6
Great Sp.	44.377	121.996	4/19/03	-90	-12.7
Great Sp.	44.377	121.996	5/15/03	-90	-12.6
Great Sp.	44.377	121.996	7/13/03	-89	-12.8
Great Sp.	44.377	121.996	8/15/03	-89	-12.8
Great Sp.	44.377	121.996	9/15/03	-92	-12.9
Great Sp.	44.377	121.996	10/14/03	-96	-12.9
Great Sp.	44.377	121.996	11/17/03	-94	-12.8
Great Sp.	44.377	121.996	7/7/04		-12.7
Hardy Cr.	44.036	122.203	8/31/02		-11.2
Ice Cap Sp.	44.345	121.998	5/12/02	-86	-12.4
Ice Cap Sp.	44.345	121.998	3/20/03	-89	-12.6
Ice Cap Sp.	44.345	121.998	6/13/03	-88	-12.5
Ice Cap Sp.	44.345	121.998	8/15/03	-89	-12.7
Ice Cap Sp.	44.345	121.998	11/17/03	-87	-12.6
Linton Cr.	44.165	121.890	8/25/03	-95	-13.5
Linton Cr.	44.165	121.890	6/29/04	-89	-13.6
Linton Lake	44.167	121.893	6/29/04	-79	-13.3
Linton Lake	44.167	121.893	9/8/04	-81	-13.3
Lost Cr.	44.174	122.051	7/25/02	-90	-12.7
Lost Cr.	44.174	122.051	8/31/02	-90	-12.8
Lost Sp.	44.161	122.017	7/25/02	-90	-12.6
Lost Sp.	44.161	122.017	8/31/02	-93	-12.9
Lost Sp.	44.161	122.017	2/17/03		-13.0

Table 1 (continued).

Site	Latitude (N)	Longitude (W)	Date	δD	δ¹⁸O
Lost Sp.	44.161	122.017	3/23/03	-91	-12.8
Lost Sp.	44.161	122.017	4/15/03		-12.8
Lost Sp.	44.161	122.017	5/15/03		-12.8
Lost Sp.	44.161	122.017	6/13/03	-91	-12.8
Lost Sp.	44.161	122.017	7/12/03		-12.8
Lost Sp.	44.161	122.017	8/14/03	-92	-12.9
Lost Sp.	44.161	122.017	9/15/03		-13.0
Lost Sp.	44.161	122.017	10/14/03	-92	-12.9
Lost Sp.	44.161	122.017	11/15/03	-94	-13.1
Lost Sp.	44.161	122.017	1/8/04		-12.9
Lost Sp.	44.161	122.017	2/19/04		-12.9
Lost Sp.	44.161	122.017	3/29/04		-12.9
Lost Sp.	44.161	122.017	5/17/04		-12.9
Lost Sp.	44.161	122.017	6/16/04		-12.9
Lost Sp.	44.161	122.017	7/1/04		-12.9
Lost Sp.	44.161	122.017	7/7/04		-12.8
Lost Sp.	44.161	122.017	7/20/04		-13.0
Lost Sp.	44.161	122.017	8/16/04		-13.0
Lost Sp.	44.161	122.017	9/23/04		-13.0
Lost Sp.	44.161	122.017	3/24/05		-13.1
Lost Lake	44.434	121.903	6/24/04	-88	-12.1
Lost Lake	44.434	121.903	9/7/04	-78	-12.2
Lost Lake Creek	44.429	121.901	9/7/04	-71	-12.8
Lost Lake Seeps	44.433	121.899	7/16/04	-77	-12.8
Lost Lake Spring	44.436	121.898	6/24/04		-12.7
Lost Lake Spring	44.436	121.898	9/7/04	-70	-12.7
McBee Cr.	43.935	122.068	2/17/03		-9.6
Obsidian Cr	44.169	121.889	6/29/04	-80	-12.2
Olallie Cr.	44.259	122.039	3/23/03	-89	-12.4
Olallie Cr.	44.259	122.039	8/21/03	-87	-12.3
Olallie Cr.	44.259	122.039	3/26/2005		-12.4
Olallie North Sp.	44.273	122.020	8/1/02	-88	-12.5
Olallie North Sp.	44.273	122.020	9/2/02	-88	-12.5
Olallie North Sp.	44.273	122.020	2/18/03	-89	-12.6
Olallie North Sp.	44.273	122.020	3/23/03	-86	-12.5
Olallie North Sp.	44.273	122.020	4/15/03	-88	-12.6
Olallie North Sp.	44.273	122.020	5/16/03	-88	-12.5
Olallie North Sp.	44.273	122.020	6/13/03	-88	-12.5
Olallie North Sp.	44.273	122.020	7/12/03	-88	-12.4
Olallie North Sp.	44.273	122.020	8/18/03	-87	-12.6
Olallie North Sp.	44.273	122.020	9/15/03	-86	-12.5
Olallie North Sp.	44.273	122.020	10/14/03	-91	-12.6
Olallie North Sp.	44.273	122.020	10/28/03	-91	-12.6
Olallie North Sp.	44.273	122.020	11/17/03	-90	-12.7
Olallie North Sp.	44.273	122.020	4/7/04	-88	-12.5
Olallie North Sp.	44.273	122.020	5/24/2004	-73	-12.5

Table 1 (continued).

Site	Latitude (N)	Longitude (W)	Date	δD	δ¹⁸O
Olallie North Sp.	44.273	122.020	6/16/2004	-71	-12.6
Olallie North Sp.	44.273	122.020	7/7/2004	-83	-12.6
Olallie North Sp.	44.273	122.020	7/20/2004	-85	-12.6
Olallie North Sp.	44.273	122.020	8/17/2004	-82	-12.6
Olallie North Sp.	44.273	122.020	10/11/2004	-79	-12.6
Olallie North Sp.	44.273	122.020	11/14/2004	-88	-12.6
Olallie North Sp.	44.273	122.020	3/25/2005	-94	-12.6
Olallie South Sp.	44.264	122.025	9/2/02	-85	-12.2
Olallie South Sp.	44.264	122.025	7/12/03	-84	-12.3
Olallie South Sp.	44.264	122.025	8/18/03	-85	-12.3
Olallie South Sp.	44.264	122.025	11/17/03	-84	-12.3
Olallie South Sp.	44.264	122.025	8/17/04		-12.3
Olallie South Sp.	44.264	122.025	3/25/05	-81	-12.3
Olallie Upper Sp.	44.272	122.018	3/23/03	-89	-12.4
Olallie Upper Sp.	44.272	122.018	5/16/03	-86	-12.5
Rebel Cr.	44.013	122.172	8/31/02		-11.9
Roaring North Sp.	43.920	122.056	7/10/03	-92	-13.0
Roaring North Sp.	43.920	122.056	8/19/03	-93	-13.1
Roaring North Sp.	43.920	122.056	9/30/03		-13.0
Roaring R. abv sp.	43.916	122.059	8/31/02		-13.0
Roaring R. blw sp.	43.934	122.066	3/23/03	-92	-12.8
Roaring R. blw sp.	43.934	122.066	8/14/03	-89	-13.0
Roaring R. un. trib.	43.946	122.080	2/17/03		-12.5
Roaring Sp.	43.948	122.067	9/2/02	-94	-13.0
Roaring Sp.	43.948	122.067	7/19/03	-93	-13.0
Roaring Sp.	43.948	122.067	8/19/03	-92	-13.0
Roaring Sp.	43.948	122.067	9/4/03		-13.0
Roaring Sp.	43.948	122.067	7/7/04		-13.0
Roaring Sp.	43.948	122.067	11/15/03	-86	-13.1
Scott Rd Seeps	44.197	122.016	8/27/2004	-69	-12.4
Separation Cr.	44.124	122.030	5/17/2004	-86	-13.3
South Fork McKenzie R.	43.960	122.063	8/30/2002		-13.0
South Fork McKenzie R.	43.958	122.083	3/23/03	-87	-12.6
South Fork McKenzie R.	43.960	122.063	6/13/03	-89	-12.7
South Fork McKenzie R.	43.960	122.063	8/14/03	-91	-12.9
South Fork McKenzie R.	43.960	122.063	2/28/2004		-12.8
Spring Lk Cr.	44.190	121.864	7/17/03	-95	-13.2
Sweetwater Sp.	44.279	122.014	8/8/03	-91	-12.7
Sweetwater Sp.	44.279	122.014	7/27/04		-12.7
Sweetwater Sp.	44.279	122.014	3/25/05	-84	-12.8
Tamolitch Sp.	44.312	122.025	9/1/02	-91	-12.7
Tamolitch Sp.	44.312	122.025	3/20/03	-88	-12.4
Tamolitch Sp.	44.312	122.025	6/13/03	-90	-12.6
Tamolitch Sp.	44.312	122.025	8/17/03	-88	-12.5
Tamolitch Sp.	44.312	122.025	11/15/03	-86	-12.7

Table 1 (continued).

Site	Latitude (N)	Longitude (W)	Date	δD	δ¹⁸O
Tamolitch Sp.	44.312	122.025	8/16/04		-12.7
Tidbits Cr.	44.224	122.268	8/31/02		-11.1
Twin Springs	43.961	122.122	6/28/04	-70	-11.8
White Branch	44.159	122.019	7/25/02	-90	-12.7
White Branch	44.159	122.019	8/31/2002	-93	-12.8
White Branch	44.159	122.019	3/23/03	-90	-12.9
White Branch	44.159	122.019	6/13/2003	-92	-12.8
White Branch	44.159	122.019	8/14/03	-92	-12.9
White Branch	44.159	122.019	7/1/2004		-12.8